Ministry of Higher Education

and Scientific Research

University of Babylon

College of Science

Department of Chemistry

Preparation of Chromatographic Column that Used to Separate and Determine of Pharmaceutical Compounds

A thesis

Submitted to the Council of College of Science – University of Babylon In Partial Fulfillment of the Requrirements for the Degree of Master in Chemistry

By

Narjis Salah Falah Mishaal AL-sultani

B.S.c. University of Babylon-2013

Supervised by

Prof. Dr. Ahmed Ali Abdul- Sahib Al-karimi

Asst. Prof. Ibtisam A. Aljazaery

2022 A.D **1444 A.H**

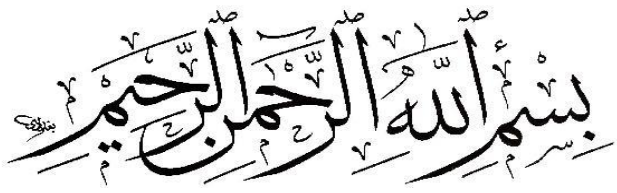

(يَرْفَعِ اللَّهُ الَّذِينَ آمَنُوا مِنْكُمْ وَالَّذِينَ أُوتُوا الْعِلْمَ دَرَجَاتٍ وَاللَّهُ بِمَا تَعْمَلُونَ خَبِيرٌ)

صدق الله العلي العظيم

المجادلة: (١١)

Supervisors Certification

We certify that this thesis was carried out under our supervision at the department of chemistry in a college of science at university of Babylon as partial fulfilment of the requirement for the degree of master's in analytical chemistry

Signature.

First supervisor

Name : Dr. Ahmed Ali Abdul sahib Alkarimi

Scientific Order: Professor

Second supervisor

Name : Asst. Prof. Ibtisam A. Aljazaery

Scientific Order: Asst. Professor

Address: University of Babylon - College of Science -Chemistry Department

Date: / /2022

Recommendation of Head of Chemistry Department

In view of the available recommendations, I forward this thesis for debate by the examining committee

Signature:

Name : Dr. Abbas Jasim Atiyah

Scientific order: Professor

Address: Head of Chemistry Department- University of Babylon - College of

Science Date: / /2022

Acknowledgements

Praise be to Allah the Lord of the worlds, and may the blessings and peace of Allah be upon the most honoured of messengers, our master Muhammad and all his family and companion.

I express my heartful thanks and deep regards to my first supervisor (Prof. Dr. Ahmed Ali Abdul sahib Alkarimi) and my second supervisor (Asst. Prof. Ibtisam A. Aljazaery) for their moral guidance, monitoring and constant encouragement throughout this work.

I take this opportunity to express my profound gratitude and deep regard to the University of Babylon, College of Science, Chemistry Department staff, colleagues, graduate students, my family and all my friends.

Narjis

Dedication

To whom I am honoured to hold his name, who did his best to get me this higher educational degree … my father, may Allah bless him.

To the spring of givings in my life …. my mother, may Allah bless her.

To that soul who supported me and stood by me … the grandfather of my children, may Allah have mercy on him.

To who supported me and stood by me…the grandmather of my children, may Allah bless her.

To that one who endured the difficulties of my path to get this precious degree and is still the best supporter to me … my husband, I dedicate to him this work with all love, elevation and dignity.

To the flowers surrounding me with their hearts … my brother and my sisters.

To my lovely children, the hope of my future, who fill my life with pleasure and warmth … Mariam, Abu Al-Fadhl and Abdullah.

Narjis

Table of Contents

Table of Figures

Table of Tables

Abbreviations

^{1}H-NMR	Proton nuclear Magnetic Resonance spectroscopy
2D	Two dimensional
3SPMA	3-sulfopropyl methacrylate
A.Am	Acryl amide
AAS	Atomic absorption sperctroscopy
AFM	Atomic force microscopy
AIBN	2 , 2, - Azobisisobutyronitrile
ATRP	Atom transfer radical polymerization
ATRP	Atom Transfer Radical Polymerization
BET	Brunauer-Emmett-Teller analyzer
BUMA	Butyl methacrylate
°C	Celsius
C18	n-Octadecyl hydrocarbon chains
C8	n-Octyl hydrocarbon chains
CEC	capillary electro chromatography
cm	centimeter
CX	Cationic exchange
CX	cation exchange
D.W	Distilled water
DAP	2, 2-Dimethoxy-2-phenylacetophenone
DVB	Divinyl benzene
ε	Molar absorption coefficient
$E_{rel.}$	Relative error
EDMA	Ethylene glycol dimethacrylate
FT-IR	Fourier Transform Infrared spectroscopy
g	gram
GC	gas chromatography
GMA	Glycidyl methacrylate
λ_{max}	The greatest wavelength
h	Hours
HCl	Hydrochloric acid
HETP	high equivalent to a theoretical plate
HI	Hydrophilic interaction

HILIC	Hydrophilic interaction liquid chromatography
HPLC	High Performance Liquid Chromatography
i.d	inner diameter
IBMK	Iso-butyl methyl ketone
IEC	Ion-Exchange chromatography
IR	Infrared spectroscopy
ISEC	Inverse size exclusion chromatography
KBr	Potassium bromide
KV	Kilo volt
L	Liter
LC	Liquid chromatography
LOD	Limit of detection
LOQ	Limit of quantitation
m	meter
M	Molarity
mg	Mili gram
min	Minute
MIP	Mercury intrusion porosimetry
mL	mili Liter
mm	Mili meter
MS	mass spectrometry
MTMS	methyltrimethoxysilane
mV	Mili volt
N	Normality
N_2	Nitrogen
$NaHSO_3$	Sodium bi sulfite
NaOH	Sodium hydroxid
NH_2	Amine
nm	Nanometer
NPLC	Normal phase liquid chromatography
o.d	outer diameter
pA	Pico amber
pH	Power Hydrogen
PMMA	poly(methyl methacrylate
ppm	Part per milion

PSI	Pressure per square inch
R^2	linear
RP	Reversed phase
RPLC	Reversed phase liquid chromatography
RP-LC	Reversed phase liquid chromatography
RSD	Relative standard deviation
SAX	Strong anion exchange
SCX	Strong cationic exchange
SEM	Scanning electron microscope
SMA	Stearyl methacrylate
TEM	Transmission electron microscopy
TEOS	tetraethyl orthosilicate
TLC	Thin layer chromatography
TMOS	tetramethyl orthosilicate
TRF	Trifluoperazine Hydrochloride
TSP	3-(Trimethoxysilyl) propyl methacrylate
UV	Ultraviolet light
WAX	Weak anion exchange
WCX	Weak cation exchange
µg	Microgram
µ-HPLC	Micro- High Performance Liquid Chromatography
µl	Microliter

Summary

High-pressure liquid chromatography (HPLC) is considered one of the most popular techniques used in analytical chemistry to separate, determine, and identify pharmaceutical compounds.

The glycidyl methacrylate-co-ethylene dimethcrylate-co- acryl amide monolithic column was synthesized as an LC column for pharmaceutical compound determination and separation.

A borosilicate tube (60 mm in length) with (1.5 mm) and (3.0 mm) inner diameter (i.d) and an outer diameter(o.d) respectively was used for in-situ copolymerization using a U.V light source. Monomers (glycidyl methacrylate and acrylamide) and crosslinker ethylene dimethacrylate and initiator (2, 2-dimethoxy-2-phenyl acetophenone) (DMPA) were dissolved in a suitable solvent consisting of (750 µL1-propanol + 900 µL Hexanol) .

The polymer was formed after (**3 min**), and the epoxy groups in glycidyl methacrylate were opened to form diol groups by pumping (**0.2 M**) HCl for 3 hours at a flow rate of (**20 µL.min^{-1}**).

The monolith was characterized using diverse techniques such as FT-IR, BET, ^{1}HNMR, and FE-SEM, and the polymer properties, such as surface area and pore size, have been studied. The optimum conditions, such as irradiation time, the permeability of the monolith, porosity, swelling, and the distance between the radiation source and the column, have been studied.

The prepared monolith was used to determine pharmaceutical compounds such as propranolol hydrochloride and trifluoperazine di hydrochloride using the HPLC technique due to their vital role in treating many human diseases.

The determination method has LOD (**0.005 µg.mL^{-1}**), LOQ (**0.036 µg.mL^{-1}**) and Sandel's sensitivity was (**0.0052 µg.cm^{-2}**) for propranolol hydrochloride, while for trifluoperazine

dihydrochloride have LOD (**0.007 µg.mL^{-1}**), LOQ (**0.036 µg.mL^{-1}**), and Sandel's sensitivity was (**0.00783**).

The prepared monolith column was used to separate pharmaceutical compounds by HPLC technology; the retention time of the first peak appeared within (**1.4min**) for propranolol hydrochloride, while for trifluoperazine dihydrochloride, it was (**2.6 min**).

It was found that these compounds interacted with the components of the prepared column, and the separation was successful. In addition, the number of theoretical plates (N) and the height of a theoretical plate for the monolithic chromatographic column after being injected with a certain amount of solution propranolol hydrochloride and trifluoperazine dihydrochloride (**110.995 plates),** (**2.19mm/plates),** (**111.102 plates**), (**2.22 mm/plate**) respectively.

The properties of the prepared monolithic column are low cost with high accuracy and precision with a life time of **(45) days**.

.

1. Introduction

Chemical separation methods are among the essential analytical methods, which are used to obtain different materials purely, without the presence of impurities suspended in them, And nuclear magnetic resonance rays, as well as atomic mass spectrometry (spectrometry mass and NMR, IR) and obtaining the pure substance, makes it easy to perform quantitative analyzes on it to know its concentration[(1)].

Chemical separation methods are essential, both in descriptive and quantitative analysis and in fact, several ways can be included within chemical separation methods, such as extraction processes of all kinds[(2)] . At present, there are many types of adsorbent materials that can be used for solid-phase extraction. Examples of these adsorbents are (1)silica-based polymers such as octadecyl-linked silica and butyl dimethyl silica, (2) copolymers or cross-linked polymers based on Characteristics of the adsorbent material, which can be hydrophobic, hydrophilic or ion-exchanger, (3) mixed-mode copolymers[(3)]. as extraction is usually used for isolation, reconcentration, modification of sample properties before separation and identification of compounds by chromatography-based techniques and others[(4)]. There has been a surge in academic and industrial interest in cross-linked polymeric supports. These were initially produced as particles and are now used to fill the columns in processes that occur under continuous flow, such as various chromatographic processes, due to recent developments in the configuration of the solid phase or separation types[(5,6)].

1.2 The Monolith

Monolith is a Greek word comprised of two related idioms: (one) and (stone). However, geologically, it is a single gigantic rock with diverse forms and sizes of holes. These materials were collected by Chinese empresses in the design and construction of their palaces[(7)]. Rock's monolith is shown in Figure (1.1)

Figure (1.1): Photograph of the porous monolith erected at Talhu Rock Museum of Fine Arts Boston[8].

In separation science, the term monolith refers to a single piece of porous material used to separate two or more substances. This is done by passing the sample inside monolithic material, which contains large pores (macropores), medium (mesopores) and small pores (micropores)[9].

The International Union of Chemists (IUPAC) defines pores in the following manner. Small pores(micropores) smaller than(2 nm), mesopores range from(2-50 nm), while the macropores are larger than (50 nm), Monolithic materials are widely used to separate both chemical and biological molecules[9].

In order to avoid high back pressures that prevent separation and cause structural defects in the monolith or the high-performance liquid chromatographic (HPLC) pump or problems connecting the pipes when working, having many macropores is critical. These pores allow enough passage of the mobile phase through to the monolith to avoid this. Because of these features, the polymeric monolith with large pores shows an efficient separation of large molecules. The medium-sized pores of mesopores increase the monolith's surface area and the monolith's carrying capacity. As for the small pores, micropores have a remarkable ability to absorb solutes in the mobile phase. The distinguishing characteristic of monoliths is that they possess large surface areas and large numbers of small pores, which leads to an increase in the active sites of the analytes present in the mobile phase, thus leading to better separating factors[(10)].

Monoliths generally contain two types: inorganic (Silica) and organic monoliths, such as methacrylates, vinyl esters, polystyrene, and ethylene glycol[(11)]. It has been used to adapt the monolithic stationary phase to a particular analysis or separation mechanism[(12)] . The simplicity of preparation and functional activity of methacrylate polymers explains why they have drawn more attention than other polymers[(13)] .

The polymeric monolith has been used in many fields because these polymeric materials could be prepared simply using a homogeneous or heterogeneous mixture inside the mould (column). Homogeneous materials possess large pores or interconnected channels; therefore, these materials could use with high flow rates and reasonable back pressures[(5)]. The polymerization mixture must always include a vinyl monomer as a cross-linker (it must contain at least a double bond) and an inert solvent or a mixture of inert solvents called (the porogen) or(pore-forming agent)[(6)]. The presence of inert solvents is necessary to prepare macroporous polymers. Different types of solvents are used to dissolve the monomers. They do not dissolve the polymeric chains formed (suitable solvents), and others that do not dissolve the monomers during polymer creation (weak or not suitable solvents)[(14)] . It has been used in recent decades as an innovative and valuable generation of

polymers used in various industries; these polymeric materials can be prepared simply using a homogenous or a heterogeneous mixture inside moulds. The materials have large interconnected pores or channels. Therefore, they can be used with high flow rates with moderate back pressures and have a wide range of applications. Polymerization mixtures consisting of only one phase can be used to prepare homogenous polymers. However, suspension polymerization reactions yield heterogenous polymer-based monoliths, which can have a greater variety of monomers mixed in than a single phase can produce in a suspension polymerization reaction. With more surface chemical structures available, it is possible to get more variety.

On the other hand, the reaction conditions tuned for one system cannot be used in the same way in another. For each unique system, it is necessary to adjust the reaction conditions[15] . As a network of interconnected large flow-through pores, the monolith column shows high axial permeability with a large internal surface area that provides less back pressure than a conventionally packed column. In addition, these channels allow better contact between the analyte and the stationary phase active sites[16] . Packet columns and monolithic columns are depicted in Figure (1.2).

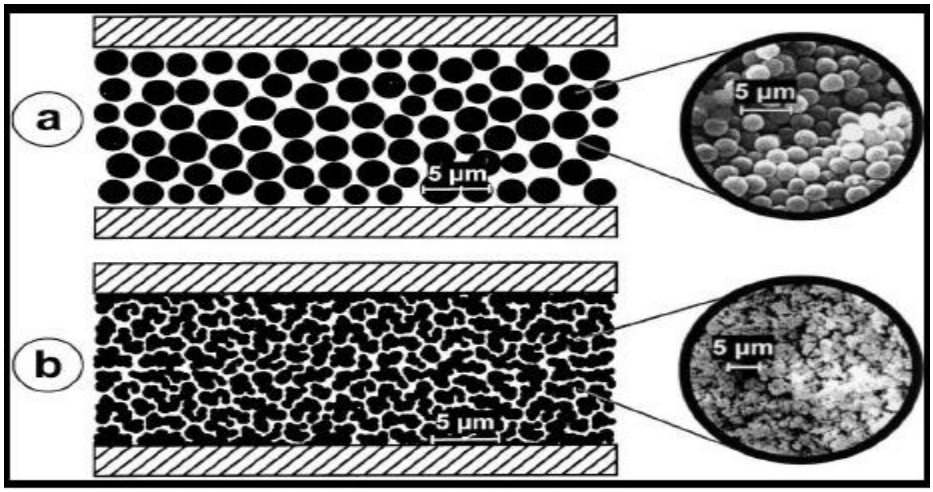

Figure (1.2): The comparison between (a) packed and (b) monolithic column[17]

Various techniques can be used to investigate the physical properties of monolithic materials, including scanning electron microscopy, transmission electron microscopy (TEM), and atomic force microscopy (AFM)[18]. Monolithic porous qualities, including pore size, hydrodynamic characteristics, and column mechanical strength, may be measured using these three approaches, providing extensive data on their shape[19] . It is possible to measure the big pores between (10 nm) and (150 nm) using mercury intrusion porosimetry (MIP), which is used to analyze the porosity and distribution of pore sizes in monolithic columns[20]. Measurement of pores smaller than 50 nm is done using inverse size exclusion chromatography ISEC and Brunauer-Emmett-Teller (BET) procedures, respectively[20][21] . Monolithic columns can be manufactured using two methods depending on the monomer(s) used in the polymerization process. Hence when alkoxysilane (silica-based monolith) is utilized, the monolith is referred to as an inorganic monolith or silica-based monolith, and the other type is an organic polymer[22] . Higher permeability, lower flow resistance, and much quicker separation periods are only moderate operation pressures of both types of packed columns. These characteristics enable them to find many applications in chromatographic techniques, for example, gas chromatography (GC), high-performance liquid chromatography (HPLC), and capillary electrochromatography (CEC), for environmental, pharmaceutical, clinical, industrial, food, and forensic analysis[23] .

1.3 Types of monoliths

1.3.1 Organic-based monoliths

Polymer-based monolithic columns have been rapidly prepared in micro-separation systems due to their preparation's simplicity and the controllability of their structure porosity and surface chemistry[24] . Liquid chromatography (LC) can use organic polymeric materials as an alternate constant phase because of their low return pressures. This depends on their chemical structures and capacity to remain stable at various pH ranges.

As these columns were used for chromatography using polyamide gel surfaces (gel chromatography), in 1990, a new technique was developed and rapidly applied to separate biomolecules[25]. The organic monolith is prepared from the polymerization of a homogeneous mixture, which includes monomers, a cross-linker, a porogenic solvent and a reaction starter Initiator[26] . The polymeric mixture is filled into a tube, and both ends of the tube are closed with a rubber stopper. The polymerization process begins with photopolymerization using ultraviolet or thermal rays for a particular time from several minutes to 24 hours, depending on the type of polymer, the resulting polymer takes the form of a mould that polymerizes inside it, where the resulting polymer can be formed according to the desire of the analyzer, as a column or disc can be prepared polymer[27]. The specific active functional groups on the surface of the polymer depend on the type of monomer used. The main groups, according to the monomer system used, are (1) styrene-based monoliths, which are highly hydrophobic, (2) methacrylates-based monoliths, which are moderately polar, and (3) acrylamide-based monoliths, which are highly polar [28].Using acrylamides, styrene, and methacrylates as monomers to yield a porous cross-linked polymer[29] .

Nowadays, three distinct types of organic monoliths can be found[30] .To begin with, the thin disks (up to three millimetres thick) are made in flat cylindrical moulds, and the most common polymerization in stainless-steel or glass tubing is used to prepare the cylindrical monolithic rod-like column as can be seen in (Figure 1.3). This column has a diameter of 1–8 mm and a length of 30–50 mm. Protein separation is made easier with the help of these columns[29,31] . The monolithic capillary is the third and final type, and it is commonly employed in capillary electrochromatography and capillary high-performance liquid chromatography[32] ,As shown in figure(1.3).

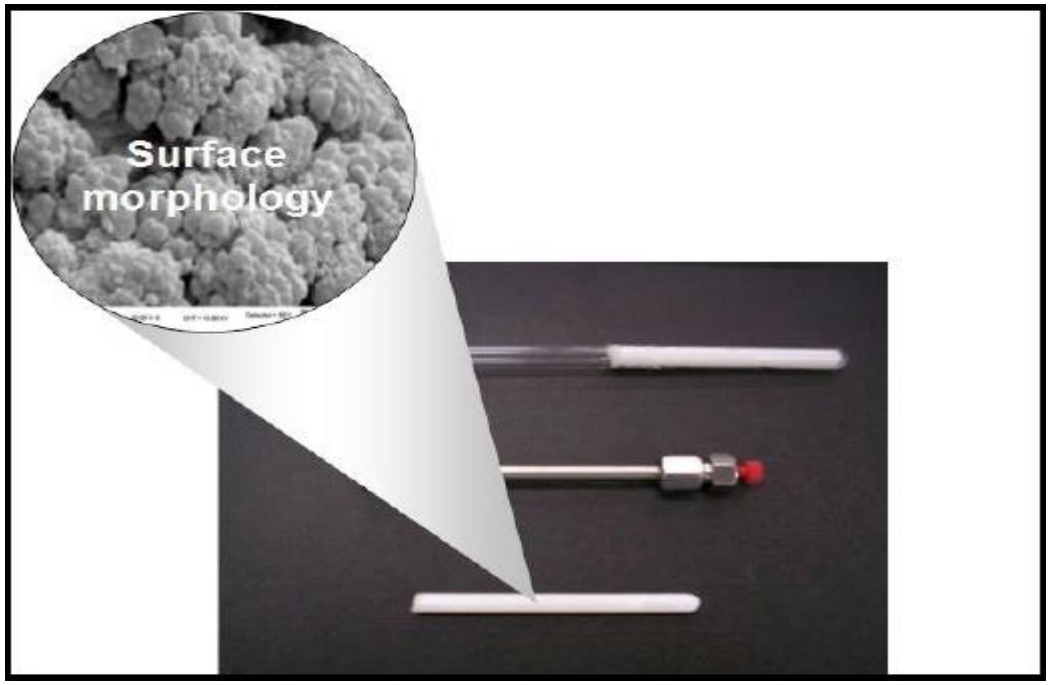

Figure (1.3): cylindrical monolith columns[5]

The advantages of organic monoliths over packed columns are as follows:(33,34)

1- Modifications that are quick and simple.

2- There is no need to keep the frits.

3- The ability to enhance mass transfer of analytes.

4- High porosity means less back pressure.

5- High selectivity.

For large molecules, such as nucleic acids [35], peptides , synthetic polymers[36], and proteins[37], organic-based monoliths are suited because of the considerable convective mass transfer and appropriate surface area.

Small molecules are difficult to separate from organic polymer monoliths under standard chromatographic settings. This drawback is caused by the material's high porosity and low mesopore[37,38] . Low-molecular-weight compounds are challenging to separate from monolith gel due to swelling caused by its porosity in the mobile phase[37]. In order to increase the separation efficiency of low molecular weight compounds to 70,000–80,000,

researchers have made significant progress. To attain this goal, many parameters and steps have been altered to examine the porosity and mass transfer in organic monoliths.

Some of these factors are as follows[27,39,40]:

1- Altering the polymerization process' starting conditions and temperature.

2-The reaction time of polymerization can be adjusted.

3- The chemistry and quantities of the polymerization mixture must be carefully optimized (functional monomers, cross linkers and porogenic solvents).

4- Modifications made to the monolith after polymerization are included in the category

5- Extending the monolithic skeleton to include more structural parts with elements

These parameters considerably impact the production of organic monoliths for chromatographic separation of low molecular weight substances. The morphology of the organic monolith is shown in Figure (1.4).

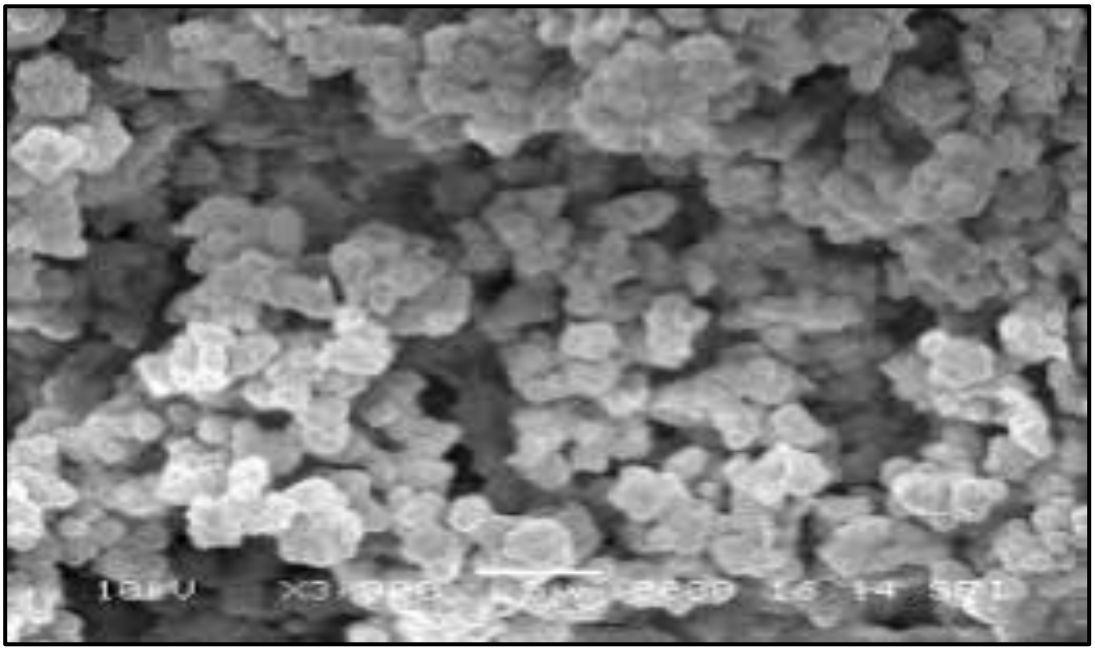

Figure (1.4): The morphology of organic monolith[41] .

1.3.2 Inorganic monolith

The inorganic monolith possesses many advantages, such as high mechanical strength, porosity, thermal stability, and not being affected by organic solvents [(42)] . compared to the organic monolith, which can shrink or swell in the presence of organic solvents[(43)]. Macro pores in the inorganic monolith can improve fluid flow through the monolith without increasing pressure. Some mesopores can increase the surface area and interact well with the materials to be studied. A silanol group (Si-OH) on the surface of the inorganic monolith can be employed to control the migration of functional groups[(44)]. The inorganic monolith is ideal for separating small molecules, as the pore sizes of the mesopores allow easy penetration of the molecules to the adsorption sites in addition to the rapid diffusion that leads to a high separation efficiency[(45)] . The bonding of groups on the surface of the inorganic monolith is more accessible than that of the organic polymeric monolith because it contains many cross-linking bonds that require hours to reach equilibrium to activate the surface[(46)] . The scientist Minakuchi and others prepared the inorganic monolith using the sol-gel method[(47)] . This method can prepare the inorganic monolith with a uniform composition, high purity and better homogeneity. Most sol-gel methods depend on using low molecular weight alkoxysilanes as generators or an essential raw material, such as (tetraethyl orthosilicate TEOS, tetramethyl orthosilicate TMOS or MTMS methyltrimethoxysilane)[(48)] . There are three reactions. The first is alkoxysilane's decomposition, aqueous silica's condensation, and the polycondensation reaction [(49)]. these reactions are illustrated in Figure (1.5) [(50)] .

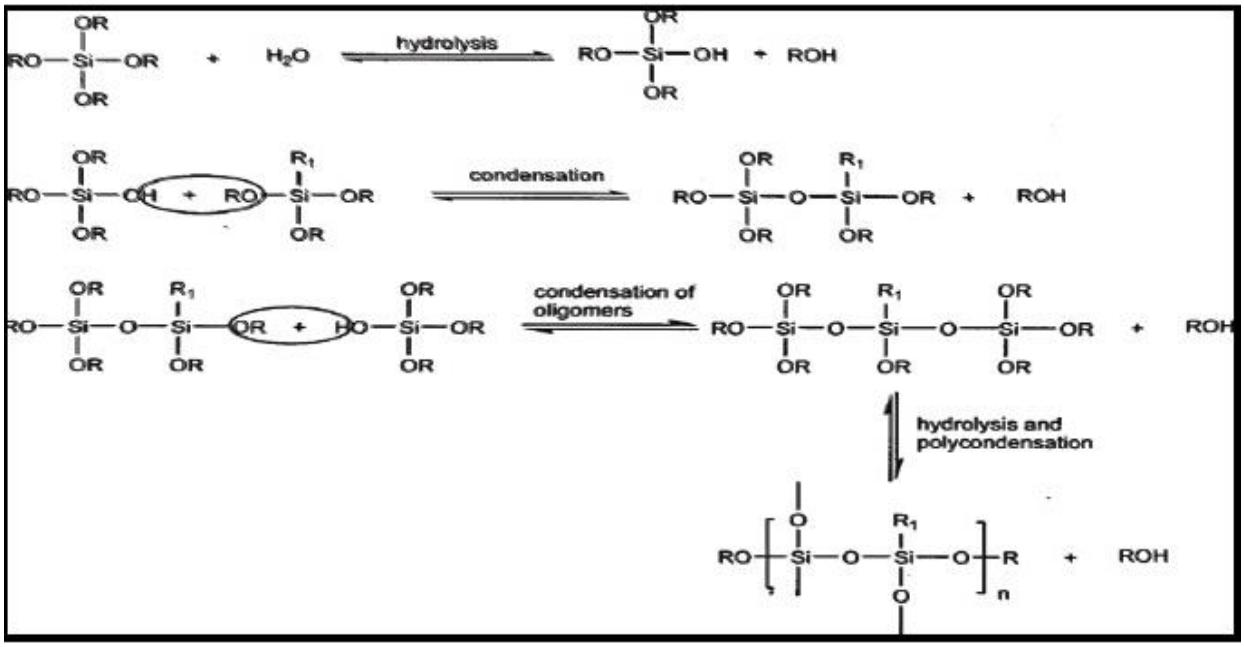

Figure (1.5): (Sol-gel) Reactions of formation of inorganic polymers[50] **.**

Monolithic Silica Columns have the following drawbacks [51][52] :

1- The column is highly permeable in a monolithic silica column with high porosity, yet the through-pore size/skeleton ratio is low.

2- Because there is less silica in a column than in a particle-packed column, the retention duration is less.

3- The k values (column permeability) are smaller than the particle-packed columns by 2–5 times and depend on the total porousness. A capillary column's k value is 90–95 percent, while a conventional-sized column's k value is 80–85 percent.

4- The phase ratio does not indicate that the sample loading capacity is as low as it appears. The separation conditions affect the loading capacity, and the mobile phase plays an integral part in this.

5- Because of the high injection volume, a 2D-HPLC column with low retention has a clear drawback: the need for exceptionally retentive columns to preserve the column efficiency.

A short-range for size exclusion mode elution, labour-intensive preparation of individual columns with the potential for repeatability issues, and limited availability are all caused by a minor internal porosity.

6- Low pH range (2-8).

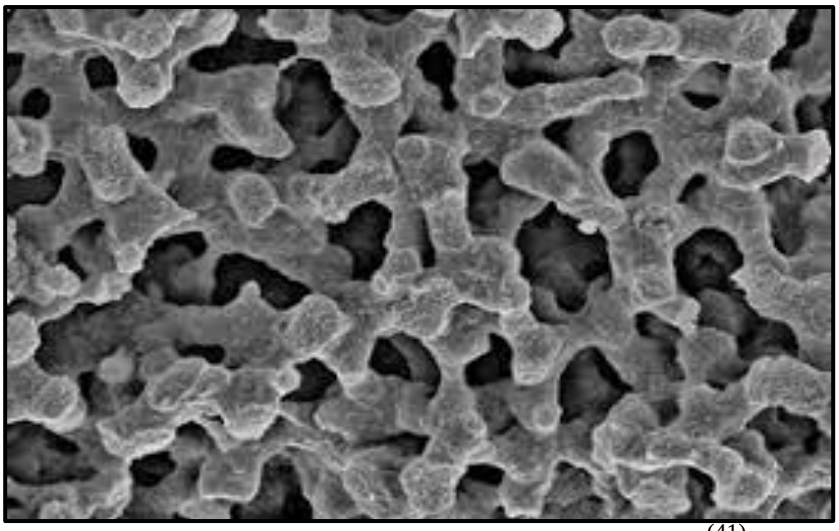

Figure (1.6): Inorganic-based monoliths[41] .

1.3.3 Hybrid Organic-Inorganic Monolith

In this monolith type, two or more components are mixed at the molecular or nanoscale level, offering notable benefits such as excellent selectivity, large surface area, thermal stability, excellent mechanical strength, long life, flexibility and excellent biocompatibility[53] when organic functional groups are evenly distributed throughout the inorganic matrix structure, excellent performance results[54] .

Different monomers can be used to polymerize inside sealed columns, so the monoliths have integrated structures like greater flexibility and higher external porosity compared with particulate-based columns[25]. Hybrid polymer-based monoliths are the first type of hybrid organic-inorganic monolith. The atom transfer radical polymerization (ATRP) has been used to construct a revolutionary hybrid polymer-based monolith for HPLC. Relying on vinyl ester resin as a monomer and $NaHSO_3$ as an initiator to regulate the free radical activity and control the molecular mass during the polymerization process. Monoliths

based on hybrid polymer have been used in a variety of applications, including separation, catalysis, and sensors[55,56].

When organic solvents are used, the monoliths might swell, resulting in mechanical instability [57] . To create a network combination copolymer, a sol-gel technique using organic and inorganic polymers yields a monolith formed from a silica precursor that contains organic moieties [58,59] . Hybrid monoliths have numerous uses, including optics[60] , electronics[61] , and biology([62] . Monoliths based on siloxane–silica nanocomposites have been studied by Noble and colleagues it was prepared using the1,3,5,7-tetramethyltetrakis (ethyltriethoxysilane)–cyclotetrasiloxane and TEOS using the sol-gel procedure, with cetyltrimethylammonium bromide as a cationic surfactant, the produced monolith had well-defined porosity[63] . For organic dyes and rare earth ions, as well as optical devices, a poly(methyl methacrylate) (PMMA)/SiO_2 hybrid monolith was created utilizing the sol-gel process based on (TEOS) [64] . Although silica-based monolithic materials have some advantages, such as superior mechanical stability and organic solvent resistance, some disadvantages, such as a narrow pH range (2–8), have been published to examine this type of monolith in various sectors of research. As a result, the preparation process is tough to monitor[65] .

1.4 Chromatography

Analytes can be separated and identified using chromatography, which is based on the fact that distinct components in a mixture tend to adsorb onto a surface or dissolve in a solvent[66] . Using essential liquid-solid chromatography, the Russian botanist Tswett was the first to recognize chromatography as an effective separation method[67] .For this type of separation (colour writing), the term chromatography was coined because of the colour patterns formed on the bed of adsorbents, but the current approach has nothing to do with colours.

In addition to the many different types of chromatography currently used, such as gas, thin-layer, paper, and liquid chromatography, all chromatographic methods require the use of a stationary phase and a mobile phase. These methods depend on the type of sample tested using the partition, ion exchange, molecular exclusion, and adsorption phenomena[68] .

The chromatographic techniques are usually named according to the physical state of the mobile phase (Figure1.7), classified as gas, liquid and supercritical fluid chromatography[1].

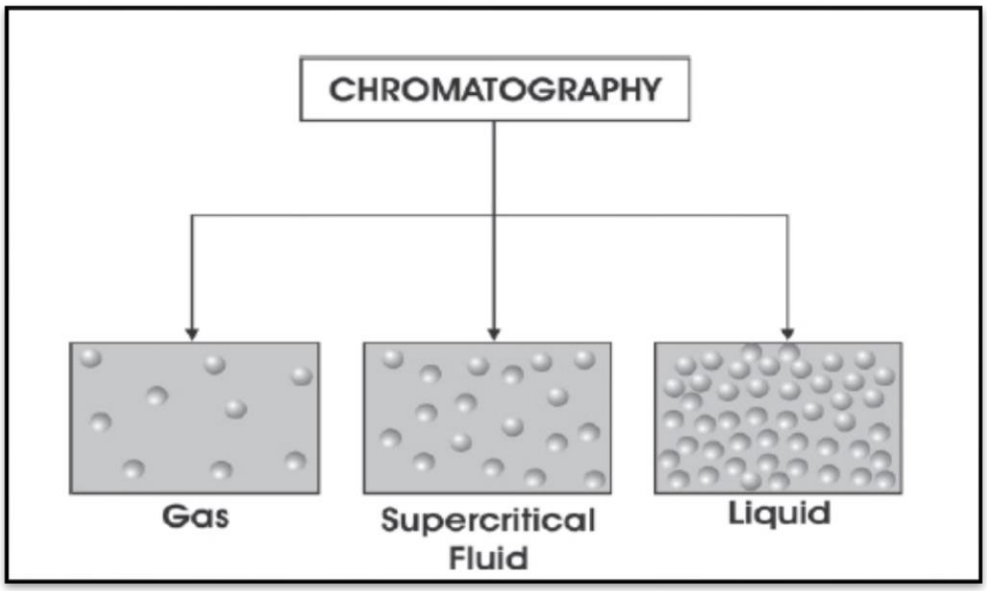

Figure(1.7): Classification of the chromatographic techniques according to the physical state of the mobile phase[1].

The essential components can be divided for the chromatographic system as follows[69]:

1-Stationary phase; this stage consists of a solid phase or layer of liquid adsorbed on the surface of a solid.

2- Mobile phase; this phase is always in the liquid state or gaseous component

3-Separated molecules; include many materials to be separated, such as ions, proteins, and nucleic acids.

1.5 High-pressure liquid chromatography (HPLC) technique

Any chromatographic technique that uses a liquid mobile phase, such as liquid chromatography, can be called "liquid chromatography." Sample separation is possible under the right conditions[68]. A liquid chromatographic technique known as High-performance liquid chromatography (HPLC) can be used to describe the method that uses a mechanical pump to pump a liquid mobile phase through a stationary phase column[68].

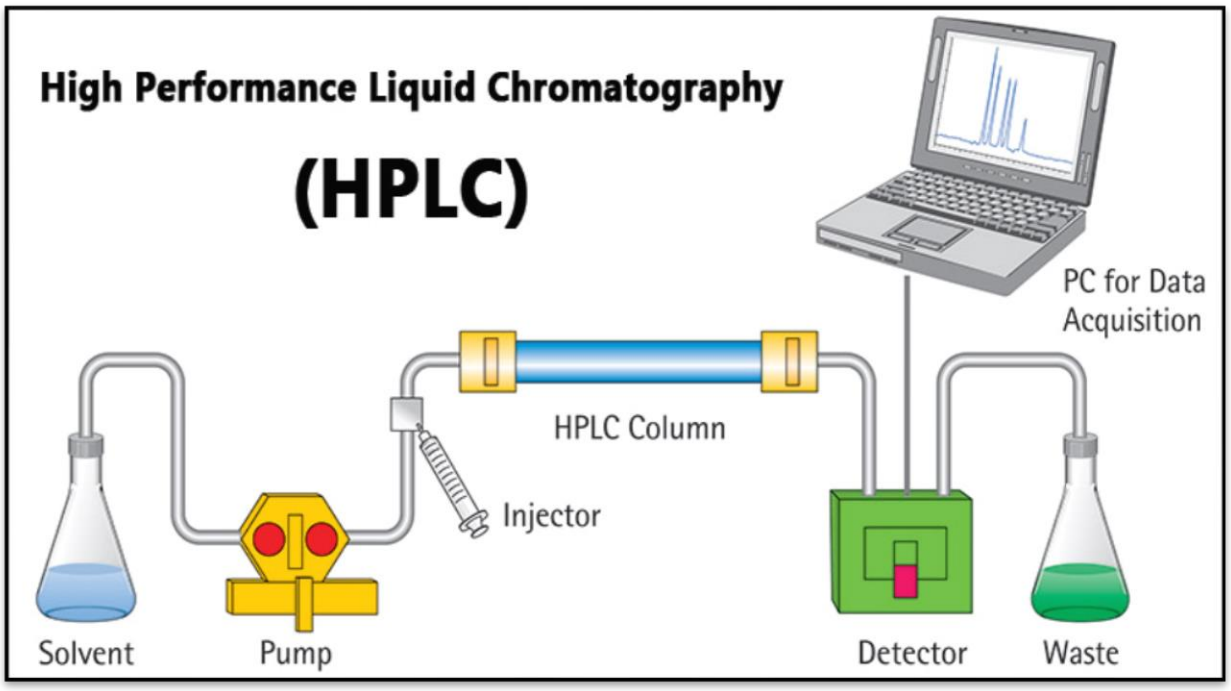

Figure (1.8): The HPLC system diagram.

Using HPLC's stationary phase column, which is typically packed with alkyl silica bonded, samples are injected into the injector and pumped through to the detector to determine the retention times of each analyte in the sample. However, retention times for each analyte can vary depending on the specific chemical and physical interactions between the analyte and the detector[70] . As a result of the composition of the mobile phase and stationary phase, the retention time for a particular analyte that elutes from the column toward the detector will be affected[71].

Hydrated methanol and acetonitrile are the most prevalent organic solvents in HPLC reservoirs. When the mobile phase composition is varied during the analysis, gradient

analysis can separate the analyte of interest as a function of the analyte's affinity to the mobile phase[72].

1.6 High-pressure liquid chromatography modes

There are several uses for high-pressure liquid chromatography (HPLC), including purification and chemical separations, as well as identification in biochemistry and analytical chemistry for clinical and pharmaceutical usage, environmental testing, forensics and food analysis[72][73] . Several modes can be used for chromatographic analysis, including normal phase, reversed, ion exchange, and size exclusion[74] .

1.6.1 Normal phase liquid chromatography (NPLC)

In normal-phase liquid chromatography, the analytes are extracted from the stationary phase using a nonpolar or moderately polar solvent, such as hexane, while the mobile phase is nonpolar or moderately polar, such as acetonitrile for the elution step[75]. Because less polar molecules move quicker and are detected first in the NPLC columns, the less polar molecules are found first, followed by the more polar ones[76].

Adsorption or partitioning is the most plausible mechanism for separation in this mode, and two models have been developed to explain how adsorption works[76].

The competition model assumes that the stationary phase is coated with mobile phase molecules; adsorption occurs because the solute and mobile phase molecules compete on adsorption sites[77] .

To begin with, there is the solvent interaction model, which states that solvent molecules form a bilayer around stationary phase particles; this bilayer is dependent on solvent concentration, and as a result, retention is due to solute molecule interactions with mobile phase adsorbed molecules in the second laye[76,77] . It takes longer for the analyte to move

through the polar stationary phase because the adsorption intensity increases with increasing polarity[78].

1.6.2 Reversed-phase liquid chromatography (RPLC)

Nowadays, HPLC separations use reversed phase mode for more than 65 percent (and maybe 90 percent) of all HPLC separations because of its adaptability, simplicity, and ability to handle molecules with a wide range of molecular masses and polarity[79] . RPLC typically uses polar solvents like acetonitrile, water, and methanol as mobile phases, whereas stationary phases like (C8) n-Octyl or (C18) n-Octadecyl hydrocarbon chains are used as stationary phases[72] . Because the functional group in the analyte is chemically bound to the stationary phase group, such as silica, reversed-phase chromatography can also be referred to as bonded-phase chromatography in the literature[79] . Due to hydrophobic interactions between the mobile phase and analyte molecules, RPLC's separation method is based on two key concepts: solvophobicity and partitioning. Solvophobicity states that the stationary phase acts more like a solid than a liquid [80][81].The analyte molecules are maintained because of the solvophobic interactions with the mobile phase rather than the stationary phase, which reduces the surface area of the analyte exposed to the mobile phase[82] . The partitioning principle proposed that the analyte molecules are entirely immersed in the stationary phase chains and are not adsorbed on the stationary phase's surface; hence these molecules are partitioned between the stationary and mobile phases[83,84] . The chain length of the stationary phase has a crucial impact on the retention process; thus, when the bonded material chain length is extended, the mechanism will approach the partitioning mechanism, while it will be comparable to the adsorption mechanism with less chain lengths[85,86]. It is widely employed in purifying and biological separation, but reversed phase chromatography can

be utilized to separate hydrophobic compounds with remarkable recovery and resolution[86].

1.6.3 Ion-Exchange chromatography (IEC)

Ion-exchange chromatography is an essential chromatographic method in which different ionic substances can be separated and identified[87]. There are two stationary phase exchangers: anion-exchangers (negative-charged) and cationic-exchangers (positive-charged). The ionic interactions between these two types of stationary phase exchangers determine the separation process[88] . However, the application of this chromatography was explicitly for separating differently charged molecules[88,89] . In addition, it was utilized to purify proteins, peptides, enzymes, amino acids, nucleic acids, antibodies, chemical compounds, and simpler carbohydrates[90–94]. Functionalized silica and synthetic polymeric resins such as methacrylic acid-divinylbenzene or styrene-divinylbenzene copolymers and various inorganic materials are used in the stationary phase of ion-exchange chromatography[94] . It is possible to use a stationary phase made of functionalized silica. However, it is limited to pH values of 8 and 2, which can lead to the silica's instability when used as a stationary phase[93] . This drawback led to synthetic polymers that can be used over a much broader pH range (pH 12 or above) but are also susceptible to swelling [94]. As part of the ion-exchange separation process, the mobile phase contains an organic solvent(85) .which is used in conjunction with an aqueous solution of salt or salt mixtures (which could include buffers), Because the stationary phase contains ionizable functional groups and has the opposite charge to that of the analyte and the mobile phase is an aqueous buffer system, the ion-exchange mechanism is based on the analyte ions being distributed in equilibrium between the stationary and mobile phases. Depending on the counter ions, this equilibrium can take one of two forms, cation or anion exchange mechanisms [89].

1.6.4 Hydrophilic interaction liquid chromatography

Hydrophilic interaction is described as "partitioning between a water-enriched mobile phase and a layer of the mobile phase that is partially immobilized on the stationary phase"[95]. However, increasing the polarity of the mobile phase decreases the retention of analyte solutes, while increasing the analyte's polarity increases it [96] . Alpert first used the term "hydrophilic interaction chromatography" (HILIC) to characterize how water-based solvents can be used to separate highly polar or highly charged solutes [97]. However, prior to Alpert's work, it was widely accepted that these separations were based on the partitioning of solutes between a bulk mobile phase and a layer richer in water partially immobilized on stationary phase surface[98] . He realized that ionic effects might be superimposed depending on the solute, stationary, and mobile phase. With its multiple applications for pharmaceutical, biological and clinical analysis of solute, HILIC has seen an upswing of interest since Irgum published a seminal overview of the approach in 2006, partly due to its suitability[99] . While reversed-phase (RP) analysis can retain many solutes, polar and ionic solutes tend to elute too readily in HILIC. Additionally, the HILIC selectivity is typically somewhat different from what can be obtained with the RP-LC method. In HILIC separations, silica and silica-based compounds are still the most often utilized components. Nevertheless, some novel substrates have been offered for HILIC columns as appropriate materials [100] .As shown in figure(1.9)

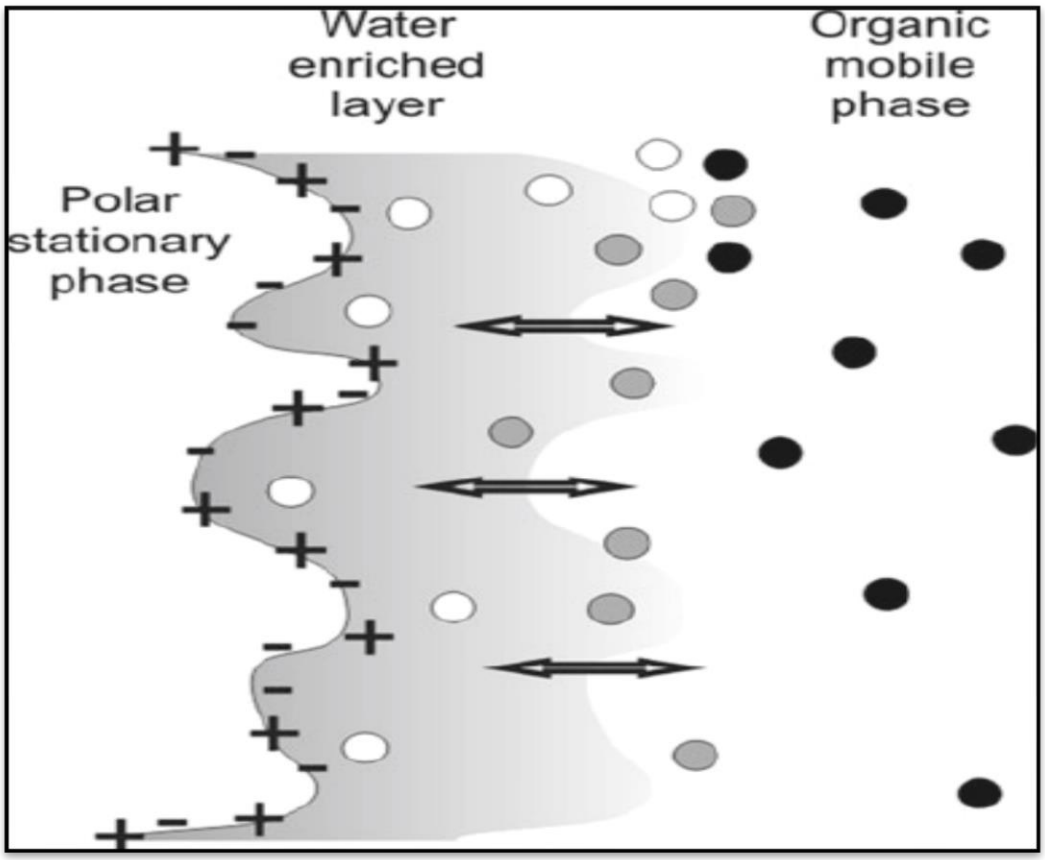

Figure (1.9): Hydrophilic interaction liquid chromatography.

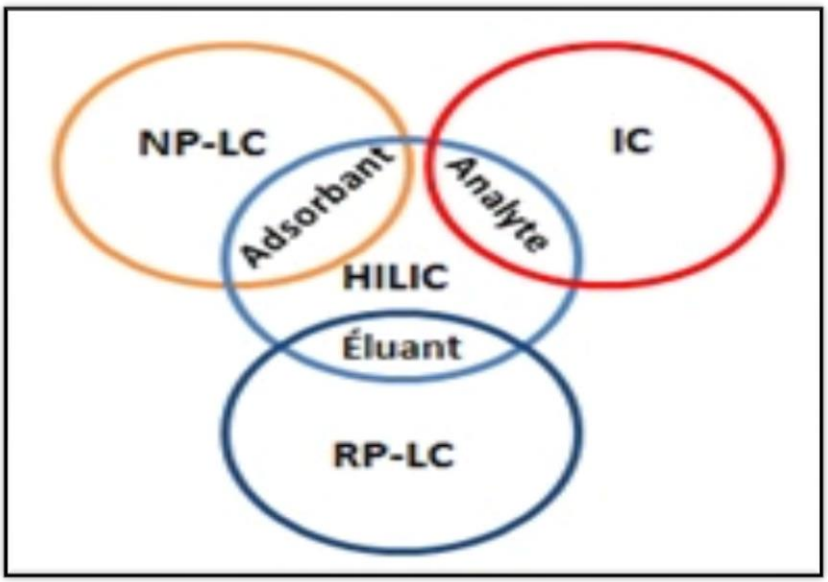

Figure(1.10): HILIC combines the characteristics of the three primary LC methods (reversed-phase LC, normal-phase LC, and ion–exchange).

1.7 Theories of chromatography[101,102]

The plate theory, developed by Martin and Synge, and the rate theory, proposed by van Deemter et al., are the two chromatographic theories that have been used to explain band broadening and column performance in modern chromatography.

1.7.1 The plate theory[68,103]

Plate theory states that chromatographic columns comprise several thin sections (plates), each allowing the solute to equilibrium between the stationary and mobile phases. This equilibration process is called plate theory. A column's more theoretical plates (N) has, the more efficient. As a result, it fails to consider the impacts of bandwidth widening and other chromatographic variables such as flow rate on the column or performance particle size and elution viscosity. The equation (1.1)can determine the number of theoretical plates (N).

$$N = L/H \qquad (1.1)$$

Where **H** is the high equivalent to a theoretical plate (HETP)

L is the length of the column (millimetres)

N is the number of theoretical plates

Suppose the mobile phase flow rate is low and the oven temperature is significant. In that case, the small particle size of the stationary phase, less viscous mobile phases, and small molecule size of the solute are all used, and the (HETP) value can be reduced while increasing the column's (N) value. Depending on the peak width, multiple approaches can be used to determine the (N) value, as illustrated in equations (1.2) and (1.3), respectively, for the peak half-height method and the Tangent method.

$$N = 5.54 \left(t_R / w_{50}\right)^2 \qquad (1.2)$$

$$N = 16 \left(t_R / w_T\right)^2 \qquad (1.3)$$

Where
t_R is the retention time of the solute
w_{50} is the half peak width
w_T is the total peak width.

Due to its simplicity, the Tangent method is considered the more popular method for calculating (N) value. The t_R, $W_{0.5}$, and W_T are shown in Figure (1.11)

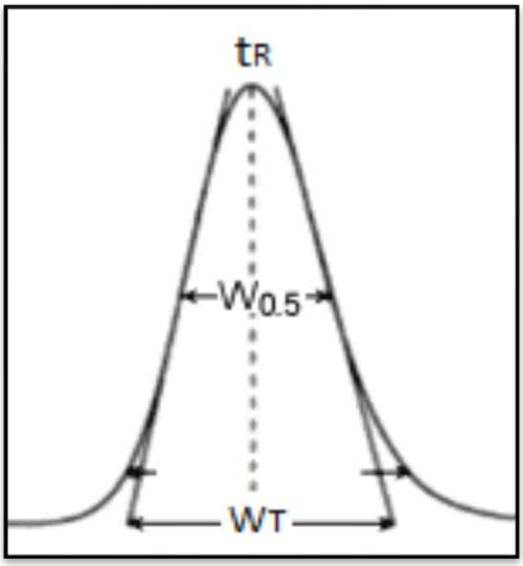

Figure(1.11): The peak half-height and the Tangent methods used to calculate the theoretical plate number (N).

1.7.2 The rate theory[68,102,104]

To explain the column efficiency and band broadening, van Deemter et al. 1956 developed this theory to describe diffusional forces that lead to the band broadening to avoid the concept of an immediate equilibrium inherent in the plate theory (1.4).

$$H = A + B/\mu + C\,\mu \qquad (1.4)$$

Where
H is the efficiency of the column

μ is the average linear velocity of the mobile phase

A is the eddy diffusion

B is longitudinal diffusion

C is the resistance to mass transfer, and the hypothetical van Deemter plot is shown in Figure (1.12).

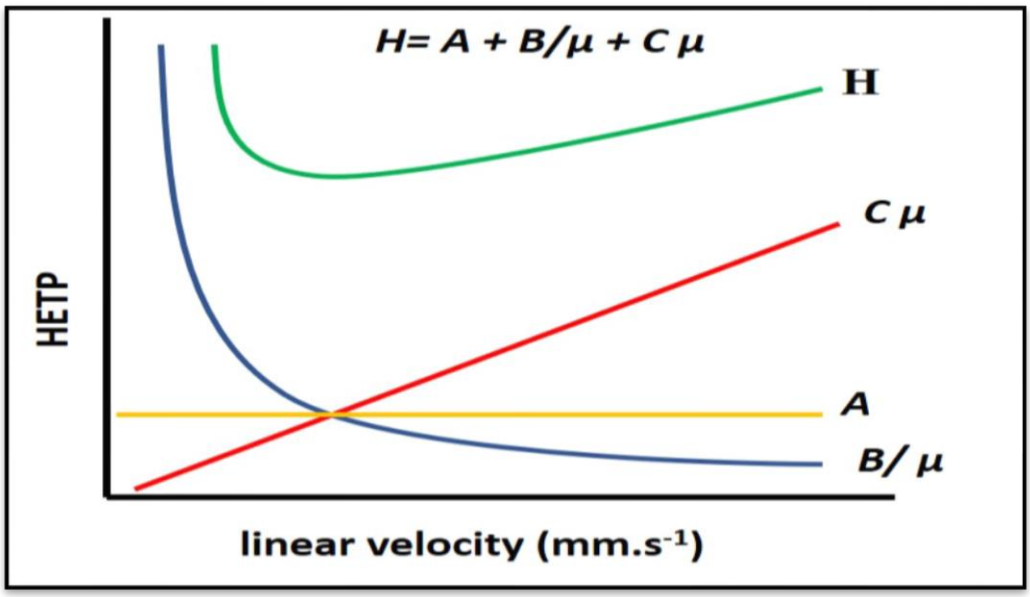

Figure (1.12): The hypothetical van Deemter plot.

The van Deemter plot shows that diffusion influences the efficiency at flow rates below the optimum (B). In contrast, the mass transfer factor (C) becomes more significant at higher flow rates. Diffusive and convective transport are the two methods by which the solute will move through the column throughout its passage. A fourth term has been added to the van Deemter equation to describe column efficiency, as illustrated in equation (Huber) (1.5)

$$H = A + B/\mu + Cs\,\mu + Cm\,\mu \qquad (1.5)$$

Cs and Cm contribute to zone broadening from resistance to mass transfer in the stationary and mobile phases. According to van Deemter's equation, the column (H) efficiency is Van Deemter's Equation states that band broadening, which affects the column's efficiency, should be kept to a minimum. Therefore, it is necessary to determine the experimental conditions to limit the zone dispersion.

1-Eddy diffusion can be minimized using well-packed columns, small stationary phase particles, and a tight particle size distribution.

2- High mobile phase flow rates, short system tubing, suitable fittings, ferrules, and nuts are used to reduce longitudinal diffusion.

3-Utilizing the stationary phase with small particles to minimize mass transfer, lowering mobile phase flow rates, and raising the column temperature all work together to achieve this goal.

1.8 Monomers

1.8.1 (2,3epoxypropyl methacrylate) Monomer

The 2,3 epoxypropyl methacrylate monomer (GMA) is an ester of methacrylic acid and glycidol. It is prevalent because it contains an epoxy group that allows many reactions to form different functional groups[105]. Methacrylate has moderate polarity because carbonyl and ester groups are present. It is commonly used in reversed-phase chromatography due to the mixing of polar and nonpolar groups and ease of preparation[106].

A nonlinear optical material, leather adhesives, resins for ion exchange chromatography, dental mixes, surface coatings, and surface modifiers were some of the industrial applications of GMA[107,108].

Other types of methacrylate monomers include methyl methacrylate, ethyl methacrylate[109], butyl methacrylate[110,111],octadecyl methacrylate[112], Methacrylic acid [113], and hydroxyethyl acrylates[114] .

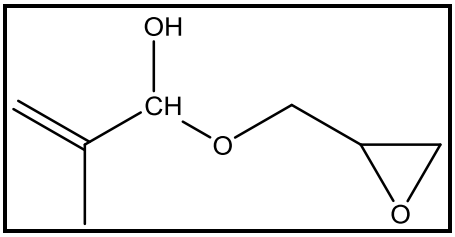

Figure(1.13): Chemical Structures of (2,3epoxypropyl methacrylate) Monomer.

Different methods were used to make GMA copolymers, but they all rely on initiating the polymerization reaction with free radicals, mainly organic peroxides or azo-catalysts[(115)]. The oxirane function does not participate in the radical polymerization of glycidyl methacrylate, as has been demonstrated by researchers[(116)].

It is possible to perform a wide range of chemical transformations and alter the functional sites on the polymer surface after the copolymer has been formed, as shown in Figure. (1.14)[(117)].

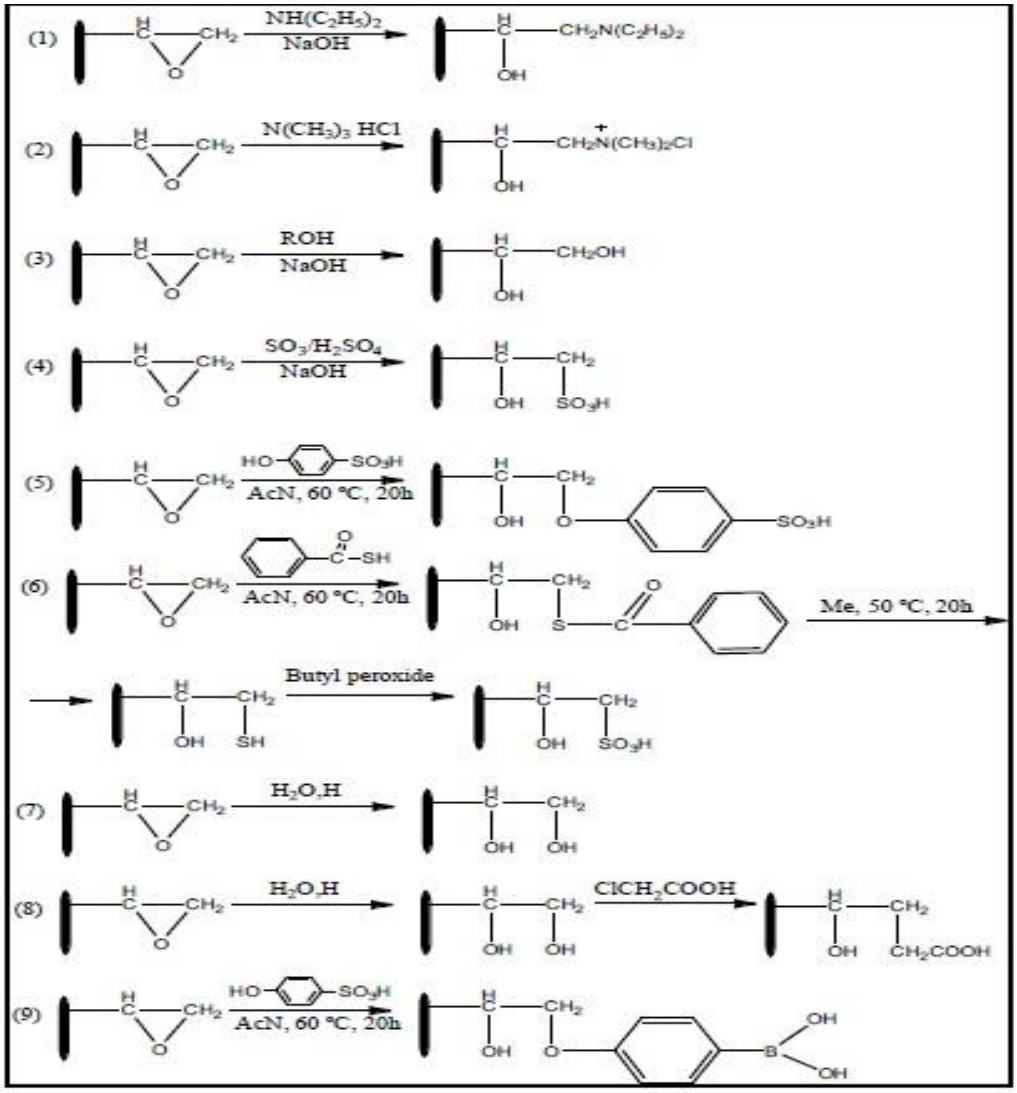

Figure (1.14): epoxy group reactions (1,2) amination, (3,4) Alkylation, (5,6) sulfonation, (7) hydrolysis, (8) carboxymethylation, (9) modification with p-hydroxy phenylboronic acid[117].

1.8.2 Acrylamide (CH_2=CH-$CONH_2$) monomer

Hydration of acrylonitrile produces acrylamide (2-propenamide) (CH2CH=CONH2) it is a colourless, odourless, crystalline solid with a melting point of 84.5 °C. In addition, it is highly mobile in soil and groundwater and biodegradable[118,119] . Acrylamide is soluble in several common organic solvents, including water, acetone, chloroform, diethyl ether, ethanol, ethyl acetate, and methanol[120].

It is used worldwide to synthesize polyacrylamide as a cement binder and in synthesising polymers and gels. Polyacrylamide polymers and copolymers are used in the paper and textile industries as flocculants in wastewater treatment, soil conditioners, ore processing, and cosmetics. It is also widely used in scientific research to selectively modify SH groups in structural and functional proteins and as a quencher of tryptophan fluorescence in studies designed to elucidate the structure and function of proteins. In addition, it is to separate proteins and other compounds by electrophoresis. Other sources of acrylamide include acrylamide entrapped in polyacrylamide, depolymerized polyacrylamide in the soil and food packaging[121,122] .

Synonyms: Acrylic acid amide; acrylic amide; ethylene carboxamide ,propenamide;propenoic acid amide; vinyl amide, Relative molecular mass : 71.08 (121,122)

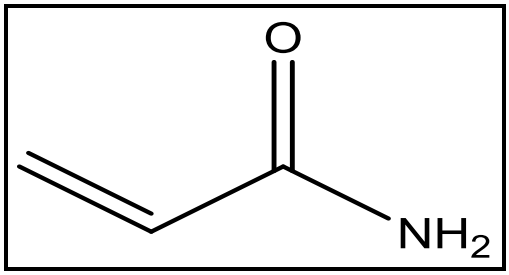

Figure(1.15): Structural Formula of Acryle amide

1.8.3 Cross-linker ethylene glycol di methacrylate (EDMA)

One of the most popular cross-linkers employed in the production of rigid macro porosity methacrylate monolithic polymers is EDMA[123] . Diethylene glycol chains play a crucial role in the cross-linking process because they allow for more cross-linking flexibility, which reduces undesirable effects like material failure due to internal tension during the polymerization process or shock from osmotic pressure [117] . The cross-linker to monomer should have a consistent ratio since any variation in this ratio will impact the monolith's porosity characteristics and chemical composition. A monolith with a wide surface area, such as hundreds of square meters, may benefit from a monolith with a higher percentage

of cross-linker to reduce the average pore size. High-surface-area monoliths, on the other hand, will have reduced solvent permeability, higher backpressure, and reduced suitability for HPLC separation; therefore, the cross-linker to monomer ratio should remain constant in these materials[14].

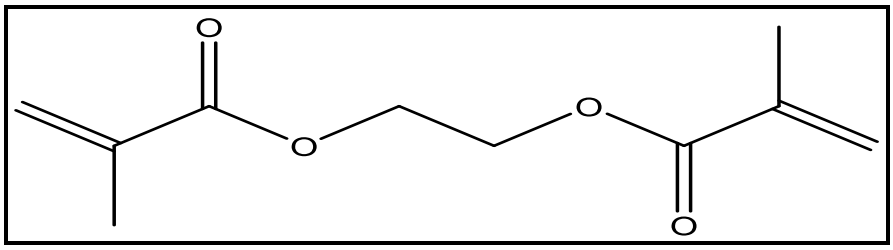

Figure(1.16): Structural Formula of Ethylene glycol di methacrylate (EDMA).

1.9 pharmaceutical compounds

1.9.1 Propranolol hydrochloride

It is s crystalline powder that ranges in colour from off-white to white and is stored at 25°C; however, variations from 15°C and 30°C [124].

Propranolol hydrochloride is a non-selective beta-blocker or inhibitor, inhibiting beta-1 and beta-2 receptors, decreasing heart rate, myocardial contractility, blood pressure, and oxygen required for the heart muscle[124] .

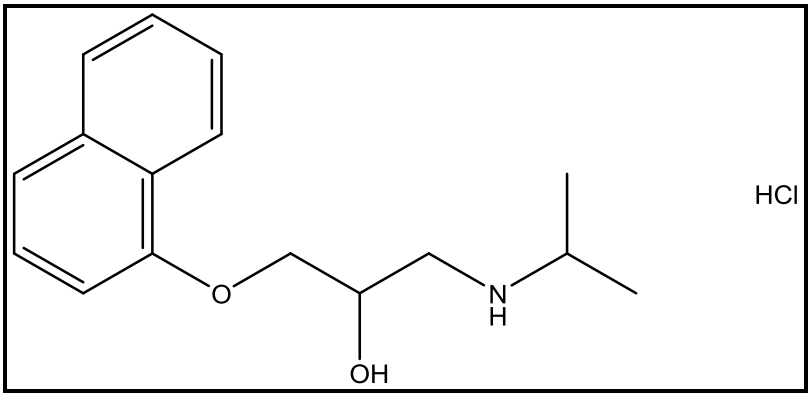

Figure(1.17): Structural Formula of Propranolol hydrochloride

1.9.2 Tri fluoperazinedi hydrochloride

The phenothiazine family includes a total of 64 members. They are made up of a variety of rings. These rings are composed of sulfur and nitrogen atoms, respectively. Trifluoperazine Hydrochloride (TRF) was one of the most important of these family compounds[(125)]. TRF has a molecular weight of 407.496 g/mole and has the following structure ($C_{21}H_{24}$ F $_3$N $_3$S.2HCl) as indicated in Figure (1.19). numerous pharmaceutical preparation names, including Iralzin, Terfluzine, Stellasil, and Stellamide, are used to promote it commercially[(126)] . When exposed to light or air, it disintegrates into white crystalline powder with a melting point of 196 ^{0}C and significant solubility in water and ethanol[(127)].

Dopamine receptors are the primary targets. Schizophrenia is the principal use of trifluoperazine. Generalized nonpsychotic anxiety disorder can be effectively treated with trifluoperazine HCl when used for a short period[(128)].

The hydrochloride salt of trifluoperazine in addition to having sulfur and nitrogen atoms in its rings is one of the phenothiazines derivatives. It operates primarily on dopamine receptors, reducing or preventing hallucinations and delusions caused by increased dopamine[(128)].

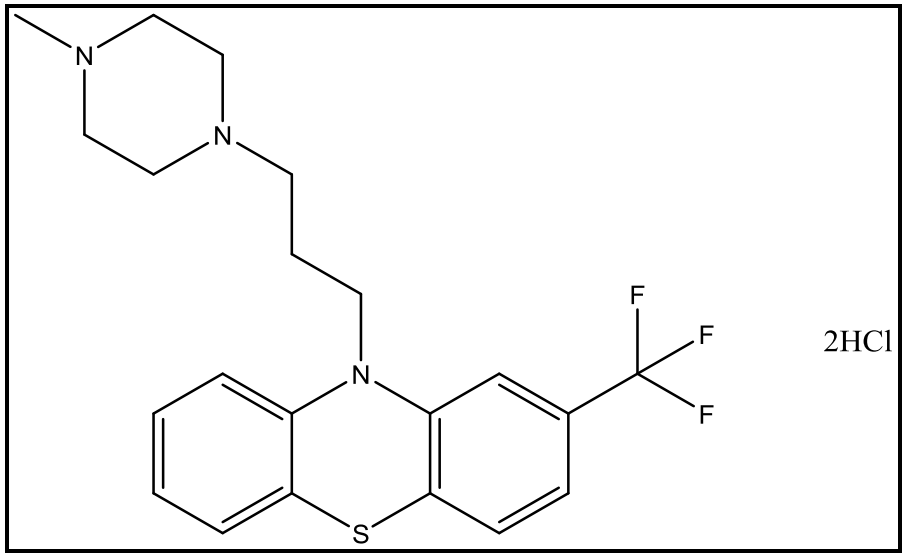

Figure(1.18): Structural Formula of Trifluoperazine dihydrochloride.

1.10 Literature Review

For the importance of pharmaceutical compounds in the treatment of many human diseases, several attempts have been made to invent methods for separating and estimating pharmaceutical compounds at the lowest cost, more accuracy and highest concentration to reach the best possible result, and this distinguishes our study from previous studies in addition to the low cost of preparing the chromatographic separation column compared to the commercially packaged column are Expensive.

NO.	Stationary phase	Technique Used	Samples	Comment	Ref.
1	HILIC/RP GMA-co-SMA-co-EDMA	HPLC	caffeine, paracetamol, and ibuprofen.	(LOD)0.1-1.0 µg/mL	(129)
2	SCX/RP GMA-co-SMA-co-EDMA	HPLC	Pharmaceutical compounds such as phenacetin and codeine.	(LOD)1.5–6.0 µg/mL	(130)
3	HI /SCX and RP/SCX GMA-co-3SPMA-co-EDMA	CEC	Narcotic pharmaceuticas		(131)
4	Iso-butyl methyl ketone (IBMK)	AAS	Propranolol Hydrochloride		(132)
5	Chromolith Flash RP-18 column 25×4.6 mm	SIC	Chloramphenicol and betamethasone	(LOD)0.5–1.0 mg/mL	(133)
6	monolithic silica column, Chromolith Performance RP-18e	HPLC	tadalafil	(LOD)100 ng mL^{-1}	(134)
7	A Chromolithm Flash RP-18e	SIC	paracetamol, caffeine, and acetylsalicylic acid	(LOD)0.022–0.060 µg mL^{-1}	(135)

8	GMA-CO-EDMA	HPLC	paracetamol and Chlorzoxazone		(136)
9	GMA-co-SPMA-co-EDMA	Pressurized CEC	Narcotine, papaverine, thebaine (kind of narcotic pharmaceuticals), codeine, and morphine	(LOD)1.5–6.0 μg/mL	(137)
10	HI /SCX and RP/SCX GMA-co-3SPMA-co-EDMA.	CEC	Basic compounds and neutral polar analytes, such as narcotic pharmaceuticals		(131)
11	GMA-CO-EDMA or BUMA-CO-EDMA-CO-SPMA	nano-liquid chromatographic	Racemic pharmaceuticals		(138)
12	GMA-CO-DVB	HPLC-UV-MS and μ-HPLC	salicin, salicylic acid, tenoxicam, ketorolac, piroxicam, tolmetin, naproxen, flurbiprofen, diclofenac and ibuprofen	r^2<0.9800, limits of detection in the low nanogram range	(139)
13	potassium permanganate in acidic medium	automated multicommutated flow system	propranolol hydrochloride	(LOD) 0.7μmol $^{-1}$	(140)
14	Supelco Discovery_ C18	HPLC	Propranolol Hydrochloride and Sodium Benzoate		(141)
15	a MicroPak NH -10 column	HPLC	Trifluoperazine hydrochloride		(142)
16	cellulose *tris*(3,5 dimethylphenylcarbamate)	HPLC	Propranolol Hydrochloride		(143)
17	Ion-exchange GMA-co-EDMA, the GMA was modified using	HPLC	Proteins		(144)

	diethylamine.				
18	Ion-exchange GMA-co-EDMA, GMA was grafted with poly(2-acrylamido-2-methyl-1-propanesulfonic acid.	HPLC	Proteins		(145)
19	GMA-co-TPGDA-co-EDMA.	HPLC	Benzene derivatives	High column efficiencies for benzene derivatives with 70,000–102,000 theoretical plates/m	(146)
20	RP, HI, and CX GMA-co-4VPBA-co-EDMA.	Nano LC separation	Alkaloids, and proteins	linear velocity of 0.265 mm/s	(147)
21	WAX GMA-co-EDMA, GMA was modifiedwith diethyl amine.	HPLC	Ligodeoxythymidilic and DNA		(148)
22	Mixed-mode GMA-co-EDMA, GMA was functionalized with thiols and coated with gold nanoparticles.	HPLC	proteins		(149)
23	WAX GMA-co-EDMA, GMA was modified with polyethyleneimine.	HPLC	proteins	velocity of 1445 cm/h	(150)
24	WCX GMA-co-EDMA, GMA was modified with ethylene diamine followed by chloro acetic acid.	HPLC	proteins		(151)
25	GMA-co-EDMA modified with diethyl amino	HPLC	Model protein mixture (ovalbumin,cytochrome C, and lysozyme)		(152)

	hydroxypropyl.				
26	GMA-co-EDMA-co-A.Am	SCX	Cu^{2+}	(LOD)0.129 $mg.L^{-1}$	(91)
27	**GMA-co-EDMA-co-A.Am**	**HPLC**	**Propranolol hydrochloride Trifluoperazine dihydrochloride**	**(LOD)0.007 µg/mL**	

Table(1.1): Summaries of previous studie.

1.11 Aim of the study

1-Preparing a monolithic chromatographic column based on some polymeric compounds that can be prepared efficiently and economically.

2-Studying the factors affecting the preparation of the column to find the best surface area and suitable pore size.

3- Identification of the prepared monolithic column using different techniques.

4-Optimizing the column features such as porosity, permeability, and swelling percentage.

5-Applying the prepared monolithic column in the determination and separation of pharmaceutical compounds (Propranolol hydrochloride ,Trifluoperazine dihydrochloride).

2. Experimental part.

2.1 Chemicals.

There are several chemicals used in this search, as shown in Table (2.1):-

Table(2.1): Chemicals used

No.	Chemical name	Chemical formula	Molecular weight g/mol	Purity %	The manufacturing company
1	Glycidyl methacrylate	$C_7H_{10}O_3$	142.15	98	Sigma-Aldrich, Poole, UK
2	Acrylamide	$CH_2CHCONH_2$	71.08	98	Sigma-Aldrich, Poole, UK
3	Ethylene dimethacrylate	$C_{10}H_{14}O_4$	198.26	98	Sigma-Aldrich, Poole, UK
4	3- (trimethoxysilyl) propylmethacrylate.	$H_2C=C(CH_3)CO_2(CH_2)_3Si(OCH_3)_3$	248.35	98	Sigma-Aldrich, Poole, UK
5	2, 2-dimethoxy-2-phenyl acetophenone	$C_6H5COC(OCH_3)_2C_6H_5$	256.30	98	Sigma-Aldrich, Poole, UK
6	1-Propanol	C_3H_8O	60.1	97	G.C.C
7	2-Butanol	$CH_3CH_2CH(OH)CH_3$	74.12	97	G.C.C
8	Hydrochloric acid	HCl	36.46	Analar	G.C.C
9	Sodium hydroxide	NaOH	40.0	99	B.D.H.
10	Acetonitrile	C_2H_3N	41.05	99.85	Scharlau
11	Aceton	C_3H_6O	58.08	99.8	Sigma-Aldrich, Poole, UK
12	2-Propanol	C_3H_8O	60.1	99.7	Merck
13	Hexanol	$C_6H_{14}O$	102.17	99.85	MerckSchuchardt
14	Formic acid	HCO_2H	46.02	85	Thomas Baker
15	Ethanol	C_2H_5OH	46.07	99.8	G.C.C
16	Chloroform	$CHCl_3$	119.38	99	Scharlau

17	**Trifluoperazine dihydrochloride**	**$C_{21}H_{24}F_3N_3S.2HCl$**	**407.496**	**99.8**	**Samarra pharmaceutical company-Iraq**
18	**Propranolol hydrochloride**	**$C_{16}H_{21}NO_2.HCl$**	**295.80**	**99.8**	**Samarra pharmaceutical company-Iraq**
19	**Methanol**	**CH_3OH**	**32.04**	**96**	**G.C.C**

2.2 Instruments

There are several techniques and devices used in this research , as shown in Table (2.2):-

Table(2.2) : Used devices

No.	Device name	The manufacturing company
1	Electronic analytical balance with four decimal places	Denver Instrument Germany TP-214
2	heater	Heidolph RM Hei-standard .Germany
3	HPLC pump (Varian Prostar system)	kD Scientific Holliiston , MAU.S.A
4	Irradiation Cabinet(220V-50HZ)	Homemade
5	U.V.- "Visible spectrophotometer" (double-beam)	(Shimadzu)(UV-1700) .Japan
6	Sonicator	ultrasonic bath India
7	FT-IR 380 spectra	Shimadzu. Japan
8	_Syringee pump_	Bioanalytical System Inc., U.S.A.
9	stirrer V.W.R.	West Chester, PA, U.S.A.
10	"Field Emission Scanning Electron Microscopy" ((FESEM))	TESCAN, Model: Mira3, Czech Republic
11	" Brunauer-Emmett-Teller " ((BET))	BEL, Model: BELSORP MINI II, Japan
12	Proton nuclear magnetic resonance(^{1}HNMR)	Model: Innova 5 Concole with an Oxford 500 Magnet, Country: United States
13	pH-meter	W.T.W. Japan
14	Oven	Jlabtech, Korea
15	Nitrogen canister	Iraq

2.3 Preparation of (0.2) M of "hydrochloric acid."

This solution was prepared by taking 1.7 mL of concentrated hydrochloric acid (that percentage of purity 35% (w/w) and specific gravity 1.18 $g.mL^{-1}$) and added to a 100mL volumetric flask containing water and then completed the volume to the mark.

2.4 Preparation (0.2) M of "sodium hydroxide."

A solution of sodium hydroxide was prepared at a concentration of (0.2M) by weighing (0.8 g) of sodium hydroxide in a clean, dry volumetric flask, adding (50 ml) distilled water. When it dissolved, the volume was completed to 100 ml to the mark.

2.5 Preparation of standard solutions of two pharmaceutical compounds

2.5.1 Preparation of Propranolol hydrochloride solutions

This solution was prepared by taking (0.3 g) of Propranolol hydrochloride in a dry and clean beaker and adding (50) mL D.W, when dissolved done the solution was transferred to (100) mL volumetric flask, then completed the volume to the mark, the standard solution for the pharmaceutical compound Propranololhydrochloride was prepared with a concentration (30 $\mu g.mL^{-1}$) and several concentrations were prepared from the standard solution (0.1-20 $\mu g.mL^{-1}$).

2.5.2 Preparation of Trifluoperazine di hydrochloride solutions

This solution was prepared by taking (0.4 g) of Propranolol hydrochloride in a dry and clean beaker and adding (50) mL D.W. The solution was transferred to (100) mL volumetric flask, then completed the volume to the mark; the standard solution for the pharmaceutical compound Trifluoperazine di hydrochloride was prepared with a concentration (40 $\mu g.mL^{-1}$), and several concentrations were prepared from the standard solution (0.1-30 $\mu g.mL^{-1}$)

2.6 Silanization Step[153]

The inner surface of the tube (borosilicate tube) was washed with ethanol and water. The borosilicate tube was then activated by washing the inner surface of the tube by pumping in a NaOH solution (0.2 M) at a flow rate of 5.0 (µl min^{-1})for (1 hour) using a syringe pump. After that, HCl (0.2M) solution was used to wash the tube at (5.0 µL min^{-1}) for (1 hour) using a syringe pump, and then washed with water and ethanol. To convert the inner tube surface into (Si-OH) groups, the final step was to silanize the tube using "3-(trimethoxysilyl) propyl methacrylate (γ-MAPS)" 20% in ethanol at pH of 5.0 through pumping at(5.0 µL/min) for (1 hour). The tube is then dried with nitrogen gas;So, it is ready for in-situ polymerization ,As shown in fig.(2.1)

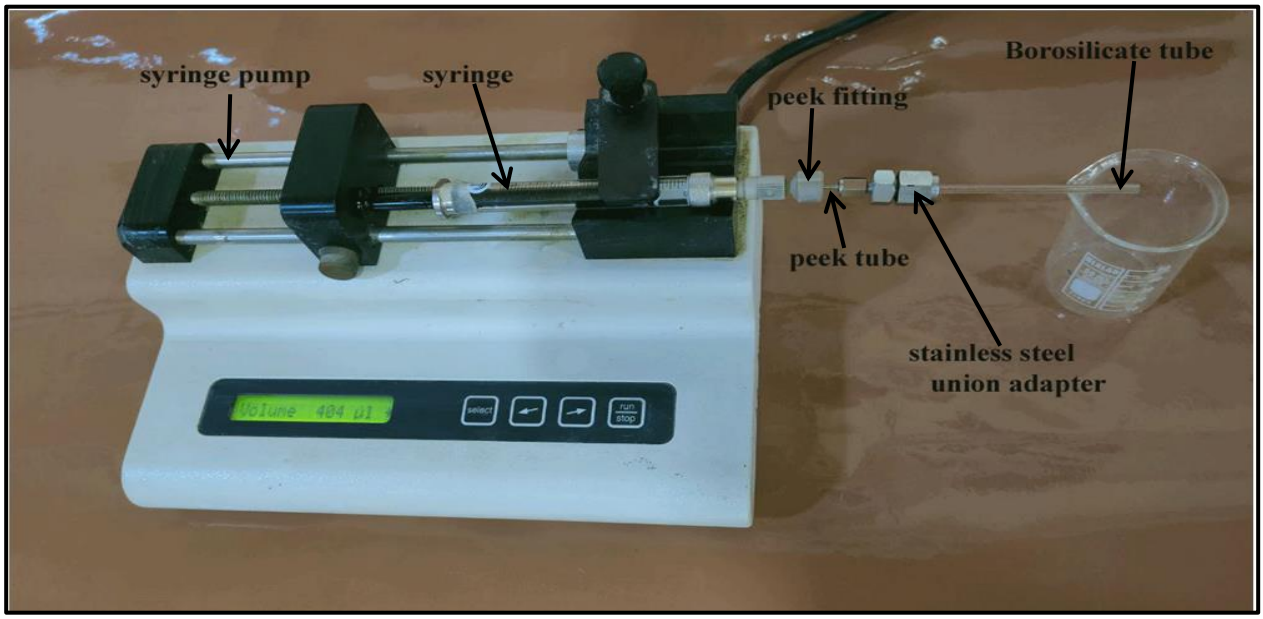

Figure (2.1) : photograph of a syringe pump.

2.7 Polymerization step

The "monolith" has been prepared inside a borosilicate tube from a mixture consisting of two monomers of 650µL (G.M.A.) with 0.282g(A.Am)&50µL ("Ethylene dimethacrylate") as cross-linker. (D.A.P.) with (1.0 Wt %) of the "monomers" were used as an abetter. "porogenic solvent" (750 µL1-propanol + 900 µL Hexanol) was used to melt"monomers" & cross-linker, In addition to the "initiator". The "polymerization" mixture was mixed well for (ten min) using a "magnetic stirrer". Ultra wave sonicator was used to sonicate the mixture for (10 min). Then oxygen was removed from the mixture by purging with nitrogen gas for (5 min). After that, the borosilicate tube was filled with the polymerization mixture using a glass syringe, then closed from both sides by a rubber stopper and exposed to U.V. light lamp for U.V. polymerization at (365 nm) for 3 min. After "monolith formation", the "column" was splashed with "ethanol" and "water" to eliminate any un-reacted component. The preparation method was based on with some modifications by Ueki et al[154] .

2.8 Investigation of optimum conditions of polymer

2.8.1 Investigation of the effect of irradiation time[155,156]

The effect of irradiation time was studied on polymer formation. The irradiation time range from (1-5) minutes.

2.8.2 Investigation of the distance between the irradiation source and the monolith column

The effect of the distance between the irradiation source and the monolith was studied to reach the appropriate dimension. This process was carried out by using a variable height stand.

2.8.3 Determination the degree of polymer swelling

Certain weights of the prepared polymer were taken. Then they were placed in (13) airtight glass cylinders, as different solvents were added as in Table (3.3), (3.4), and (3.5) for each cylinder separately and completely cover the monolith or polymer with the solvent by adding (3mL) of these solvents to know the degree of polymer swelling over time.

2.8.4 porosity calculation[157]

By using Fletcher *et al*. method, the overall porosity for the prepared monolith was calculated using the equation below :

$$\emptyset_t = (W_M - W_T) / dLR^2 \pi \qquad (2.1)$$

Whereas $\emptyset_t$: is the overall porosity,($W_{.M.}$): Weight of the prepared monolith loaded with water, (W.T.**):** Weight of the prepared monolith desiccated,(**d):** Density of water at 25 °C =1, **L:** Length of the prepared monolith column, and R^2**:** The cylindrical radius of the column.

2.8.5 Test Permeability of the monolith [144]

The prepared monolith's permeability was studied using an HPLC pump where the pump provided with distilled water with various flow rates through the monolith. The return pressure value is recorded when the return pressure is stable.

2.9 The morphological characteristics of the prepared polymer

The morphological properties were tested using an (S.E.M.), (B.E.T.), FT-IR, and ^{1}HNMR:-

2.9.1 "Scanning electron microscope" (S.E.M.) [16,158]

This technique was used to describe the morphological of the prepared monolith column. The samples were covered with a fragile layer of "gold" and "platinum" about(2 nm) thick through a spray coating machine. Then the images were acquired using an acceleration voltage of (20 kV) and the current of (100 pA) in the high–discharge style.

2.9.2 Brunauer-Emmett-Teller (B.E.T.)

This device examines the prepared monolithic's surface area, pore size, and average pore diameter. The monolith was prepared using the method described in the previous paragraph(2-7), and paragraph(2.6). After that, the prepared monolith was removed and non-reactive materials by washed with "ethanol" and "water". Then the prepared monolith was dried in oven at (80 °C) to find the surface area, the pore size and average pore diameter of the prepared monolith.

2.9.3 "Fourier Transform Infrared" (FT-IR) spectroscopy [159]

FT-IR spectra were observed by FT-IR 380 (Shimadzu) spectra, where two samples were taken, purified, and dried well. The first sample was taken directly for measurement after being triturated with KBr to prove the formation of the polymer. As for the second sample, the ring was opened as in paragraph (3.6), then it was triturated with KBr, and its I.R. spectrum was measured to prove the ring's success through a comparison of I.R. spectrum with the I.R. spectrum of the first sample.

2.9.4 Nuclear Magnetic Resonance ^{1}H-NMR spectroscopy [160,161]

The ^{1}H - N.M.R. spectra of the prepared monolith GMA-co-EDMA-co-A.AM was studied to show the formation of the monolith by observing the displacements given in the test result.

2.9.5 Ring opening by hydrolysis [131]

After polymer formation, the epoxy ring of the glycidyl methacrylate monomer was opened by pumping 0.2 M hydrochloric acid at 20 µL/min^{-1} for 3 hours to form the diol groups.

2.10 use of monoliths GMA-co-EDMA-co-A.AM for the pharmaceutical compounds determination

The prepared monolith was used to determine propranolol hydrochloride and tri trifluoperazine dihydrochloride. It was tested using several standard solutions of propranolol hydrochloride (0.1-20 µg.mL^{-1})and trifluoperazine dihydrochloride(0.1-30 µg.mL^{-1}) at room temperature. Then the test solution of propranolol hydrochloride and trifluoperazine di hydrochloride supplied from different companies were tested using the HPLC technique.

Chapter Three

3. Results and discussion

3.1 Preparation of the monolith column

The preparation of the monolith column in a borosilicate tube, which was (60mm) in length, (1.5 mm) in inner diameter and (3 mm) in outer diameter, as shown in Figure (3.1), was explaind as shown in (3.3), (3.2) to prepare the internal surface of the tube and the polymerization step.

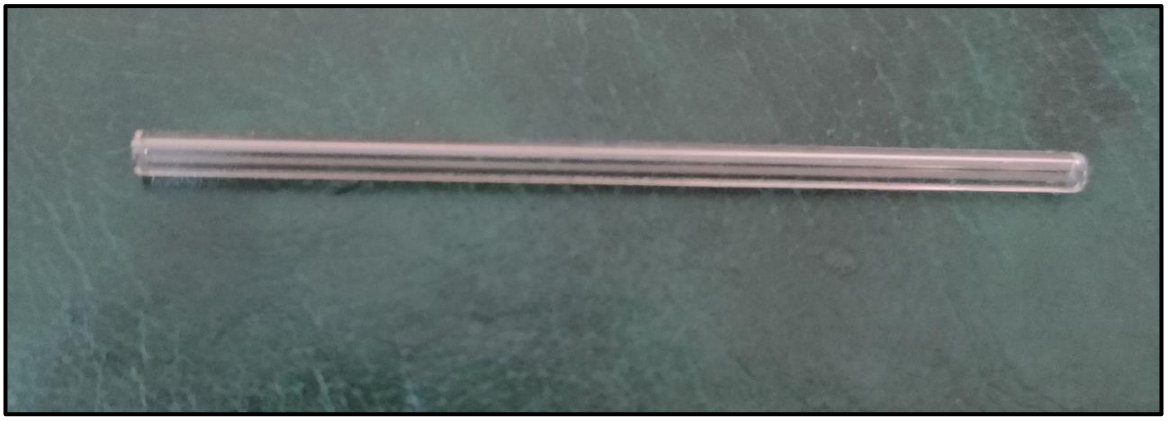

Figure (3.1): Photograph of the borosilicate tube before preparing the internal surface of the tube.

3.2 Preparing the internal surface of the tube [24,162]

The process of preparing the internal surface of the tube borosilicate is the essential step in the figuration of the monolith in a tube, as it includes the reaction of(3-trimethoxysilyl) propyl methacrylate with “silanol groups” ((Si-OH)) on the internal wall of the borosilicate tube, The benefit of this is installing the monolith on the inner wall of the tube and ensuring that the polymer does not come out or dislodge when using a high pumping speed, Besides, it helps prevent the shrinkage effect during the polymerization process, Moreover, avoid interactions between silanol groups and pharmaceutical compounds if the analysis sample contains pharmaceutical compounds. The process of preparing the inner surface of the tube includes several steps. In each of these steps, the solutions necessary for

the preparation process are pumped into the borosilicate tube using a syringe at a flow rate of (5µL min^{-1}) for 1 hour [23]. The first step was to wash the inner wall of the tube using ethanol to remove any organic matter, then rinse with distilled water to remove any ethanol residue. After that, a sodium hydroxide solution was used at a concentration of(0.2M) to decompose the siloxane groups and increase the silanol groups' density. Then, it was washed with D.W to take out every residual basic solution.

Furthermore, an (HCl) solution at a concentration of (0.2M) was utilized to take out every residual alkali mineral ion. After that, "the borosilicate tube" was rinsed with distilled water to take out every remaining (hydrochloric acid HCl), and then it was washed with "ethanol" to take out the distilled water. Allowed , (3- trimethoxysilyl) propyl methacrylate was inoculated into the borosilicate tube and pliable to interact for (one hour), after that the tube was harsh with (N_2) gas. Nevertheless, the trimethoxysilane groups are attached to the "silanol groups "on the surface of the tube, and the linked methacrylate groups will participate in "the polymerization reaction", binding the monolith to the internal walls of "the glass tube". The procedures for preparing the tube's inner surface are shown in Fig. (3.2)[163]

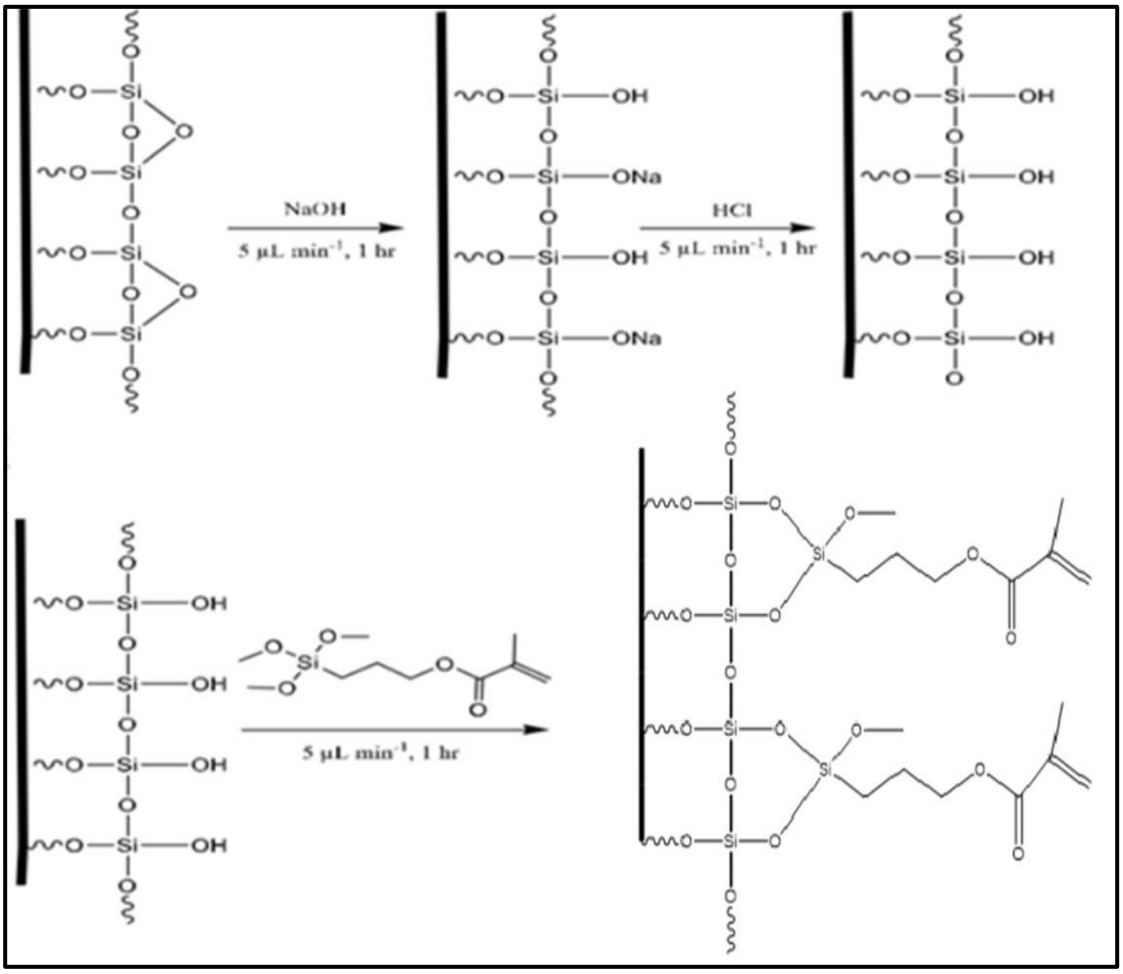

Figure (3.2) : Steps for preparing the internal surface of the borosilicate tube[163].

3.3 The polymerization process

The polymerization mixture was based on the published study modification with a few changes [91] including monomers species according to the properties of a prepared monolith and the structure of "porogenic solvent".

Two monomers, glycidyl methacrylate and acryl amide, are used in the polymerization process of the polymer combination. There are two functional groups in GMA, the methacrylate double bond that participates in photopolymerization and the epoxide groups

that can be used in various chemical reactions, as well as in post polymerization modification reactions to produce different functional groups that can provide multiple separation mechanisms. The cross-linker, porous solvents, and a reaction initiator are vital in the polymerization reaction and the polymer's final morphology. The cross-linking agent "(ethylene glycol dimethacrylate)(EDMA)" is a common cross-linking agent used to prepare solid large-pore monolithic polymers.The cross-linker-to-monomer ratio must remain constant because any variation will affect the porosity properties and the cross-linked chemical composition. For example, increasing the bond percentage reduces the average pore size by forming high cross-linking microspheres, which may be advantageous for obtaining a monolith with a large surface area. Due to its large surface area and restricted solvent permeation, the bond-to-monomer ratio must be maintained consistently. A binary solvent consisted of 1-propanol and Hexanol was used in the polymerization mixture. The primary role of this solvent is to dissolve the monomers, the linker and the initiator. At the same time, it does not contribute to dissolving the polymer. The polymerization process was carried out by photopolymerization using ultraviolet rays to start the process of free radical polymerization to form the monolith inside the borosilicate tube. because It has many (advantages) such as controlling pore size, short preparation time, avoiding high temperatures that lead to polymer cracking, controlling the position and length of the porous monolith, and high mechanical strength. In order to initiate the polymerization process, 2,2-dimethoxy-2 phenyl acetophenone was cleaved, and free radicals formed, which attacked double bonds in monomers to form a glycidyl methacrylate/ethylene methacrylate/acrylamide monolithic column. This monolithic column was then filled with the polymerization solution described above,As shown in figure(3.3).

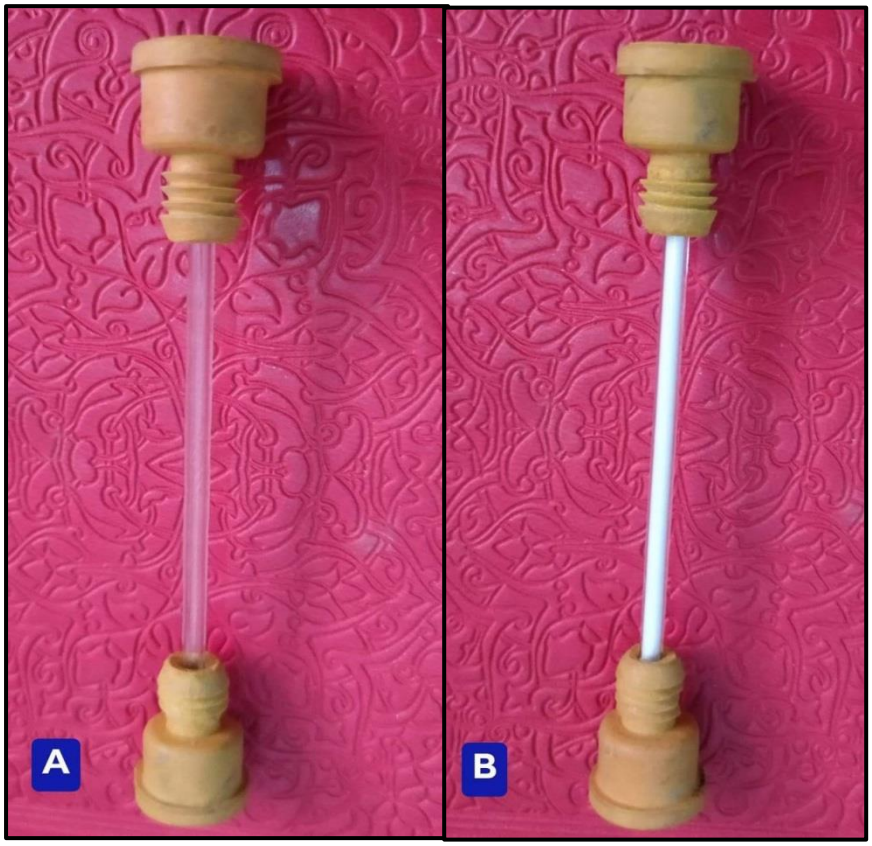

Figure (3.3): (A) borosilicate tube after the step of preparing the inner surface of the tube, (B) borosilicate tube after polymerization and monolith formation.

Since the porosity of the prepared monolith in this study is large (**0.0823**) and pore size (**5.26 nm**), this is due to the large-sized pharmaceutical compounds estimated through this prepared monolith to pass easily without any obstruction affecting the monolith. In comparison, the porosity of the prepared monolith in the published research is and it is smaller than (**0.0360**) and pore size (**5.1859 nm**) because this monolith was used to separate ions of small size that can pass through small pores easily and without high return pressure that leads to polymer breakdown.

The steps of the free radical polymerization process can be explained as follows [104,164]

1- Cleavage step of the initiator (2,2-dimethoxy-2-phenyl acetophenone)

This step consists of dismantling the initiator using ultraviolet light to form two parts of (benzoyl) that start the polymerization reaction and an(acetal)part that acts as an inhibitor to inhibit the polymerization process as shown in Figure (3.4).

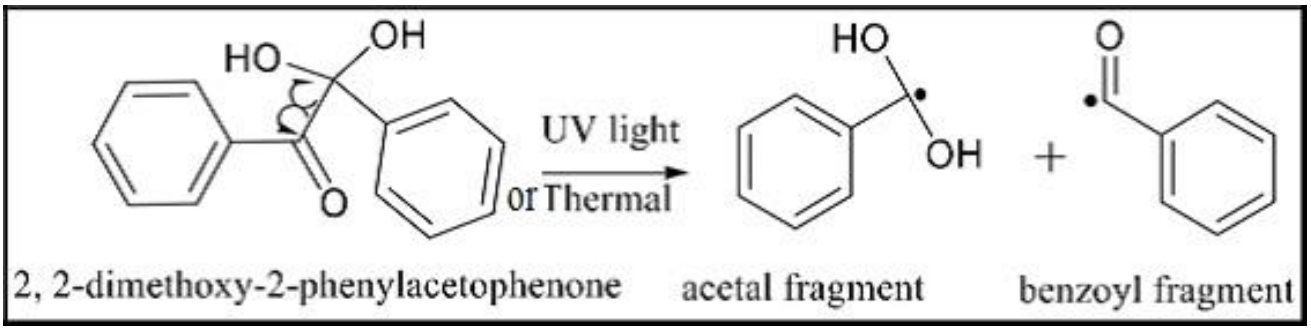

Figure (3.4): the initiator cleavage step.

2- The initiation step

This step involves the free radicals attacking the benzoyl "double bond" of the monomer to compose new free radicals on the monomer that can be attacked by the double bond of the" cross linker "or another "monomer" as shown in Figure (3.5).

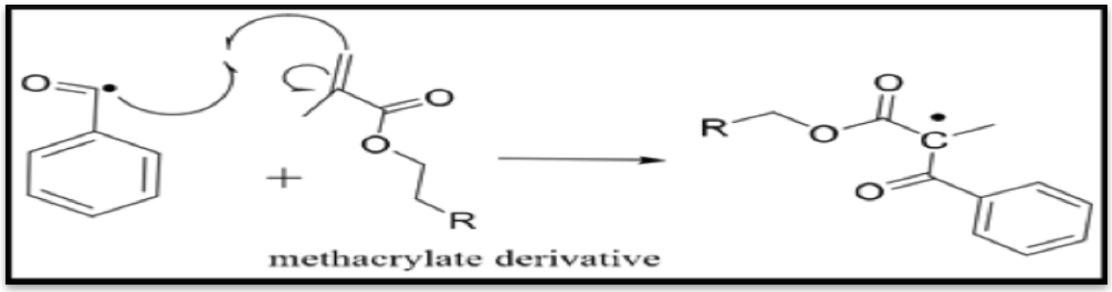

Figure(3.5) :The initiation step

3- The growth step

This step includes free radical interactions between monomers and cross-linker for the growth of the polymer chain, as shown in Figure (3.6).

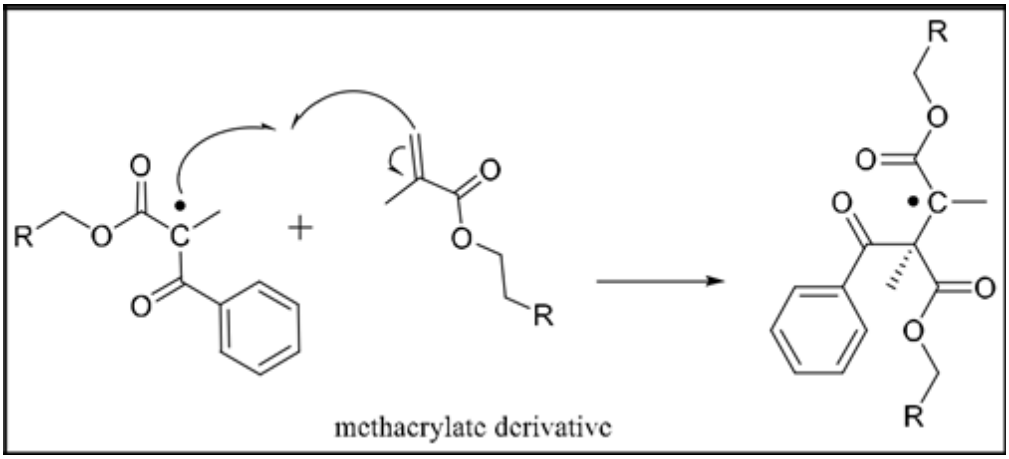

Figure (3.6): the propagation step.

4- Ending step

In this step, the polymerization process is finished due to the interaction of each free radical with the other, as shown in Figure (3.7).

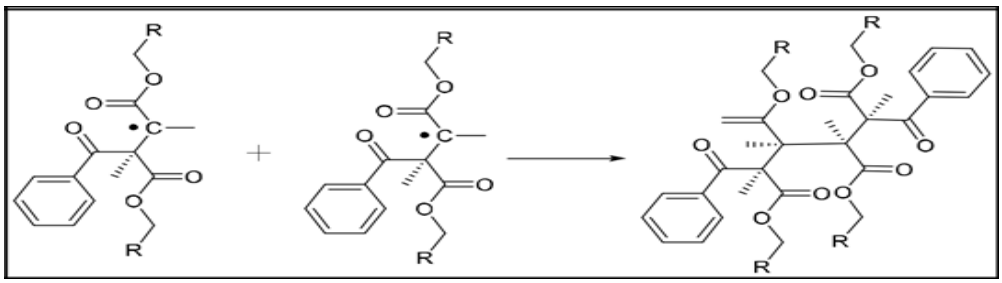

Figure (3.7) :The finalization step

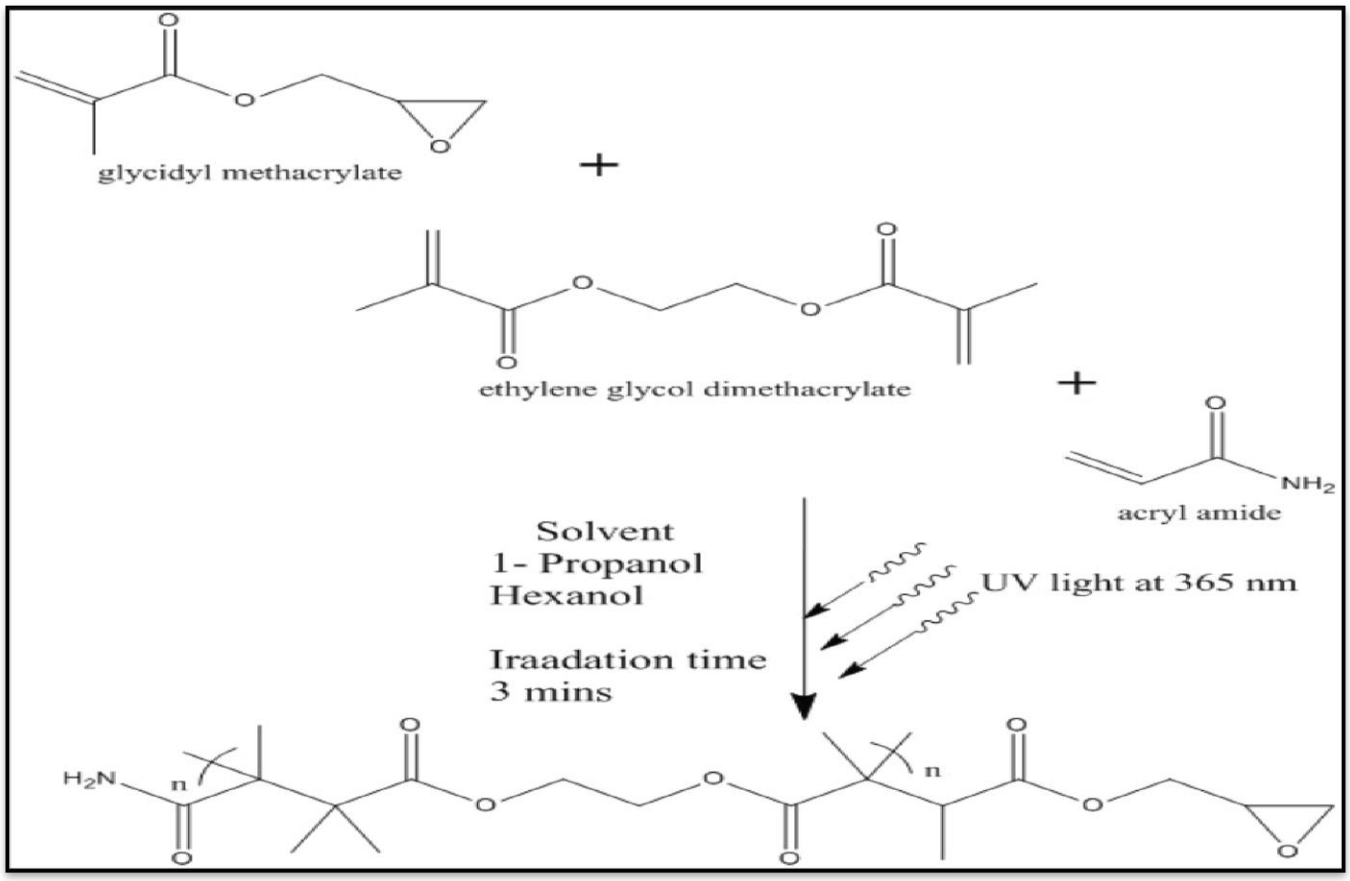

Figure (3.8) : final formula of the polymer after the polymerization process is completed.

3.4 The morphological characteristics of the monolithic column

3.4.1 Scanning electron microscope (SEM) of the prepared monolith column GMA-co-EDMA-co-A.AM [8,165]

The scanning electron microscope is used to study the composition of the sample's outer surface, giving a three-dimensional image. As a torrent of electrons with a very short wavelength is used, it can obtain a very high amplification power. The electron microscope consists of a tightly closed vertical tube that maintains a constant vacuum of air, so the electron stream can only be magnified in a vacuum complete, because the electrons lose their speed and diverge if they collide with the dispersed molecules of oxygen and nitrogen, in addition to the discharge, a high, stable and balanced electric

current is needed. The condenser lens works perfectly, called the electromagnetic condenser lens, to focus the electrons. The electron beam passes over the sample to be examined, and there is a set of detectors to collect the signals emitted from the sample. The electrons are received on a fluorescent screen that can be viewed directly or using magnifying lenses, as shown in Figure (3.9)

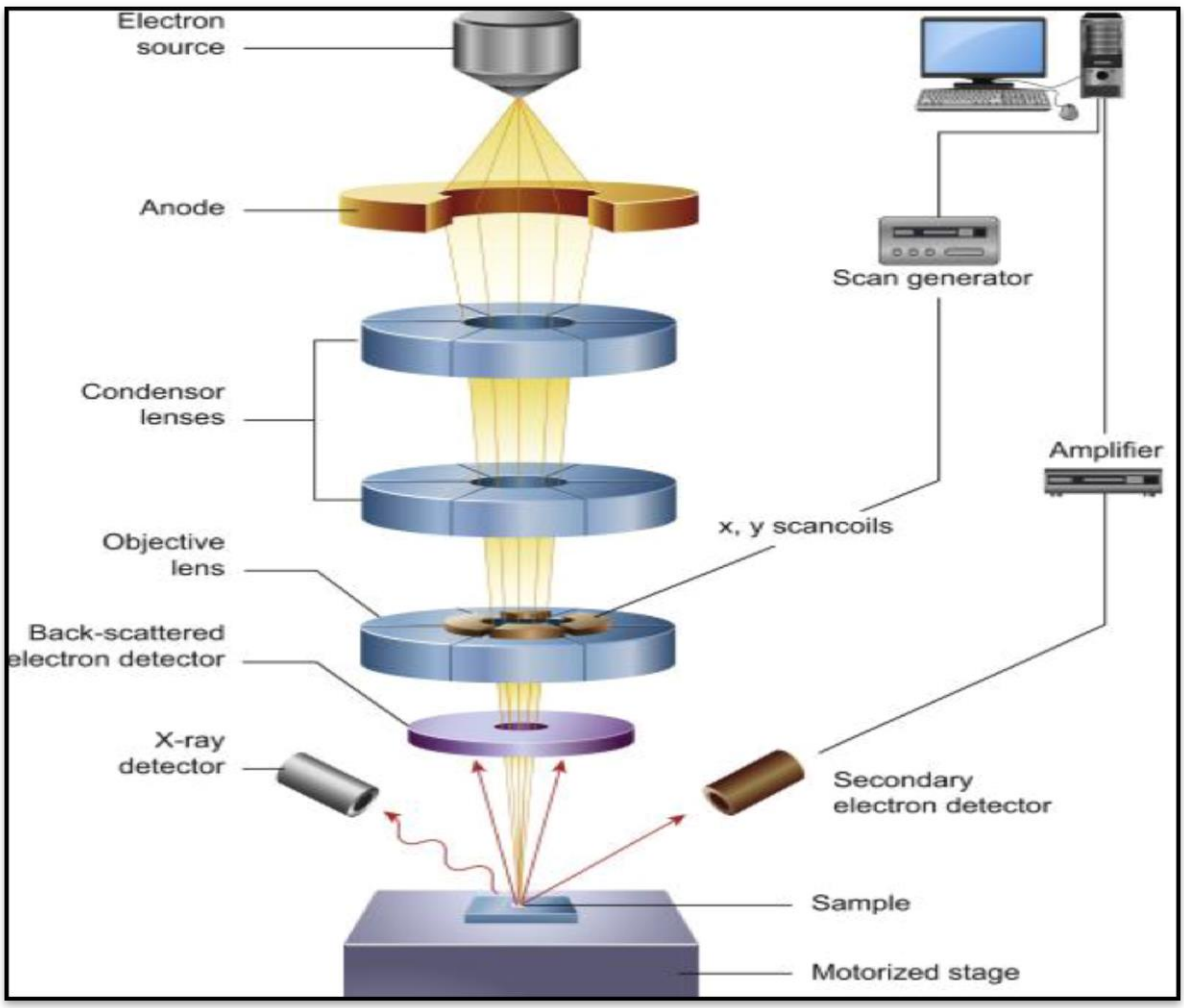

Figure (3.9): Structure of the scanning electron microscope[164,165]

The morphological properties of the monolith (GMA-co-EDMA-co-AAm) have been investigated using an (SEM) technique. SEM Cluster groups and macropores are visible in the monolith's shape, as seen in Figure (3.10) reveals a number of critical informational for the finished Figure (3.10). A network of massive channels is one way to conceptualize monolithic media. As a second benefit, these pores allow the mobile phase to move past

them efficiently, which helps to reduce back pressure. Furthermore, "the surface area" of the monolith may be raised due to the micropores and mesopores; these pores can share in increasing the surface loading ability of the monolith. Further, they increase the interactions using a high flow rate and minimum return pressure.

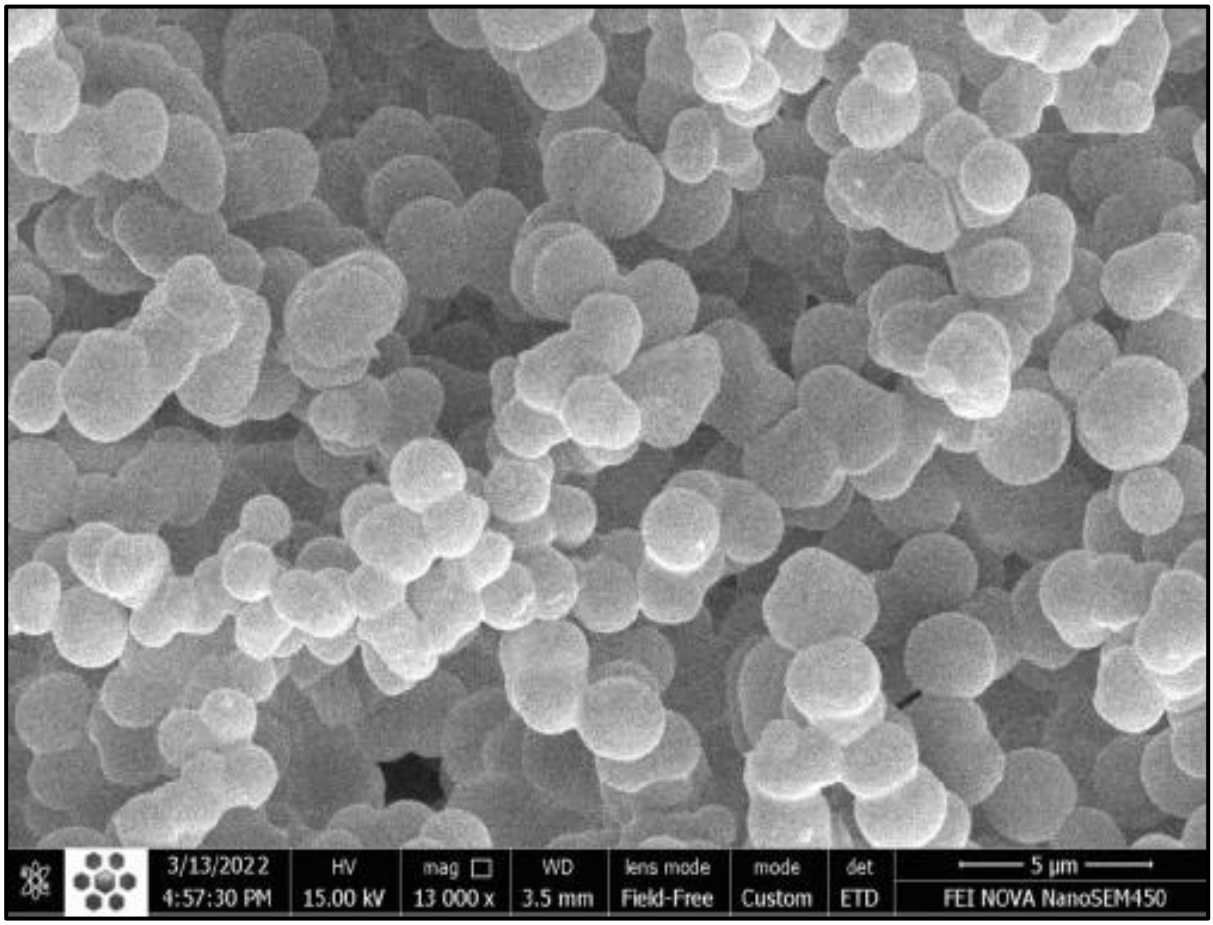

Figure (3.10) : SEM image of the prepared monolith column GMA-co-EDMA-co-A.AM

3.4.2 "Brunauer-Emmett-Telle" (BET) analysis for GMA-co-EDMA-co-A.AM monolith [166,167]

Brunauer, Emmett and Teller found a method for calculating a specific surface area of a sample, including the pore size distribution of gas adsorption. The amount of gas adsorbed depends on (the exposed surface, temperature, Gas pressure, and interaction strength between gas and solid matter) In the BET surface area analysis, nitrogen is usually used because of its high purity and intense interaction with most solids .because the interaction between the gas phase and the solid is usually weak, the gas volume is measured (usually nitrogen) adsorbed on the surface of the particles at the boiling point of nitrogen(-196 °C) At this temperature, the nitrogen gas is less than the critical temperature. It, therefore, will adsorb on the surface of the particles. Then known quantities of nitrogen gas are gradually released into the sample cell . When the relative pressures less than atmospheric pressure are achieved by creating conditions of partial vacuum and formation of adsorption layers; the sample is removed from the nitrogen atmosphere and heated to release the adsorbed nitrogen from the material and determine its quantity. The collected results are presented in the form of temperature BET, which determines the amount of adsorbed gas as a function of relative pressure, as shown in Figure (3.11)

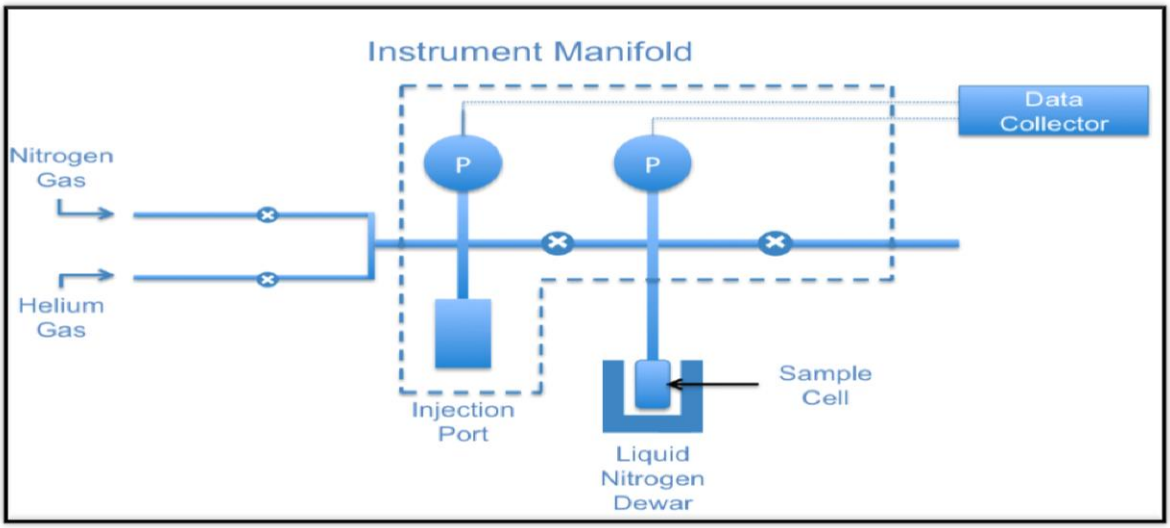

Figure (3.11) :The principle of operation of the BET device

Brauer-Emmett-Teller (BET) analyses established "the surface area" and the "pore size" of the GMA-co-EDMA -co- A.AM monolithic column. The results of Brunauer-Emmett-Teller (BET) analyses were (**5.26nm**), (**14.461m^2/g**) of pore size and surface area, respectively; in this case, pore size and surface area are interrelated as pore size is needed for flow rate and surface area is required to provide a morphological environment to create reactions on the surface. The results are satisfactory, as high flow rates are obtained with moderate back pressures, and the reactions are carried out on the surface without hindrances.

3.4.3 FT-IR spectroscopy for GMA-co-EDMA-co-A.AM monolith

The FT-IR spectrum clearly indicates polymer fashioning via monitoring the essential peaks in the monomers and the formed polymer. Yet, in the (GMA) monomer, the essential peaks (1716.41cm $^{-1}$)for (C=O), (1636.97cm^{-1})for (C=C), (907.70cm^{-1}) for (epoxy ring) (159). Furthermore the(FT-IR) spectra for(A.Am) exhibit essential peaks for (C=C) at (1609.83cm^{-1}), (C=O) at (1667.02cm $^{-1}$), and (NH2) at (3339.67cm^{-1}) . The FT-IR spectra of (GMA-co-EDMA-co-A.Am) showed clear peaks for (C=O), (NH_2), and epoxying. At the same time, the (C=C) peaks in the monomers and cross-linker spectra disappeared, this being a strong evidence of polymer formation. The FT-IR for the prepared monolith is shown in Fig. (3.12)

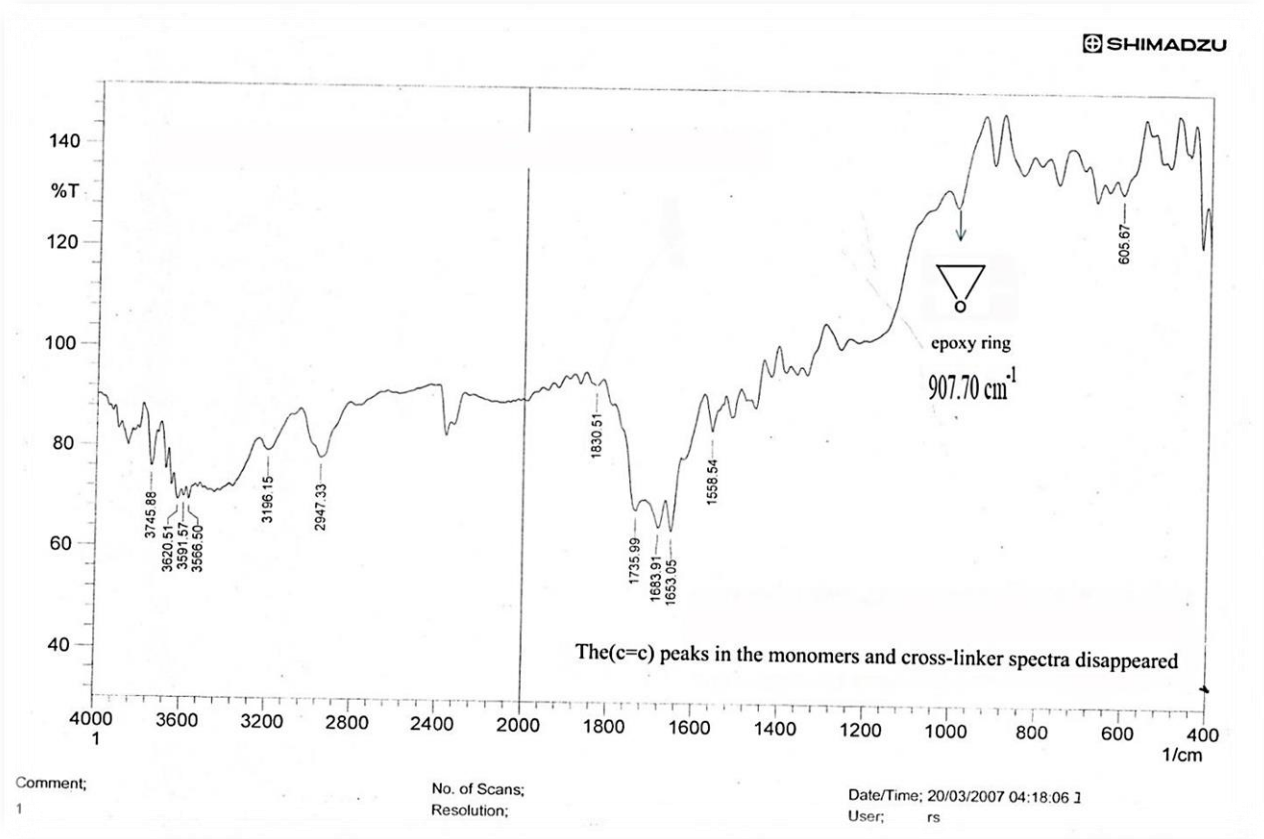

Figure (3.12) : FT-IR spectrum of prepared monolithic polymer

3.4.4 Ring-openingof[GMA-co-EDMA-co -A.AM]monolithic column

Hydrolysis of the epoxy ring using hydrochloric acid to open the monolith's epoxy ring using a dual syringe (flow rate of 20µL) and pumping hydrochloric acid (0.2 M) for (3hours)[91], this procedure is completed. The epoxy group was changed to diol groups for the ring opening reactions, and diol synthesis to be demonstrated employing FT-IR spectra is shown in Fig. (3.13).

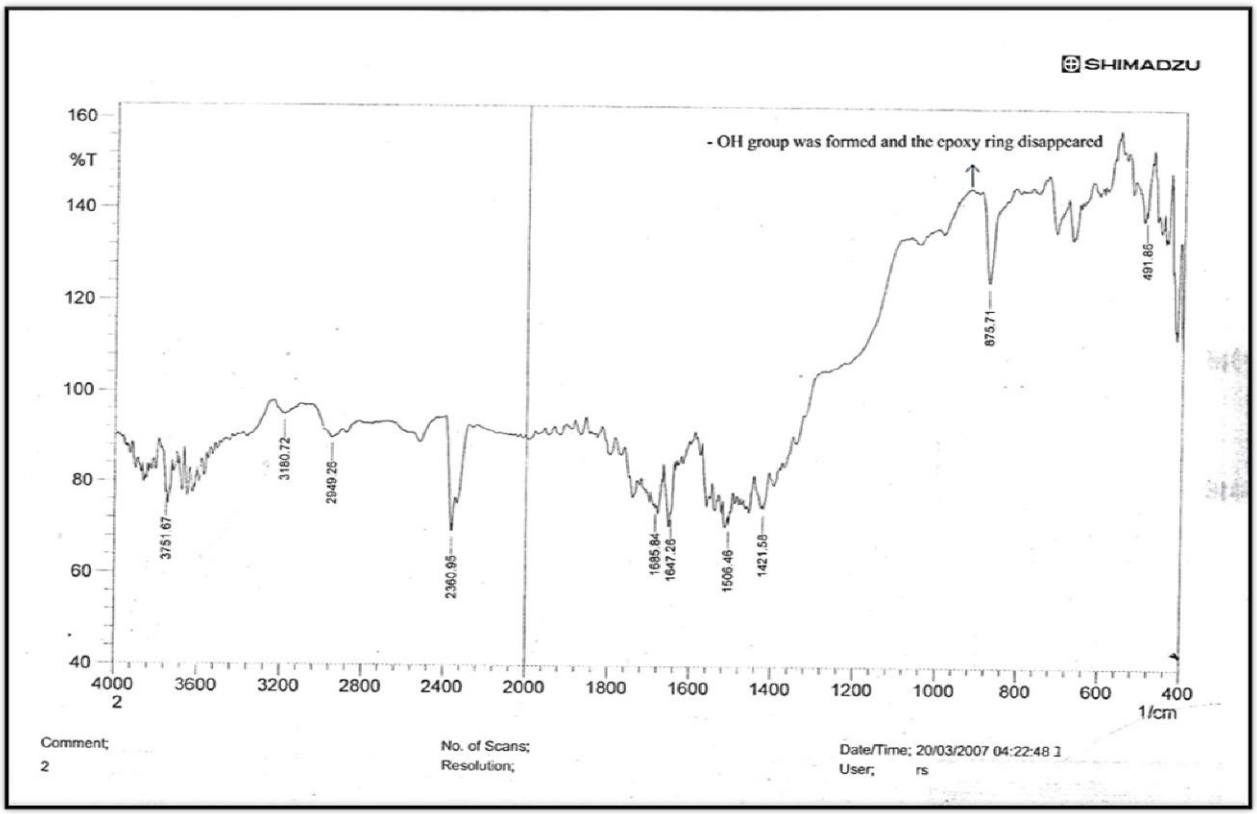

Figure(3.13) : FT-IR spectra of the monolith after a ring-opening reaction.

From figure (3.13), it can be seen that the epoxy group at (907 cm^{-1})disappeared and the peak of the OH group at (3751 cm^{-1}), which is an evidence of the epoxy ring opening, whereas this peak was not found in the FT-IR spectra of the monolith before the epoxy group opening.

Figure (3.14) shows the polymer's final formula after opening the prepared monolith's epoxy ring.

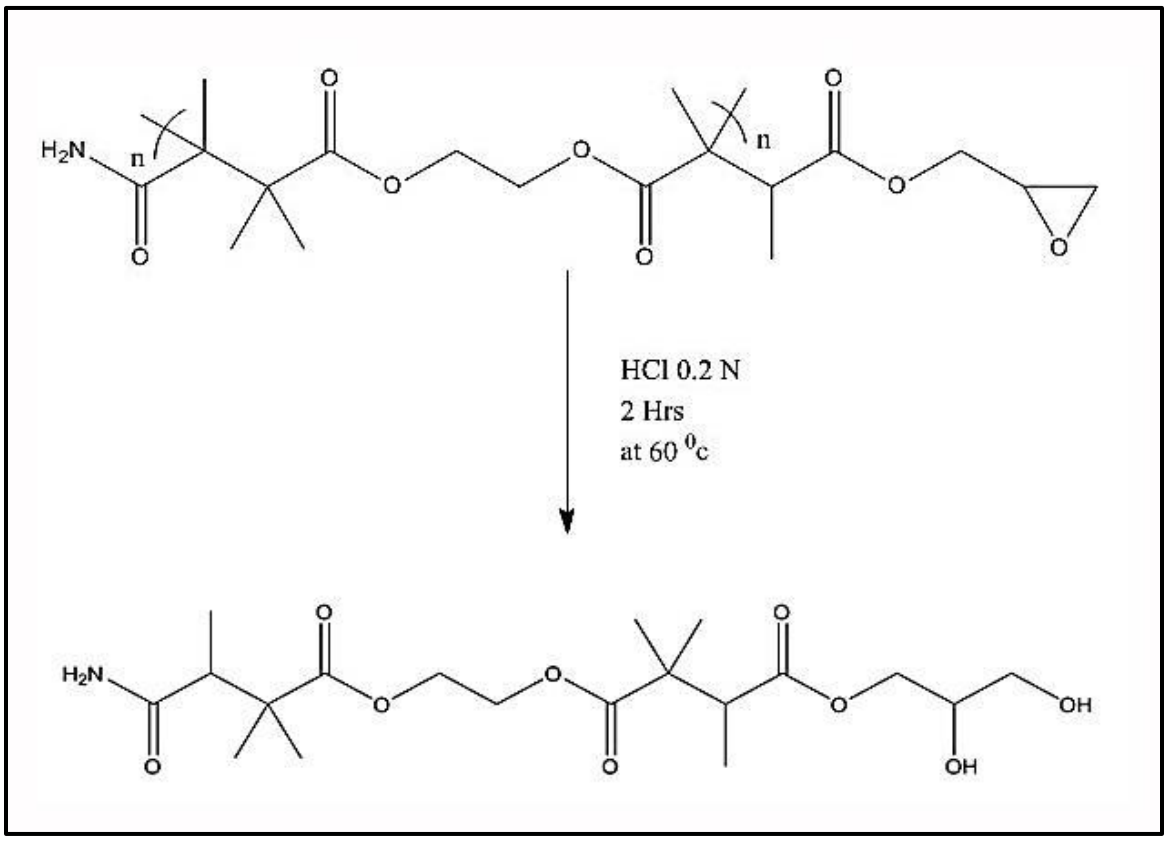

Figure (3.14) : The final formula of the polymer after opening the epoxy ring of the prepared monolith.

3.4.5 Nuclear Magnetic Resonance ^{1}H-NMR spectroscopy for GMA-co-EDMA-co-A.AM monolith

The prepared polymer (GMA-co-EDMA -co-A.AM) is studied using nuclear magnetic resonance spectrometry (^{1}H NMR); concerning the monomers, it contains CH_2, Alkene CH_2, and CH_3 the ^{1}H NMR spectrum for the prepared polymer Figure (3.15) showed a signal at (3.4 µg.mL^{-1})that it belongs to the CH_2 group, it also gives a signal at (2.5 µg.mL^{-1})which belongs to th CH_3 group noting that there is no indication of CH_2 alkene, which appears within (6-7 µg.mL^{-1}) in all monomers before polymer formation, and this is good evidence of the formation of the polymer.

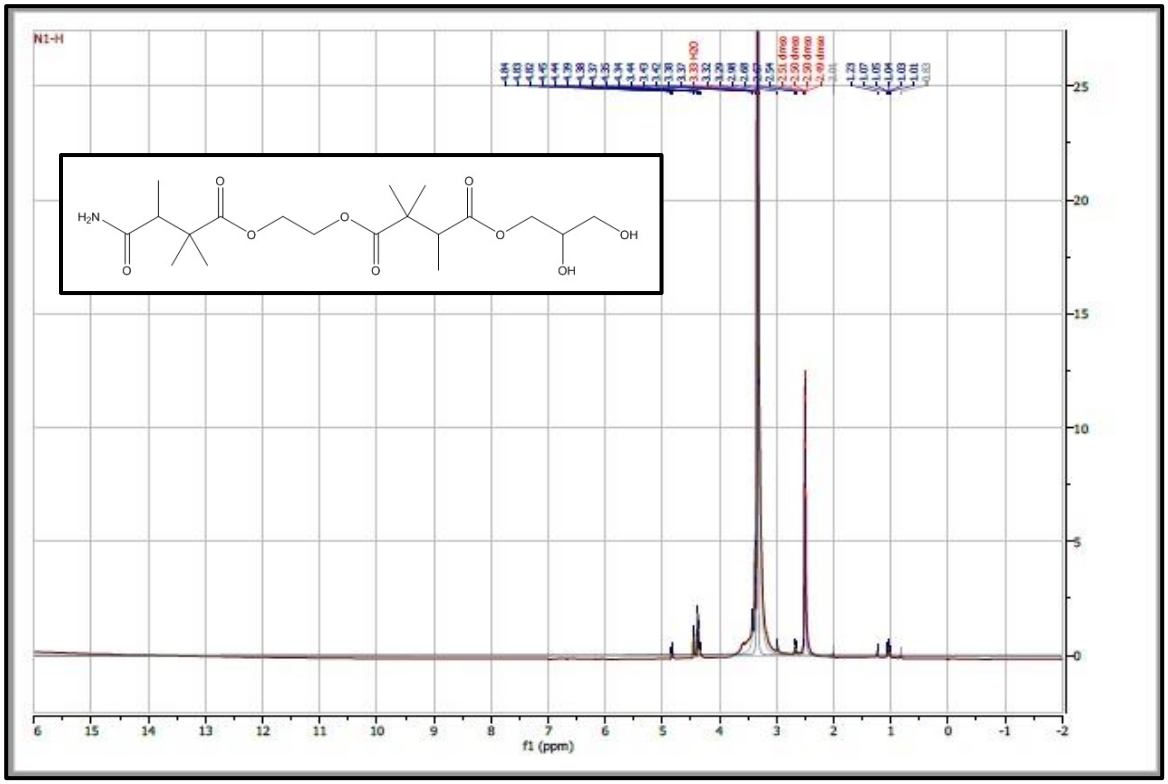

Figure (3.15) : ^{1}HNMR spectroscopy for (GMA-co-EDMA -co-A.AM).

3.5 Investigation of optimum conditions of the polymer prepared

3.5.1 The effect of irradiation time

After determining the monomer ratio and the distance between the irradiation source and the prepared column, the most appropriate irradiation time for polymer formation was studied. Different irradiation times ranged from (1-5 minutes), and the results are shown according to Table (3-1).

Table(3.1): Shows The effect of irradiation time effect on monolith formation.

(Irradiation time) (minutes)	(Result)
1	The monolith did not form
2	The monolith initiate form
3	**The monolith formed with suitable return pressure**
4	The monolith formed but blocked
5	The monolith formed but blocked

can be observed from Table (3.1) that the irradiation time is the essential factor that metamorphoses the mixture of monomers to the rigid polymer, so when using a high irradiation time of (4) minutes or more, the polymer chains grow and consequently, the polymer branches increase rapidly and form a monolith with a porous structure small as shown in Figure (3.16)((C)). On the other hand, when the irradiation time decreases to less than (2) minutes, this may lead to the formation of a little polymerized material in the borosilicate tube, and the polymer will not form properly and affect the performance of the prepared monolith, as shown in Fig. (3.16)((A)) whilst when using the irradiation time (3) minutes will give return pressure and good surface area as shown in Figure(3.16)((B))(168)

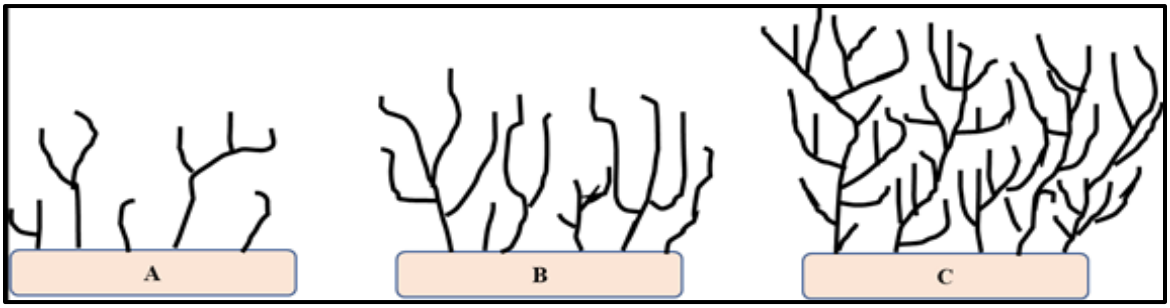

Figure (3.16):Effect of increasing the irradiation time on the growth of polymer chains.

3.5.2 Investigation of the distance between the irradiation source and the monolith column

The effect of the distance between the irradiation source and the prepared separation column was studied to find the best distance that the polymer can form inside the separation column. The distance from the irradiation source ranged between (3-16cm), and the results are shown according to Table (3.2).

Table (3.2):Effect of the distance between the irradiation source and the monolith column.

Distance /cm	The result of the polymer formed
3	The polymer is formed, but it cannot be washed
6	The polymer is formed, but it cannot be washed
10	**The polymer is inside the separation column and can be washed easily with good back pressure**
13	The polymer is inside the separation column but with low back pressure
16	the polymer is inside the separation column, but incompletely

It can be noted from Table (3.2) that the polymerization process cannot be controlled when the distance between (3-6 cm), which causes small pores and unable to wash the prepared column and use it for the estimation and separation of pharmaceutical compounds. When the distance between (6-10cm) was used, the rate of The pore size is very small as it can be controlled, while the polymerization process and polymer formation can be controlled well when using a distance of(10 cm), as the polymer is homogeneous and can be washed easily with good return pressure, while when using a distance of (13-16cm) the polymer is inside the separation column, but in an incomplete form. As shown in Figure (3.17)

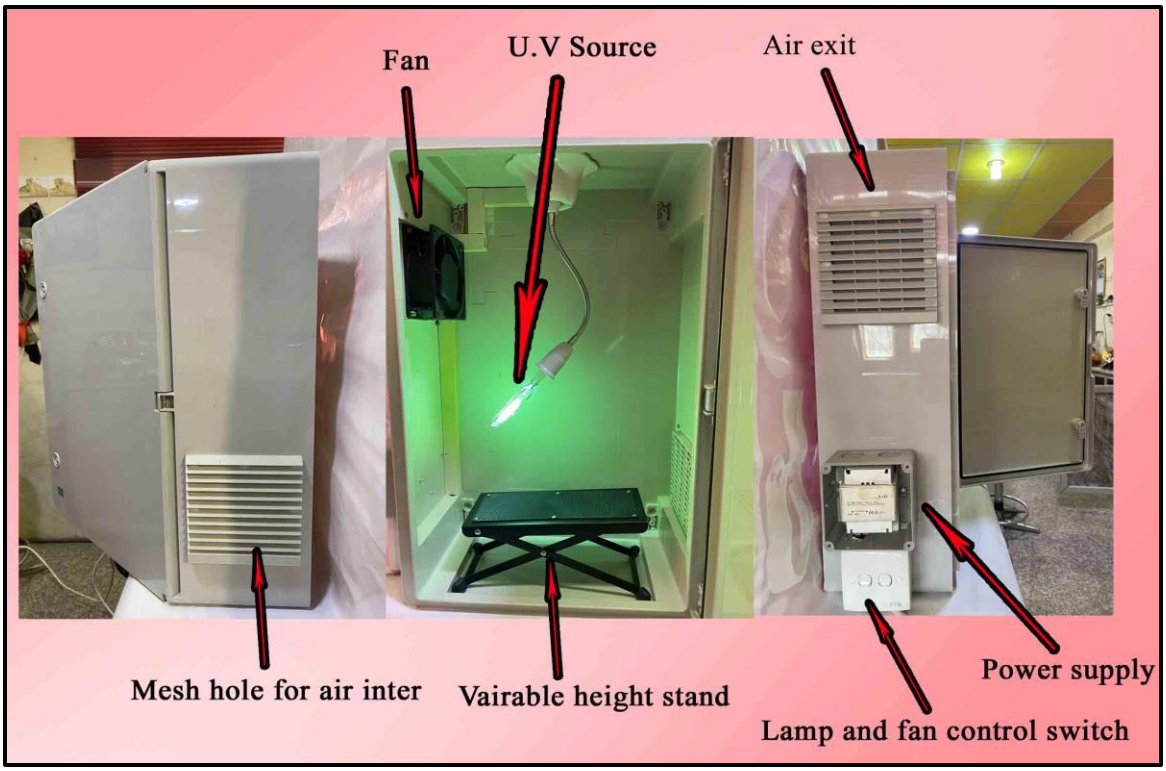

Figure(3.17): Photograph of Irradiation cabinet set.

3.5.3 The percentage of polymer swelling

Cross-linked polymers swell because the solvent molecules diffuse into the crystal lattice of high molecular weight polymers and cause a change in size. This leads to polymer breakdown during exposure to mechanical stress or high pressure. The type of permeable solvent can also have a significant effect and cause the prepared polymer to dissolve. The percentage of swelling was calculated by applying the following equation:

$$\boldsymbol{swlling}\% = \frac{\boldsymbol{mt-mo}}{\boldsymbol{mo}} \times \mathbf{100} \qquad \textbf{(3-1)}$$

As $\mathbf{m_o}$: weight of the polymer before swelling, $\mathbf{m_t}$: weight of the polymer after swelling. Alcohol solvents, different polar solvents and a mixture of solvents were used to test the degree of swelling of the polymer, and when applying the equation, the results appeared as in tables (3.3), (3.4), and (3.5)

Table (3.3) : shows the percentages of polymer swelling prepared using different alcohol solvents.

Time/hour	Swelling% Methanol	Swelling% Ethanol	Swelling% 2-propanol	Swelling% 2-butanol	Swelling% Hexanol
1	0.5	2.04	3.04	0.07	7.9
2	0.5	2.04	3.04	0.07	7.9
24	0.66	2.04	3.33	0.14	8
95	0.73	2.24	3.47	0.22	8.1
119	0.73	2.44	3.62	0.29	8.1
338	0.73	2.44	3.62	0.44	8.1

We note from Table (3.3) that the polymer swells to a high degree when using (**Hexanol**), and this may be attributed to the polymer saturation with the solvent and its insolubility, as well as the lack of cleavage of the polymeric chain, which causes a small pore, and reduces the mechanical properties when using high pressures rates and the inability to load pharmaceutical compounds, while the lowest degree of swelling when using (**methanol**), where an excellent porous structure is obtained as shown in the Figure (3.18).

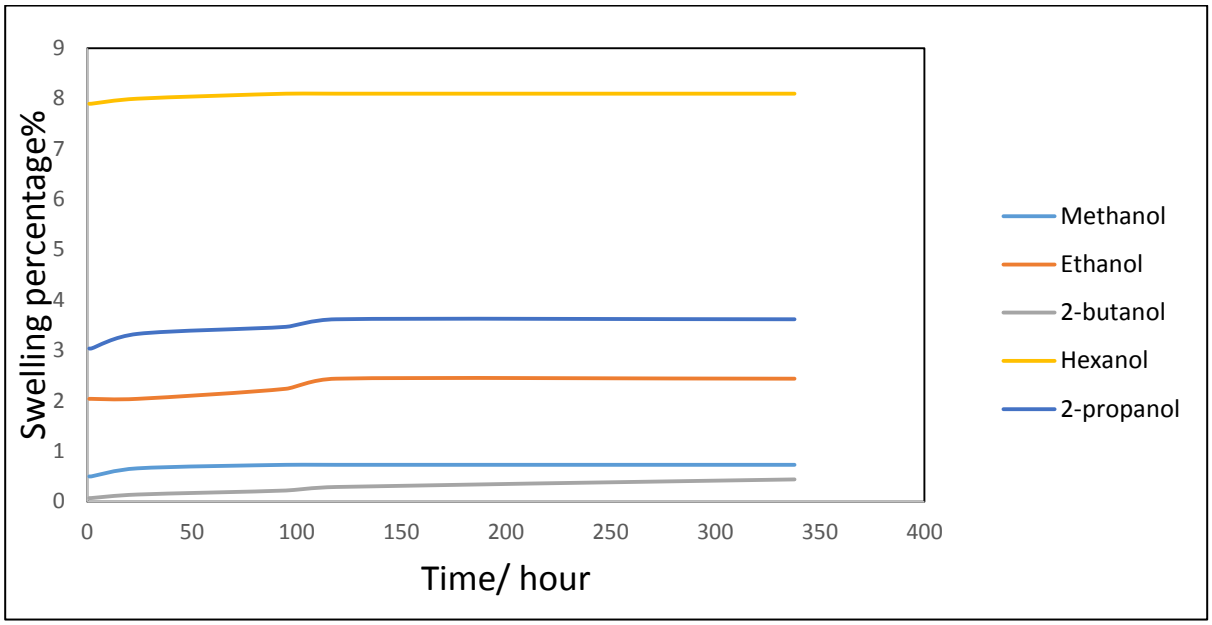

Figure (3.18): The percentage of polymer swelling using different alcohol solvents.

When using different polar solvents, it can be seen from Table (3.4) that when using **acetonitrile** and **formic acid**, the polymer begins to swell up to (**119**) hours and(**24**) hours, respectively. Then the polymer disintegrates as a result of the penetration of the solvent into the crystal lattice, which suffers either from chemical decomposition or as a result of swelling pressure, resulting in the polymer breaking, while the polymer suffers only swelling. In contrast, the polymer suffers from a slight, almost imperceptible swelling as it maintains its crystal lattice and pore size when using **water, acetone and chloroform**, as shown in Figure (3.19).

Table (3.4) : shows the percentages of swelling of the polymer prepared using different solvents of polarity.

Time/hour	Swelling% water	Swelling% acetonitrile	Swelling% aceton	Swelling% formic acid	Swelling% chloroform
1	1.5	0.3	4.1	1.7	16.4
2	1.5	0.4	4.1	2.7	16.4
24	1.5	0.48	4.2	2.8	16.4
95	1.6	0.56	4.31	Not found	16.54
119	1.68	0.65	4.37	Not found	16.60
338	1.68	-	4.37	Not found	16.65

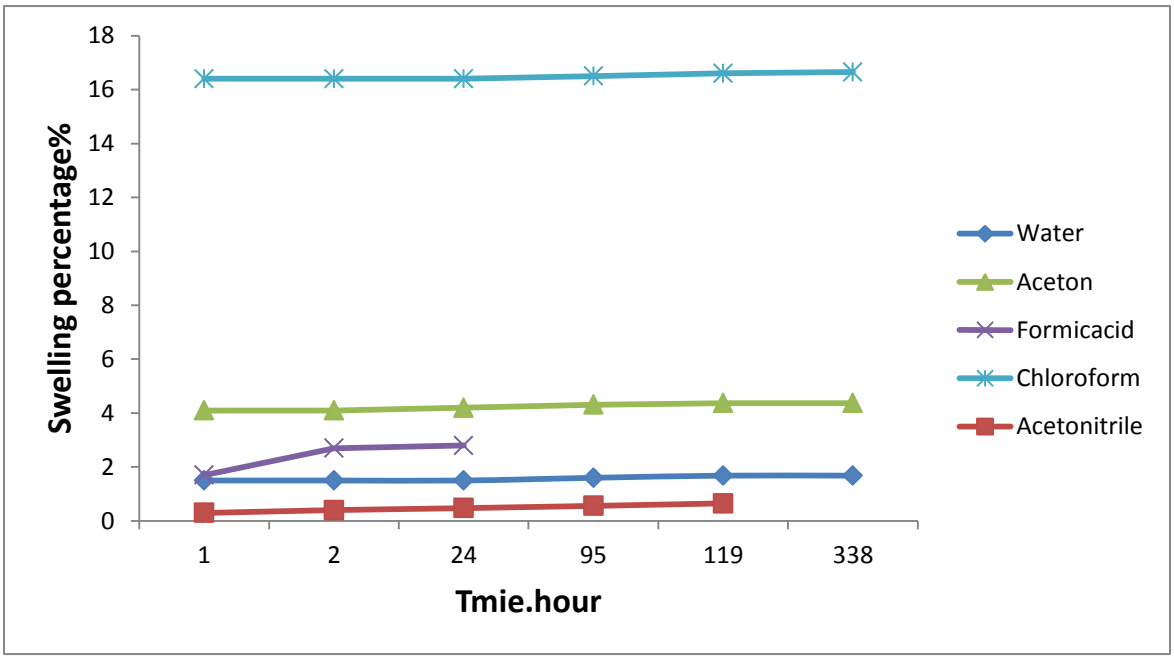

Figure (3.19) : The percentage of swelling of the polymer using different polar solvents.

However, when using a mixture of **water with acetonitrile**, the polymer is exposed to swelling at first. The reason may be attributed to the interaction between the molecules of

the mixture and the polymer. Eventually, the polymer disintegrates as a result of the chemical decomposition of the polymer. However, the polymer suffers from swelling when using the **ethanol-water** mixture and a mixture of **1-propanol and water**. Very slight does not affect the pore size. In contrast, the polymer retains its general structure; this indicates no interaction between polymer molecules and no chemical decomposition, as shown in Table (3.5)**.**

Table (3.5): shows the percentage of swelling of the polymer prepared using a mixture of two different solvents.

Time\hour	Swelling% Ethanol + water	Swelling% 1-propanol + water	Swelling% Acetonitrile + water
1	1.6	11.5	16.8
2	1.7	11.5	16.9
24	1.78	11.7	17.04
95	1.85	12	17.2
119	1.9	12	17.37
338	1.9	12	Not found

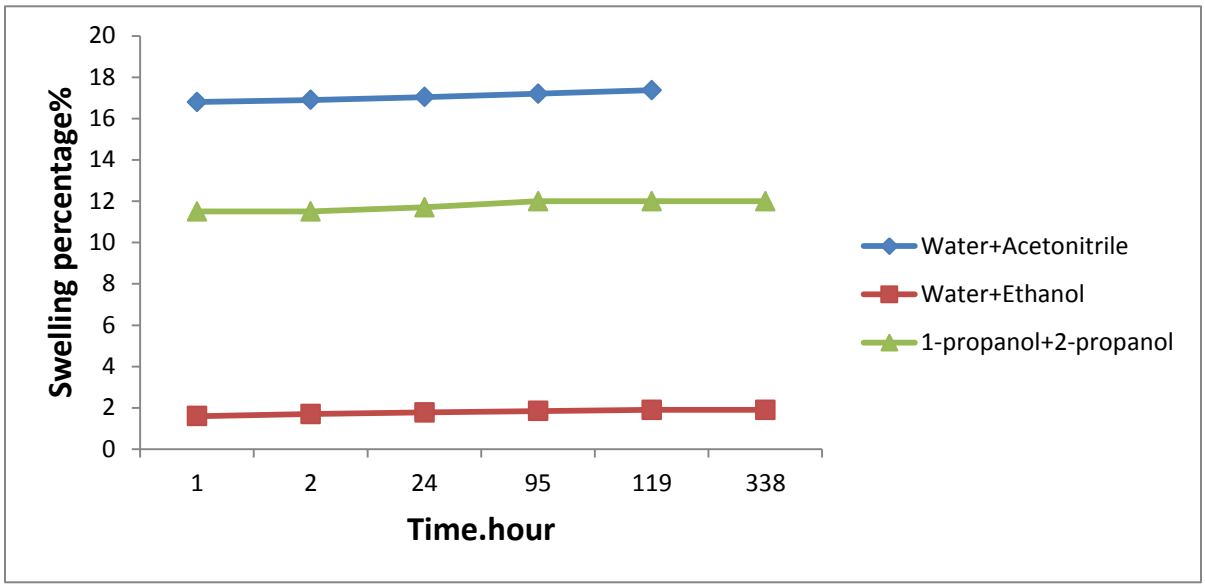

Figure (3.20): The percentage of swelling of the polymer using a mixture of two different solvents.

Through the swelling experiments that were conducted on the polymer, we can see that its importance lies in giving indications about the mechanism of choosing the mobile phase and, on the other hand, knowing which solvent is best used as a preservation solution for the column, as it was found that **water** is the best solution used to keep the column, as the age of the column was when it was saved with distilled water up to **(45) days**.

3.5.4 Permeability and the porosity of the prepared monolith

The permeability of the prepared monolith was studied by evaluating the return pressure generated by the electronic pump using distilled water with different flow rates through the monolith, as shown in Figure (3.21)

Figure (3.21): The electronic pump 980 - PU for measuring pressure and flow rate.

Figure (3.21) clarifies that the back pressure generated in the pump rises with the rise in the flow rate until it reaches a flow rate of 300 µL.m^{-1}and the pressure is stable at this point by (355.5828) PSI, when the flow rate increases more than 300 µL.mL^{-1}, the pump gives an error signal. The system shuts down, or the monolith column slips from the connections due to the pressure reaching a critical point, so the flow rate through the column was determined from(10 –0.3) µL.mL^{-1} ., the result is shown in Figure (3.22).

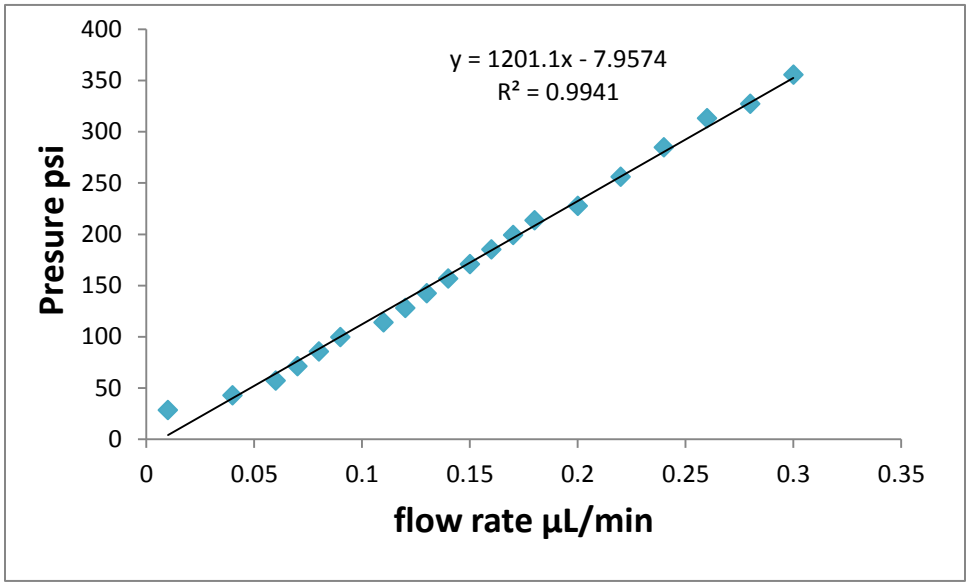

Figure (3.22): The relation between pressure and flow rate

the porosity of the monolith was calculated according to the equation **($Øt = (W_M - W_T) / dLR^2 \pi$)** as a result, the porosity was (**0.0823**)

3.6 Calibration curve

A calibration curve was made for each of the pharmaceutical compounds Trifluoperazine di hydrochloride and Propranolol hydrochloride at a range of concentrations between (0.1-30 µg.mL^{-1}), as it was measured at a wavelength of (370nm), had a detection limit (0.007 µg.mL^{-1}), Quantitative detection (0.054 µg.mL^{-1}), and Sandel sensitivity equal to (0.00783 µg/cm^2) for a calibration curve Trifluoperazine di hydrochloride, while the calibration curve Propranolol hydrochloride at a range of concentrations between (0.1-20 µg.mL^{-1}), as it was measured at a wavelength of (290 nm). had a detection limit (0.005 µg.mL^{-1}), a quantitative detection limit (0.036 µg.mL^{-1}), and Sandel's sensitivity is equal to (0.0052 µg/cm^2) as in Figure (3.23), (3.24).

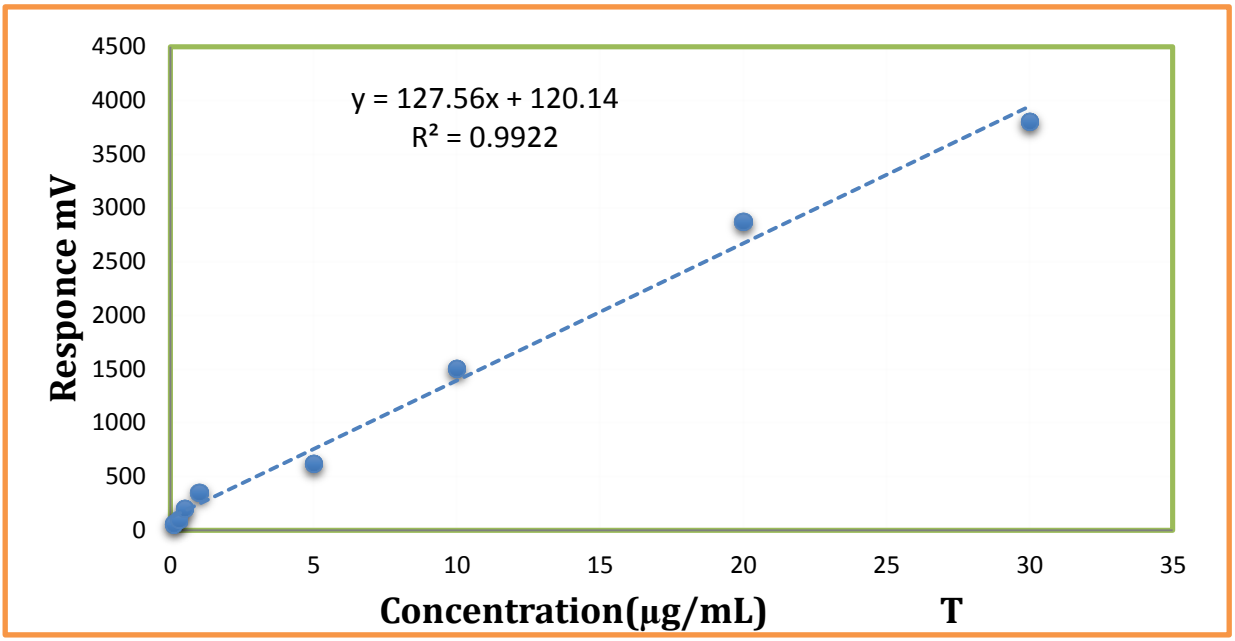

Figure (3.23): calibration curve for Trifluoperazine dihydrochloride.

Table (3.6):Calibration curve Parameters for Trifluoperazine dihydrochloride.

Parameters	Values
Range	(0.1-30 µg.mL^{-1})
slope	127.56
λ_{max}	370nm
R^2	0.9922
LOD.	0.007 µg.mL^{-1}
LOQ.	0.054 µg.mL^{-1}
Sandlle Index µg/cm^2	0.00783 µg/cm^2
ε.(L/mol.cm)	5198×10^4

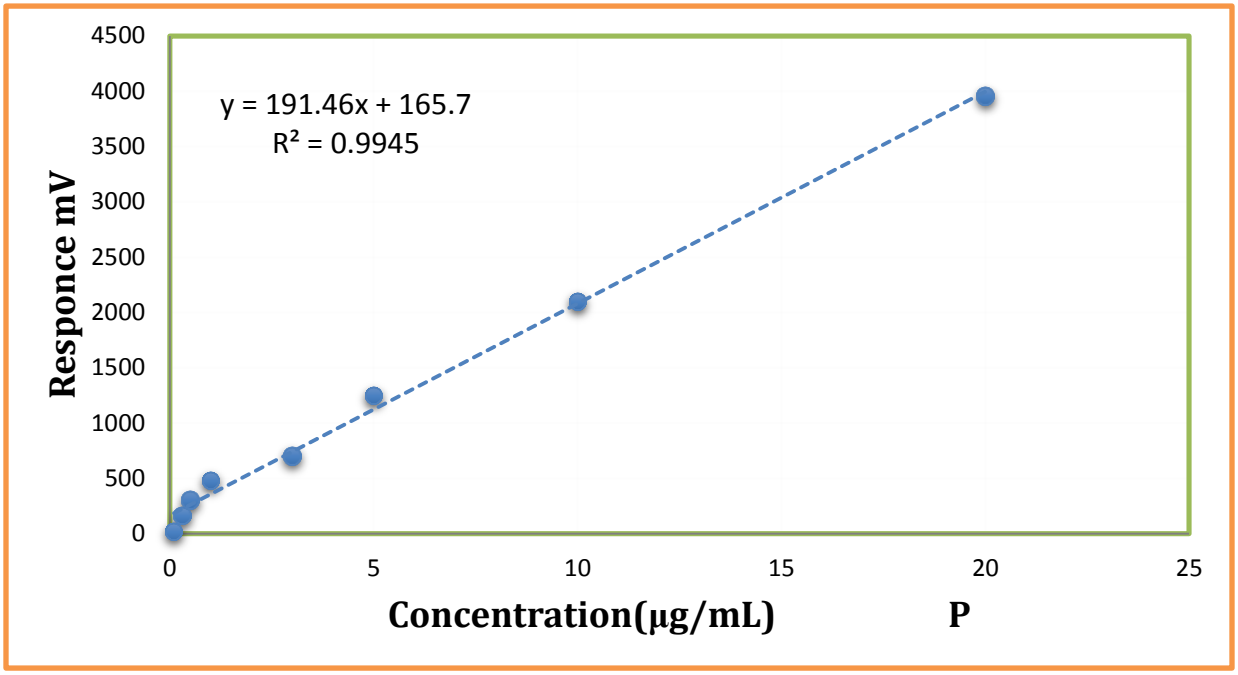

Figure (3.24): calibration curve for Propranolol hydrochloride.

Table (3.7):Calibration curve Parameters for Propranolol hydrochloride

Parameters	Values
Range	(0.1-20µ g.mL^{-1})
slope	191.46
λ_{max}	290nm
R^2	0.9945
LOD	0.005 µg.mL^{-1}
LOQ	0.036 µg.mL^{-1}
Sandlle Index µg/cm^2	0.0052 µg/cm^2
ε.(L/mol.cm)	5663 ×10^4

3.7 Separation of The pharmaceutical compounds by HPLC technology

By HPLC technology, the monolithic chromatographic column prepared in this study that was connected to the HPLC device and has been injected with a certain amount of Propranolol hydrochloride with wavelength 290 nm . A peak appeared after a period of time (**1.4min**) and it was found that this compound interacted with the components of the prepared column and the separation was successful. As shown in the figure (3.25).

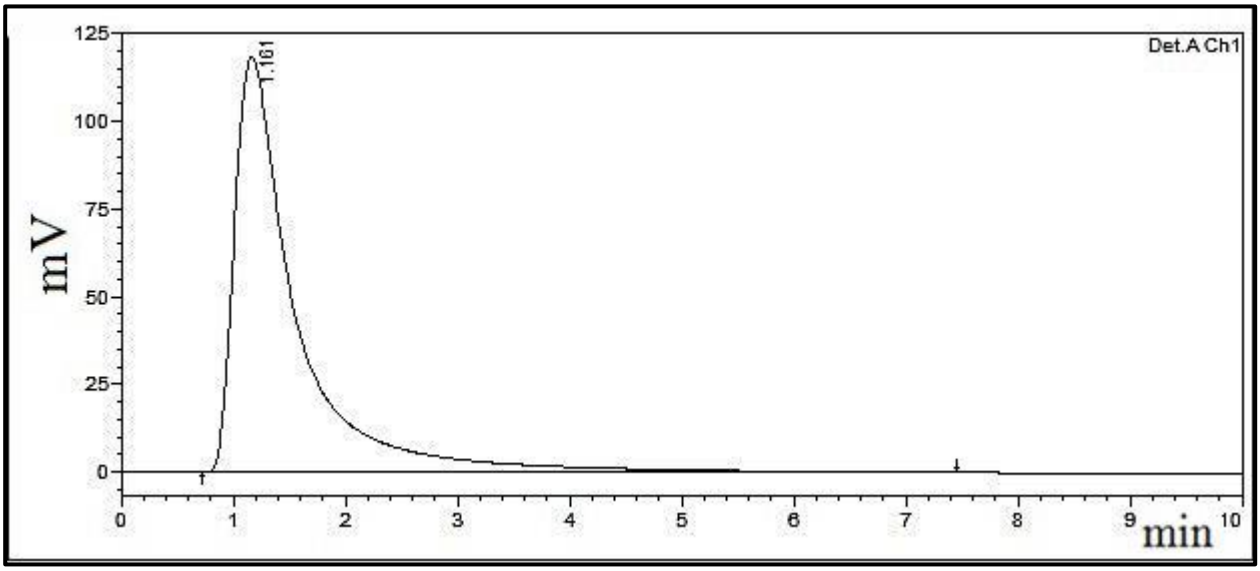

Figure (3.25): HPLC chromatogram for Propranolol hydrochloride (0.3 µg.mL^{-1}), at flow rate 1 mL.min^{-1}, (80:20)% water/ACN, λ=290 nm

By HPLC technology, the monolithic chromatographic column prepared in this study that was connected to the HPLC device and has been injected with a certain amount of trifluoperazine dihydrochloride with wavelength 370 nm . A peak appeared after a period of time (**2.6 min**) and it was found that this compound interacted with the components of the prepared column and the separation was successful. As shown in the figure (3.26).

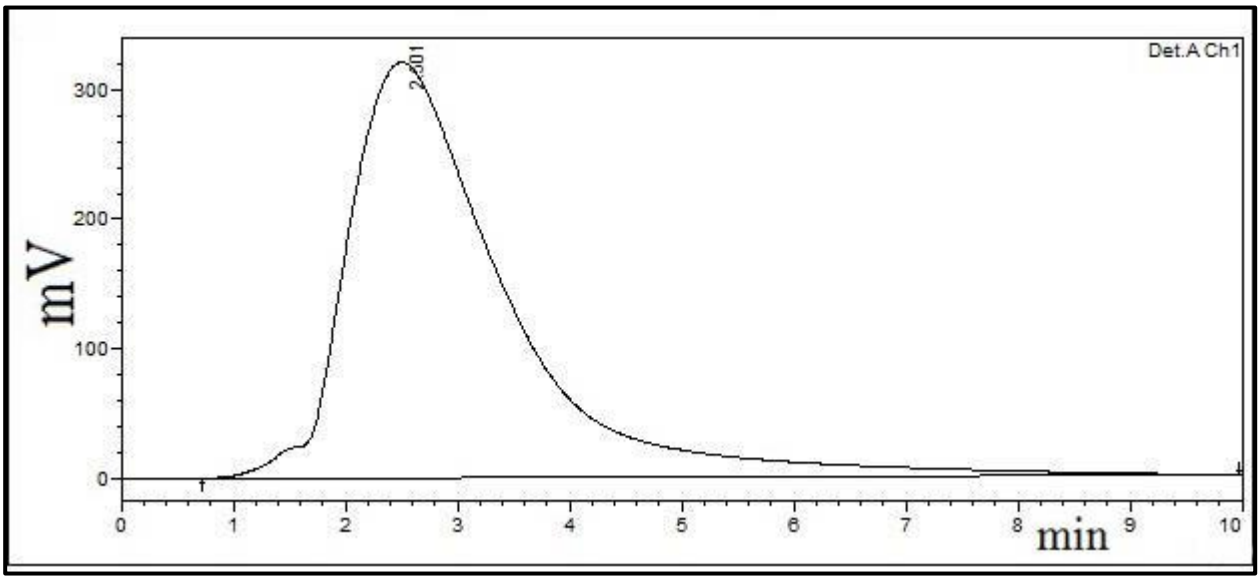

Figure (3.26): HPLC chromatogram for trifluoperazine dihydrochloride (0.3 µg/mL), at flow rate 1 mL.min^{-1}, (80:20)% water/ACN, λ=370 nm.

Certain amount of both pharmaceutical compounds were taken and mixed and injected into the prepared column connected to the HPLC device. A wide peak appeared,as in the figure(3.27).

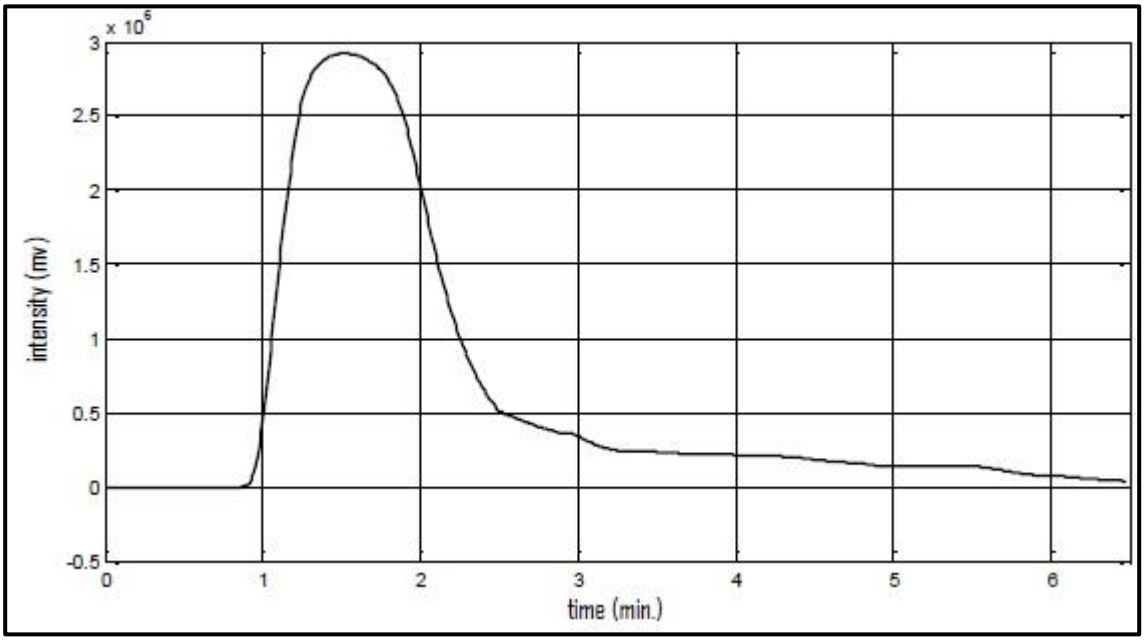

Figure (3.27): HPLC chromatogram for mixture of the pharmaceutical compounds (Propranolol hydrochloride, trifluoperazine dihydrochloride) (0.3 µg.mL^{-1}), flow rate 1 mL.min^{-1}, (80:20)% water/ACN, λ=290 nm

This broad peak of the mixture of the two compounds was treated by the first derivative and peaks of both compounds appeared, but unsatisfactorily as in the figure(3.28).

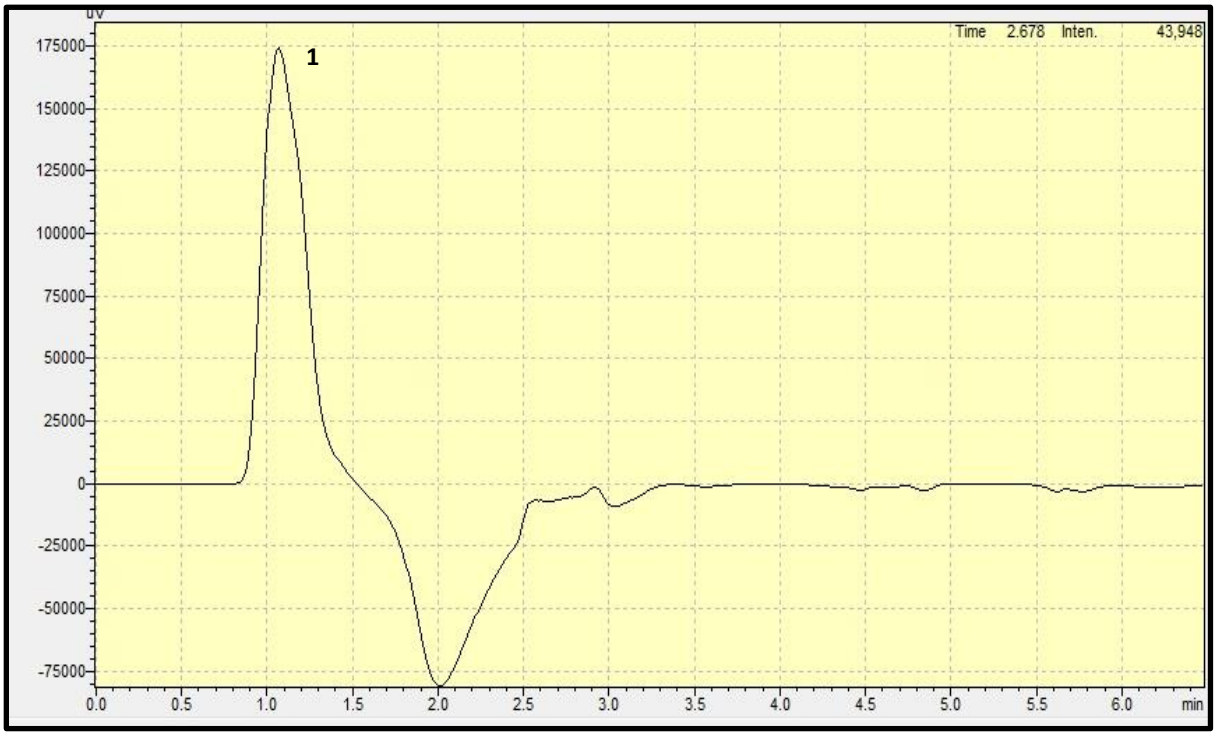

Figure (3.28):First derivative for a mixture of the pharmaceutical compounds (Propranolol hydrochloride, trifluoperazine dihydrochloride) (0.3 µg.mL^{-1}), at flow rate 1 mL.min^{-1}, (80:20)% water/ACN, λ=290 nm

But when using the second derivative, sharp and clear peaks appeared for both pharmaceutical compounds, and this indicates that the prepared column was separated by both compounds at different periods of time, although both compounds have the same interaction because they have the same active groups as in the figure(3.29).

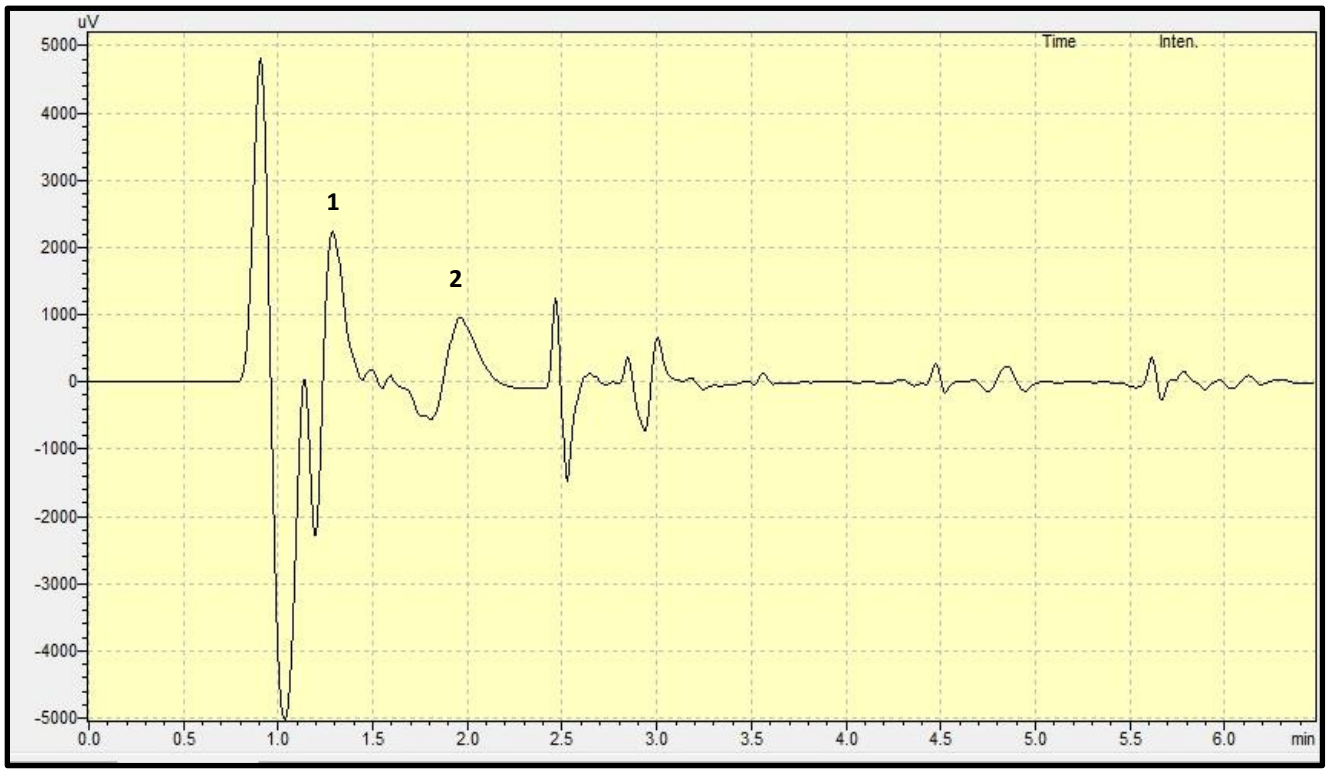

Figure (3.29) : second derivative for a pharmaceutical (Propranolol hydrochloride, trifluoperazine dihydrochloride) (0.3 µg.mL^{-1}), at flow rate 1 mL.min^{-1}, (80:20)% water/ACN, λ=290 nm

3.8 The efficiency of the monolithic column [103]

According to the plate theory, when the average number of theoretical plates (N) value is raised, the monolithic column's efficiency is raised within reason rise the instant equilibrium of the solute between the mobile phase and the stationary phase. The efficiency of the monolithic column was examined by computation (N) and (Rs) valuable, whereas The average number of theoretical plates (N) and the resolution value (Rs) for propranolol hydrochloride and trifluoperazine dihydrochloride employment HILC /HPLC monolithic column inside HPLC instrument (n=three).

Equations(3.1),(3.2) can calculate the number of theoretical plates (N) values.

N = L/H **(3.1)**

$N = 16(t_R / w_t)^2$ **(3.2)**

H: the height of a theoretical plate,**$w_{1/2}$**: is the width of the chromatographic peak at half its height, **t_R** : retention time.

By applying the above equation, it was found that the number of theoretical plates (N) values for the monolithic chromatographic column after being injected with a certain amount of solution propranolol hydrochloride is (**10.995 plates**) and the height of a theoretical plate is(**2.19mm/plates)** while the number of theoretical plates (N) values for the monolithic chromatographic column after being injected with a certain amount of solution trifluoperazine dihydrochloride is equal to (**11.102 plates**) and the height of a theoretical plate is (**2.22 mm/plate**).

3.9 Applications

The performance of the monolith column was evaluated by calculating the RSD% values for the process of propranolol hydrochloride and trifluoperazinedihydrochloride using the prepared monolithic, which was connected to the HPLC system (Shimadzu 2010A). The conditions were the mobile phase is (70:30)acetonitrile to water with a flow rate of 1 mL. min^{-1}, the wavelength is (290 nm) for propranolol hydrochloride, and the wavelength is (370nm) for tri fluo perazine dihydrochloride. The determination process of pharmaceutical compounds was carried out three times.

Table(3.8): shows the calculation of RSD values for the estimation process for each propranolol hydrochloride and trifluoperazine dihydrochloride.

Pharmaceutcal compounds	Theoretical value mg	Experimental value1 mg	Experimental value2 mg	Experimental value3 mg	RSD % n=3	E rel. %	t-test	f-test
Propanolol (accord)	10	9.62	9.67	9.73	1.02	-0.038	0.117	0.142
Triflupromazine (Hicma)	10	9.39	9.23	9.4	1.41	-0.061		

3.10 Conclusions

- The (GMA-co- EDMA-co-A.Am) monolithic column was successfully prepared inside a borosilicate tube using the UV polymerization method to produce HPLC monolithic columns (Chromatographic Column).
- The epoxy group in (GMA) were converted to form (diol groups) using HCl (0.2M); these groups can assist in determining various compounds such as pharmaceutical, biological and ionic compounds.
- It is found that the (GMA-co- EDMA-co-A.Am) monolithic column is formed after (3 min) irradiation time. The distance between the monolith column is investigated.
- The percentage of polymer swelling is tested using different solvents (polar, alcohol and mixture solvents), the result shows that water concedes a good solution for column solvent storage.
- The prepared monolithic column was demonstrated using SEM, BET, FTIR and ^{1}HNMR analysis. The results show that the polymer has three peaks denoting the presence of (C=O), epoxy group, and an NH_2 group. Whilst (C=C) peak in (the monomers) and (cross-linker) vanished, this is suitable proof for the figuration of the polymer by incorporation of both monomers and cross-linker using (C=C) bonds.
- The ^{1}HNMR analysis shows that the ($C=CH_2$) bonds around in the monomers and cross-linker have disappeared in the polymer ^{1}HNMR spectrum.
- The results of Brunauer-Emmett-Teller (BET) analyses are of large pore size and surface area, respectively. The results are satisfactory, as high flow rates are obtained with moderate back pressures, and the reactions are carried out on the surface without hindrances.
- The prepared monolithic column (GMA-co-EDMA-co-A.Am) was successfully used as a chromatographic column (HPLC Column) after opening the epoxy ring to determine

and separation pharmaceutical compounds (propranolol hydrochloride, trifluoperazine dihydrochloride)using(HPLC)technique.

3.11 Future Work

With the results conducted in this research, address some proposals for future work which would support this research, which is as follows:

- Development of monolithic columns using different monomers that have different properties for estimating and separating various samples.
- Study different porous (porogenic) solvents that can enhance the prepared monolith's morphological properties in this study.
- Investigate the length of the GMA-co- EDMA -co- A.Am monolithic columns and the effect on the separation performance.
- Developing more ways to modify the epoxy ring to expand the separation range of differentparticles.

References

1. Lanças FM. The role of the separation sciences in the 21th century. J Braz Chem Soc. 2003;14(2):183–97.
2. Harvey D. Modern Analytic Chemistry Spectroscopy. 2000;1–817.
3. Andrade-Eiroa A, Canle M, Leroy-Cancellieri V, Cerdà V. Solid-phase extraction of organic compounds: A critical review (Part I). TrAC - Trends Anal Chem [Internet]. 2016;80:641–54. Available from: http://dx.doi.org/10.1016/j.trac.2015.08.015
4. Poole CF. extraction [Internet]. Solid-Phase Extraction. Elsevier Inc.; 2020. 1–36 p. Available from: http://dx.doi.org/10.1016/B978-0-12-816906-3.00001-7
5. Arrua RD, Strumia MC, Igarzabal CIA. Macroporous monolithic polymers: Preparation and applications. Vol. 2, Materials. 2009. 2429–2466 p.
6. Qi T, Sonoda A, Makita Y, Kanoh H, Ooi K, Hirotsu T. Synthesis and borate uptake of two novel chelating resins. Ind Eng Chem Res. 2002;41(2):133–8.
7. Guiochon G. Monolithic columns in high-performance liquid chromatography. J Chromatogr A. 2007;1168(1–2):101–68.
8. Chiriac AE, Azoicai D, Coroaba A, Doroftei F, Timpu D, Chiriac A, et al. Raman spectroscopy, x-ray diffraction, and scanning electron microscopy as noninvasive methods for microstructural alterations in psoriatic nails. Molecules. 2021;26(2).
9. Union I, Pure OF, Chemistry A. Recommendations for the characterization of porous solids (Technical Report). Pure Appl Chem.

1994;66(8):1739–58.

10. Ma F wei, Kong S yuan, Tan H sheng, Wu R, Xia B, Zhou Y, et al. Structural characterization and antiviral effect of a novel polysaccharide PSP-2B from Prunellae Spica. Carbohydr Polym [Internet]. 2016;152:699–709. Available from: http://dx.doi.org/10.1016/j.carbpol.2016.07.062
11. Svec F, Fréchet JMJ. Continuous Rods of Macroporous Polymer as High-Performance Liquid Chromatography Separation Media. Anal Chem. 1992;64(7):820–2.
12. Barut M, Podgornik A, Urbas L, Gabor B, Brne P, Vidič J, et al. Methacrylate-based short monolithic columns: Enabling tools for rapid and efficient analyses of biomolecules and nanoparticles. J Sep Sci. 2008;31(11):1867–80.
13. Svec F. Porous polymer monoliths: Amazingly wide variety of techniques enabling their preparation. J Chromatogr A. 2010;1217(6):902–24.
14. Viklund C, Svec F, Fréchet JMJ, Irgum K. Monolithic, “molded”, porous materials with high flow characteristics for separations, catalysis, or solid-phase chemistry: Control of porous properties during polymerization. Chem Mater. 1996;8(3):744–50.
15. Khodabandeh A, Arrua RD, Thickett SC, Hilder EF. Utilizing RAFT Polymerization for the Preparation of Well-Defined Bicontinuous Porous Polymeric Supports: Application to Liquid Chromatography Separation of Biomolecules. ACS Appl Mater Interfaces. 2021;13(27):32075–83.
16. Unger KK, Skudas R, Schulte MM. Particle packed columns and

monolithic columns in high-performance liquid chromatography-comparison and critical appraisal. J Chromatogr A. 2008;1184(1–2):393–415.

17. Oberacher H, Huber CG. Capillary monoliths for the analysis of nucleic acids by high-performance liquid chromatography-electrospray ionization mass spectrometry. TrAC - Trends Anal Chem. 2002;21(3):166–74.
18. Pawlowski S, Nayak N, Meireles M, Portugal CAM, Velizarov S, Crespo JG. CFD modelling of flow patterns, tortuosity and residence time distribution in monolithic porous columns reconstructed from X-ray tomography data. Chem Eng J [Internet]. 2018;350:757–66. Available from: https://doi.org/10.1016/j.cej.2018.06.017
19. Liu Y, Zhou W, Mao Z, Chen Z. Analysis of Evodiae Fructus by capillary electrochromatography-mass spectrometry with methyl-vinylimidazole functionalized organic polymer monolilth as stationary phases. J Chromatogr A [Internet]. 2019;1602:474–80. Available from: https://doi.org/10.1016/j.chroma.2019.06.011
20. Alzahrani E. Polycarbonate Microchip Containing CuBTC-Monopol Monolith for Solid-Phase Extraction of Dyes. Int J Anal Chem. 2020;2020.
21. Zou H, Huang X, Ye M, Luo Q. Monolithic stationary phases for liquid chromatography and capillary electrochromatography. J Chromatogr A. 2002;954(1–2):5–32.
22. Li W, Xu P, Zhou H, Yang L, Liu H. Advanced functional nanomaterials with microemulsion phase. Sci China Technol Sci. 2012;55(2):387–416.

23. Dores-Sousa JL, Fernández-Pumarega A, De Vos J, Lämmerhofer M, Desmet G, Eeltink S. Guidelines for tuning the macropore structure of monolithic columns for high-performance liquid chromatography. J Sep Sci. 2019;42(2):522–33.
24. Carolius Angga S, Septiana D, Amalia S, Warsito, Dhiaul Iftitah E, Sabarudin A. Preparation of poly-(Gma-eda-β-cd-co-tmptma) monolith as high-performance liquid chromatography chiral stationary phase column. Indones J Chem. 2019;19(4):951–8.
25. Hoshina K, Horiyama S, Matsunaga H, Haginaka J. Molecularly imprinted polymers for simultaneous determination of antiepileptics in river water samples by liquid chromatography-tandem mass spectrometry. J Chromatogr A. 2009;1216(25):4957–62.
26. Carrasco-Correa EJ, Martínez-Vilata A, Herrero-Martínez JM, Parra JB, Maya F, Cerdà V, et al. Incorporation of zeolitic imidazolate framework (ZIF-8)-derived nanoporous carbons in methacrylate polymeric monoliths for capillary electrochromatography. Talanta [Internet]. 2017;164:348–54. Available from: http://dx.doi.org/10.1016/j.talanta.2016.11.027
27. Mansour FR, Arrua RD, Desire CT, Hilder EF. Non-ionic Surface Active Agents as Additives toward a Universal Porogen System for Porous Polymer Monoliths. Anal Chem. 2021;93(5):2802–10.
28. Aydoğan C, Gökaltun A, Denizli A, El Rassi Z. Biochromatographic applications of polymethacrylate monolithic columns used in electro- and liquid phase-separationsΨ. J Liq Chromatogr Relat Technol [Internet]. 2018;41(10):572–82. Available from:

https://doi.org/10.1080/10826076.2018.1462204

29. Dores-Sousa JL, Terryn H, Eeltink S. Morphology optimization and assessment of the performance limits of high-porosity nanostructured polymer monolithic capillary columns for proteomics analysis. Anal Chim Acta [Internet]. 2020;1124:176–83. Available from: https://doi.org/10.1016/j.aca.2020.05.019
30. Svec F. My favorite materials: Porous polymer monoliths. J Sep Sci. 2009;32(1):3–9.
31. Patrushev Y, Yudina Y, Sidelnikov V. Monolithic rod columns for HPLC based on divinylbenzene-styrene copolymer with 1-vinylimidazole and 4-vinylpyridine. J Liq Chromatogr Relat Technol [Internet]. 2018;41(8):458–66. Available from: https://doi.org/10.1080/10826076.2018.1455149
32. Lubomirsky E, Khodabandeh A, Preis J, Susewind M, Hofe T, Hilder EF, et al. Polymeric stationary phases for size exclusion chromatography: A review. Anal Chim Acta [Internet]. 2021;1151:338244. Available from: https://doi.org/10.1016/j.aca.2021.338244
33. NISHIMURA N, NAITO T, KUBO T, OTSUKA K. Suppression of Hydrophobicity and Optimizations of a Ligand-Immobilization for Effective Affinity Chromatography Using a Spongy Monolith. Chromatography. 2018;39(3):113–8.
34. Pack BW, Risley DS. Evaluation of a monolithic silica column operated in the hydrophilic interaction chromatography mode with evaporative light scattering detection for the separation and detection of counter-ions. J

Chromatogr A. 2005;1073(1–2):269–75.

35. Echevarría RN, Keunchkarian S, Villarroel-Rocha J, Sapag K, Reta M. Organic monolithic capillary columns coated with cellulose tris(3,5-dimethylphenyl carbamate) for enantioseparations by capillary HPLC. Microchem J [Internet]. 2019;149:104011. Available from: https://doi.org/10.1016/j.microc.2019.104011
36. Trojer L, Lubbad SH, Bisjak CP, Wieder W, Bonn GK. Comparison between monolithic conventional size, microbore and capillary poly(p-methylstyrene-co-1,2-bis(p-vinylphenyl)ethane) high-performance liquid chromatography columns. Synthesis, application, long-term stability and reproducibility. J Chromatogr A. 2007;1146(2):216–24.
37. Meunier DM, Smith PB, Baker SA. Separation of polymers by molecular topology using monolithic columns. Macromolecules. 2005;38(12):5313–20.
38. Li M, Lei X, Huang Y, Guo Y, Zhang B, Tang F, et al. Ternary thiol-ene photopolymerization for facile preparation of ionic liquid-functionalized hybrid monolithic columns based on polyhedral oligomeric silsesquioxanes. J Chromatogr A [Internet]. 2019;1597:167–78. Available from: https://doi.org/10.1016/j.chroma.2019.03.032
39. Karabat RR, Rasheed AS, Hassan MJM. A new method in some german grape wines using ZIC-HILIC technology with UV detection to separate and identify quercetin. Plant Arch. 2020;20(1):2692–6.
40. Svec F. Quest for organic polymer-based monolithic columns affording enhanced efficiency in high performance liquid chromatography

separations of small molecules in isocratic mode. J Chromatogr A [Internet]. 2012;1228:250–62. Available from: http://dx.doi.org/10.1016/j.chroma.2011.07.019

41. Jandera P. Advances in the development of organic polymer monolithic columns and their applications in food analysis - A review. J Chromatogr A [Internet]. 2013;1313:37–53. Available from: http://dx.doi.org/10.1016/j.chroma.2013.08.010
42. Gambero A, Kubota LT, Gushikem Y, Airoldi C, Granjeiro JM, Taga EM, et al. Use of chemically modified silica with β-diketoamine groups for separation of α-lactoalbumin from bovine milk whey by affinity chromatography. J Colloid Interface Sci. 1997;185(2):313–6.
43. WEN X, ZHENG HJ, ZHANG Y, JIA Q. Progress in Monolithic Column-based Separation and Enrichment of Glycoproteins. Chinese J Anal Chem [Internet]. 2020;48(1):13–21. Available from: http://dx.doi.org/10.1016/S1872-2040(19)61207-7
44. Patil AA, Chiang CK, Wen CH, Peng WP. Forced dried droplet method for MALDI sample preparation. Anal Chim Acta [Internet]. 2018;1031:128–33. Available from: https://doi.org/10.1016/j.aca.2018.05.056
45. Bignardi C, Elviri L, Penna A, Careri M, Mangia A. Particle-packed column versus silica-based monolithic column for liquid chromatography-electrospray-linear ion trap-tandem mass spectrometry multiallergen trace analysis in foods. J Chromatogr A [Internet]. 2010;1217(48):7579–85. Available from: http://dx.doi.org/10.1016/j.chroma.2010.10.037

46. Jal PK, Patel S, Mishra BK. Chemical modification of silica surface by immobilization of functional groups for extractive concentration of metal ions. Talanta. 2004;62(5):1005–28.
47. Moravcová D, Planeta J. Silica Monolithic Capillary Columns for Hilic Separations. Hungarian J Ind Chem. 2018;46(1):39–42.
48. Gao YR, Cao JF, Shu Y, Wang JH. Research progress of ionic liquids-based gels in energy storage, sensors and antibacterial. Green Chem Eng [Internet]. 2021;2(4):368–83. Available from: https://doi.org/10.1016/j.gce.2021.07.012
49. Kato M, Sakai-Kato K, Toyo'oka T. Silica sol-gel monolithic materials and their use in a variety of applications. J Sep Sci. 2005;28(15):1893–908.
50. Zarcula C, Claudia K, Corici L, Croitoru R, Csunderlik C, Peter F. Combined sol-gel entrapment and adsorption method to obtain solid-phase lipase biocatalyts. Rev Chim. 2009;60(9):922–7.
51. Gill I, Ballesteros A. Bioencapsulation within synthetic polymers (Part 1): sol-gel encapsulated biologicals. Trends Biotechnol [Internet]. 2000;18(7):282–96. Available from: http://www.ncbi.nlm.nih.gov/pubmed/10950510
52. Kobayashi H, Ikegami T, Kimura H, Hara T, Tokuda D, Tanaka N. Properties of monolithic silica columns for HPLC. Anal Sci. 2006;22(4):491–501.
53. Bai L, Liu H, Liu Y, Zhang X, Yang G, Ma Z. Preparation of a novel hybrid organic-inorganic monolith for the separation of lysozyme by high

performance liquid chromatography. J Chromatogr A [Internet]. 2011;1218(1):100–6. Available from: http://dx.doi.org/10.1016/j.chroma.2010.10.115

54. Xu L, Lee HK. Preparation, characterization and analytical application of a hybrid organic-inorganic silica-based monolith. J Chromatogr A. 2008;1195(1–2):78–84.
55. Jandera P, Urban J, Moravcová D. Polymetacrylate and hybrid interparticle monolithic columns for fast separations of proteins by capillary liquid chromatography. J Chromatogr A. 2006;1109(1):60–73.
56. Nakanishi K, Shikata H, Ishizuka N, Koheiya N, Soga N. Tailoring mesopores in monolithic macroporous silica for HPLC. HRC J High Resolut Chromatogr. 2000;23(1):106–10.
57. Nema T, Chan ECY, Ho PC. Application of silica-based monolith as solid phase extraction cartridge for extracting polar compounds from urine. Talanta. 2010;82(2):488–94.
58. Poddar S, Sharmeen S, Hage DS. Affinity monolith chromatography: A review of general principles and recent developments. Electrophoresis. 2021;42(24):2577–98.
59. Wu C, Liang Y, Zhu X, Zhao Q, Fang F, Zhang X, et al. Macro-mesoporous organosilica monoliths with bridged-ethylene and terminal-vinyl: High-density click functionalization for chromatographic separation. Anal Chim Acta. 2018;1038:198–205.
60. Nassar EJ, Gonçalves RR, Ferrari M, Messaddeq Y, Ribeiro SJL. Titania-based organic-inorganic hybrid planar waveguides. J Alloys Compd.

2002;344(1–2):221–5.

61. Nishio K, Tsuchiya T. Organic-inorganic hybrid ionic conductor prepared by sol-gel process. Sol Energy Mater Sol Cells. 2001;68(3–4):295–306.
62. Wei Y, Jin D, Xu J, Baran G, Qiu KY. Mechanical properties of interface-free polycrylate-silica hybrid sol-gel materials for potential dental applications. Polym Adv Technol. 2001;12(6):361–8.
63. Noble K, Seddon AB. Porous Siloxane-Silica Hybrid Materials by Sol-Gel Processing. 2003;2003.
64. Sun J, Akdogan EK, Klein LC, Safari A. Characterization and optical properties of sol-gel processed PMMA/SiO2 hybrid monoliths. J Non Cryst Solids. 2007;353(29):2807–12.
65. Zhu T, Row KH. Preparation and applications of hybrid organic-inorganic monoliths: A review. J Sep Sci. 2012;35(10–11):1294–302.
66. Past T. + 1) (1). 1991;116(December):1237–44.
67. Duemichen E, Braun U, Senz R, Fabian G, Sturm H. Assessment of a new method for the analysis of decomposition gases of polymers by a combining thermogravimetric solid-phase extraction and thermal desorption gas chromatography mass spectrometry. J Chromatogr A [Internet]. 2014;1354:117–28. Available from: http://dx.doi.org/10.1016/j.chroma.2014.05.057
68. Hassan SA, Nashat NW, Elghobashy MR, Abbas SS, Moustafa AA. Stability-indicating rp-hplc and ce methods for simultaneous determination of bisoprolol and perindopril in pharmaceutical formulation: A comparative study. J Chromatogr Sci. 2020;58(8):747–58.

69. Bhoj Y, Tharmavaram M, Pandey G, Rawtani D, Mustansar Hussain C. Chromatographic Techniques for Forensic Investigations. Technol Forensic Sci. 2020;129–49.
70. Chen A, Liu S, Yang Y, Xiang P. Liquid chromatographic separation using a 2 μm i.d. open tubular column at elevated temperature. Anal Chem. 2021;93(10):4361–4.
71. Maraie NK, Neamah MJ. Application of proniosomal powder technology to prepare fast water dissolving tablets for dutasteride. J Glob Pharma Technol. 2018;10(3):916–27.
72. Abidi SL. High-performance liquid chromatography of phosphatidic acids and related polar lipids. J Chromatogr A. 1991;587(2):193–203.
73. Ma Y, Tanaka N, Vaniya A, Kind T, Fiehn O. Ultrafast Polyphenol Metabolomics of Red Wines Using MicroLC-MS/MS. J Agric Food Chem. 2016;64(2):505–12.
74. Miller JD, Knapp EE, Key CH, Skinner CN, Isbell CJ, Creasy RM, et al. Calibration and validation of the relative differenced Normalized Burn Ratio (RdNBR) to three measures of fire severity in the Sierra Nevada and Klamath Mountains, California, USA. Remote Sens Environ [Internet]. 2009;113(3):645–56. Available from: http://dx.doi.org/10.1016/j.rse.2008.11.009
75. Scott RPW. Chrom-Ed Book Series LIQUID.
76. Tamer MA, Ahmed KK, Muhsin Z. Nanocrystal technology as a tool for improving dissolution of poorly soluble drugs. J Glob Pharma Technol. 2019;11(5):180–92.

77. Davis DP, Bramwell KJ, Hamilton RS, Williams SR. Ethylene glycol poisoning: Case report of a record-high level and a review. J Emerg Med. 1997;15(5):653–67.
78. Zhu BY, Mant CT, Hodges RS. Mixed-mode hydrophilic and ionic interaction chromatography rivals reversed-phase liquid chromatography for the separation of peptides. J Chromatogr A. 1992;594(1–2):75–86.
79. Poole CF. Stationary phases for packed-column supercritical fluid chromatography. J Chromatogr A [Internet]. 2012;1250:157–71. Available from: http://dx.doi.org/10.1016/j.chroma.2011.12.040
80. Wells MJM, Clark CR. Hydrophobic Substituent Constants Derived by Intracolumn Biiogarithmic Analysis of Reversed-Phase Liquid Chromatographic Retention of 4,4'-Disubstituted Benzanilides and Benzamides. Anal Chem. 1992;64(15):1660–8.
81. Gritti F, Hlushkou D, Tallarek U. Faster dewetting of water from C8- than from C18-bonded silica particles used in reversed-phase liquid chromatography: Solving the paradox. J Chromatogr A [Internet]. 2019;1602:253–65. Available from: https://doi.org/10.1016/j.chroma.2019.05.041
82. Marcos S, Werner JS, Burns SA, Merigan WH, Artal P, Atchison DA, et al. Vision science and adaptive optics, the state of the field. Vision Res [Internet]. 2017;132:3–33. Available from: http://dx.doi.org/10.1016/j.visres.2017.01.006
83. Martire DE, Boehm RE. Unified theory of retention and selectivity in liquid chromatography. 2. Reversed-phase liquid chromatography with

chemically bonded phases. J Phys Chem. 1983;87(6):1045–62.

84. Dill KA. The mechanism of solute retention in reversed-phase liquid chromatography. J Phys Chem. 1987;91(7):1980–8.
85. Dill KA, Naghizadeh J, Marqusee JA. Chain molecules at high densities at interfaces. Annu Rev Phys Chem. 1988;39:425–61.
86. Mallik AK, Qiu H, Takafuji M, Ihara H. High molecular-shape-selective stationary phases for reversed-phase liquid chromatography: A review. TrAC - Trends Anal Chem [Internet]. 2018;108:381–404. Available from: https://doi.org/10.1016/j.trac.2018.09.003
87. Hamed YAAH, Rasheed AS. Zwitterionic ion chromatography coupled with ultraviolet detection for the quantification of 2-deoxyguanosine in human serum. Syst Rev Pharm. 2020;11(3):240–6.
88. Review M, Ec E, Ib O, Va W. Applications of Column, Paper, Thin Layer and Ion Exchange Chromatography in Purifying Samples: Mini Review OPEN ACCESS Background: Historical Perspective. SF J Pharm Anal Chem [Internet]. 2019;2(November). Available from: https://scienceforecastoa.com/
89. Lucy CA. Evolution of ion-exchange: From Moses to the Manhattan Project to Modern Times. J Chromatogr A. 2003;1000(1–2):711–24.
90. Mant CT, Hodges RS. Mixed-mode hydrophilic interaction/cation-exchange chromatography (HILIC/CEX) of peptides and proteins. J Sep Sci. 2008;31(15):2754–73.
91. Abed EF, Alkarimi AA. Ion Exchange Monolithic Column for Copper Determination. Acta Chem Iasi. 2021;29(2):151–65.

92. Knudsen HL, Fahrner RL, Xu Y, Norling LA, Blank GS. Membrane ion-exchange chromatography for process-scale antibody purification. J Chromatogr A. 2001;907(1–2):145–54.
93. Lukács D, Horváth K, Hajós P. Development of retention mechanism for the separation of carboxylic acids and inorganic anions in cryptand-based ion chromatography. J Chromatogr A. 2020;1621(xxxx).
94. Jose S, Kingdom U. Elsevier Science Publishers B . V ., Amsterdam - Printed in The Netherlands © 1987 Elsevier Science Publishers B . V . 1987;44:305–16.
95. Alpert AJ. Effect of salts on retention in hydrophilic interaction chromatography. J Chromatogr A [Internet]. 2018;1538:45–53. Available from: http://dx.doi.org/10.1016/j.chroma.2018.01.038
96. Li Q, Huang Y, Zhang Y, Cui H, Yin L, Li Y, et al. A novel HPLC method for analysis of atosiban and its five related substances in atosiban acetate injection. J Pharm Biomed Anal [Internet]. 2020;177:112808. Available from: https://doi.org/10.1016/j.jpba.2019.112808
97. Alpert AJ. Hydrophilic-interaction chromatography for the separation of peptides, nucleic acids and other polar compounds. J Chromatogr A. 1990;499(C):177–96.
98. Yeung D, Klaassen N, Mizero B, Spicer V, Krokhin O V. Peptide retention time prediction in hydrophilic interaction liquid chromatography: Zwitter-ionic sulfoalkylbetaine and phosphorylcholine stationary phases. J Chromatogr A. 2020;1619(xxxx):1–8.
99. Hemström P, Irgum K. Hydrophilic interaction chromatography. Vol. 29,

Journal of Separation Science. 2006. 1784–1821 p.

100. Ibrahim MEA, Wahab MF, Lucy CA. Hybrid carbon nanoparticles modified core-shell silica: A high efficiency carbon-based phase for hydrophilic interaction liquid chromatography. Anal Chim Acta [Internet]. 2014;820:187–94. Available from: http://dx.doi.org/10.1016/j.aca.2014.02.034
101. Snyder LR. A rapid approach to selecting the best experimental conditions for high-speed liquid column chromatography part ii—estimating column length, operating pressure and separation time for some required sample resolution. J Chromatogr Sci. 1972;10(6):369–79.
102. Antakli S, Nejem L, Shawa D. Determination of height equivalent to a theoretical plate and van deemter constants for C8 and C18 columns by using high performance liquid chromatography. Res J Pharm Technol. 2018;11(4):1603–11.
103. Harvey D. Modern Analyitical Chemistry - David Harvey. 2004;1–817.
104. Klinkenberg A, Zuiderweg FJ. Longitudinal diffusion and resistance to mass transfer as causes of nonideality in chromatography. Chem Eng Sci. 1956;5(6):271–89.
105. Carrasco-Correa EJ, Ramis-Ramos G, Herrero-Martínez JM. Hybrid methacrylate monolithic columns containing magnetic nanoparticles for capillary electrochromatography. J Chromatogr A [Internet]. 2015;1385:77–84. Available from: http://dx.doi.org/10.1016/j.chroma.2015.01.044
106. Tang S, Duan Y, Chang F, Jiang W, Zhang F, Liu Z, et al. The fabrication

of carboxylic acid-functionalized porous layer open tube column and its application in hydrophilic interaction chromatography for small polar molecules. J Liq Chromatogr Relat Technol [Internet]. 2020;43(19–20):913–24. Available from: https://doi.org/10.1080/10826076.2020.1848864

107. Wang X, Hao T, Qu J, Wang C, Chen H. Synthesis of thermal polymerizable alginate-GMA hydrogel for cell encapsulation. J Nanomater. 2015;2015.
108. He S, Wu W, Wang R, Pu W, Chen Y. Investigation on the polyamide 6/SEBS-g-MA/organoclay nanocomposites with glycidyl methacrylate as a compatibilizer. Polym - Plast Technol Eng. 2011;50(7):719–26.
109. Bandari R, Elsner C, Knolle W, Kühnel C, Decker U, Buchmeiser MR. Separation behavior of electron-beam curing derived, acrylate-based monoliths. J Sep Sci. 2007;30(17):2821–7.
110. Fernández-Pumarega A, Dores-Sousa JL, Eeltink S. A comprehensive investigation of the peak capacity for the reversed-phase gradient liquid-chromatographic analysis of intact proteins using a polymer-monolithic capillary column. J Chromatogr A. 2020;1609.
111. Oktavia B, Prasmi Kardi R. Fabrication of methacrylate polymer-based on the silica capillary modified with dimethylamine. J Phys Conf Ser. 2020;1481(1).
112. do Nascimento FH, Moraes AH, Trazzi CRL, Velasques CM, Masini JC. Fast construction of polymer monolithic columns inside fluorinated ethylene propylene (FEP) tubes for separation of proteins by reversed-

phase liquid chromatography. Talanta [Internet]. 2020;217(April):121063. Available from: https://doi.org/10.1016/j.talanta.2020.121063

113. Huang L, Yu W, Guo X, Huang Y, Zhou Q, Zhai H. Chip-based multi-molecularly imprinted monolithic capillary array columns coated Fe3O4/GO for selective extraction and simultaneous determination of tetracycline, chlortetracycline and deoxytetracycline in eggs. Microchem J [Internet]. 2019;150:104097. Available from: https://doi.org/10.1016/j.microc.2019.104097
114. Krenkova J, Lacher NA, Svec F. Control of selectivity via nanochemistry: Monolithic capillary column containing hydroxyapatite nanoparticles for separation of proteins and enrichment of phosphopeptides. Anal Chem. 2010;82(19):8335–41.
115. Krishnasamy B, Shanmugaraj BP, Murugavel SC, Dai L, Petri DFS. Investigation on dual functional epoxy resins containing photosensitive group in the main chain for photoresist applications. Int J Polym Anal Charact [Internet]. 2020;25(4):198–215. Available from: https://doi.org/10.1080/1023666X.2020.1780849
116. Goswami PK, Kashyap M, Das PP, Saikia PJ, Handique JG. Poly(Glycidyl Methacrylate-co-Octadecyl Methacrylate) particles by dispersion radical copolymerization. J Dispers Sci Technol [Internet]. 2020;41(12):1768–76. Available from: https://doi.org/10.1080/01932691.2019.1635026
117. Tennikova TB. Review Preparation of methacrylate monoliths. 2007;2801–13.

118. Ehme FRWO. Environmental Degradation of Polyacrylamides . 1 . Effects of Artificial Environmental Conditions : Temperature , Light , and pH. 1996;135:121–35.
119. Sun J, Li M, Zou F, Bai S, Jiang X, Tian L, et al. Protection of cyanidin-3-O-glucoside against acrylamide- and glycidamide-induced reproductive toxicity in leydig cells. Food Chem Toxicol [Internet]. 2018; Available from: https://doi.org/10.1016/j.fct.2018.03.027
120. Mallevialle J, Bruchet A, Fiessinger F. How Safe Are Organic Polymers in Water Treatment ? 1984;(C):87–93.
121. Bologna LS, Andrawes FF, Barvenik FW, Lentz RD, Sojka RE. Analysis of Residual Acrylamide In Field Crops. 1999;37(July):240–4.
122. Leibl N, Haupt K, Gonzato C, Duma L. Molecularly Imprinted Polymers for Chemical Sensing : A Tutorial Review. 2021;1–19.
123. Yu C, Xu M, Svec F, Fréchet JMJ. Preparation of monolithic polymers with controlled porous properties for microfluidic chip applications using photoinitiated free-radical polymerization. J Polym Sci Part A Polym Chem. 2002;40(6):755–69.
124. del Mar Orta M, Martín J, Medina-Carrasco S, Santos JL, Aparicio I, Alonso E. Adsorption of propranolol onto montmorillonite: Kinetic, isotherm and pH studies. Appl Clay Sci [Internet]. 2019;173(July 2018):107–14. Available from: https://doi.org/10.1016/j.clay.2019.03.015
125. Attimarad M, Alkadham A, Almosawi MH, Venugopala KN. Development of rapid and validated RP-HPLC method for concurrent quantification of rosuvastatin and aspirin form solid dosage form. Indian J

Pharm Educ Res. 2018;52(1):151–8.

126. Hptlc V, For M, Estimation S, Sodium OFD, In CP, Form TD. Validated Hptlc Method for Simultaneous Estimation of Dicloxacillin Sodium and Cefpodoxime Proxetil in. 2018;7(9):1048–57.
127. Hamzah MH, Taqi RMM, Hasan MM, Al-Timimi RJM. Spectrophotometeric Determination of Trifluoperazine HCL in Pure Forms and Pharmaceutical Preperations. Int J Pharm Clin Res. 2017;9(5):337–42.
128. Kiran Kumari Subhankar Nanda, M.J.Saxena, K. Ravikanth and Shivi Maini SPT. Studies on comparative efficacy of herbal amino acid Studies on comparative efficacy of herbal amino acid (Methiorep) supplement with synthetic DL methionine on broiler growth performance and carcass quality traits. Ijser. 2012;2(8):307–9.
129. Hara T, Izumi Y, Hata K, Baron VG, Bamba T, Desmet G. Performance of small-domain monolithic silica columns in nano-liquid chromatography and comparison with commercial packed bed columns with 2 μm particles. J Chromatogr A [Internet]. 2020;1616:460804. Available from: https://doi.org/10.1016/j.chroma.2019.460804
130. Kubín M, Špaček P, Chromeček R. Gel permeation chromatography on porous poly(ethylene glycol methacrylate). Collect Czechoslov Chem Commun. 1967;32(11):3881–7.
131. Wang J, Lü H, Lin X, Xie Z. Monolithic column with double mixed-modes of hydrophilic interaction/ cation-exchange and reverse-phase/cation-exchange stationary phase for pressurized capillary

electrochromatography. Electrophoresis. 2008;29(4):928–35.

132. El-Ries MA, Abou Attia FM, Ibrahim SA. AAS and spectrophotometric determination of propranolol HCl and metoprolol tartrate. J Pharm Biomed Anal. 2000;24(2):179–87.

133. Šatínský D, Chocholouš P, Salabová M, Solich P. Simple determination of betamethasone and chloramphenicol in a pharmaceutical preparation using a short monolithic column coupled to a sequential injection system. J Sep Sci. 2006;29(16):2494–9.

134. Aboul-Enein HY, Ali I. Determination of tadalafil in pharmaceutical preparation by HPLC using monolithic silica column. Talanta. 2005;65(1):276–80.

135. Albekairi N, Aqel A, ALOthman ZA. Simultaneous Capillary Liquid Chromatography Determination of Drugs in Pharmaceutical Preparations Using Tunable Platforms of Polymethacrylate Monolithic Columns Modified with Octadecylamine. Chromatographia. 2019;82(7):1003–15.

136. Mutaz ES, Aqel A, Abdulkhair BY, Obbed MS, ALOthman ZA, Badjah-Hadj-Ahmed Y, et al. Preparation and Characterization of Glycidyl Polymethacrylate Monolith Column and its Application for Simultaneous Determination of Paracetamol and Chlorzoxazone in Their Combined Pharmaceutical Formulations. J Anal Chem. 2020;75(11):1435–42.

137. Lin X, Wang J, Li L, Wang X, Lü H, Xie Z. Separation and determination of five major opium alkaloids with mixed mode of hydrophilic/cation-exchange monolith by pressurized capillary electrochromatography. J Sep Sci. 2007;30(17):3011–7.

138. Ahmed M, Yajadda MMA, Han ZJ, Su D, Wang G, Ostrikov KK, et al. Single-walled carbon nanotube-based polymer monoliths for the enantioselective nano-liquid chromatographic separation of racemic pharmaceuticals. J Chromatogr A [Internet]. 2014;1360:100–9. Available from: http://dx.doi.org/10.1016/j.chroma.2014.07.052
139. Sultan M, Stecher G, Stoggl W, Bakry R, Zaborski P, Huck C, et al. Sample Pretreatment and Determination of Non Steroidal Anti-Inflammatory Drugs (NSAIDs) in Pharmaceutical Formulations and Biological Samples (Blood, Plasma, Erythrocytes) by HPLC-UV-MS and μ-HPLC. Curr Med Chem. 2012;12(5):573–88.
140. Marques KL, Santos JLM, Lima JLFC. Chemiluminometric determination of propranolol in an automated multicommutated flow system. J Pharm Biomed Anal. 2005;39(5):886–91.
141. Zahálka L, Matysová L, Šklubalová Z, Klovrzová S, Solich P. Simultaneous determination of propranolol hydrochloride and sodium benzoate in oral liquid preparations by HPLC. Chromatographia. 2013;76(21–22):1553–8.
142. Abdel-Moety EM, Al-Deeb OA. Stability-indicating liquid chromatographic determination of trifluoperazine hydrochloride in bulk form and tablets. Eur J Pharm Sci. 1997;5(1):1–5.
143. Chen L, Ma H, Liu X, Sheng XJ. Semipreparative enantiomer separation of propranolol hydrochloride by high-performance liquid chromatography using cellulose tris(3,5- dimethylphenylcarbamate) chiral stationary phase. J Chromatogr Sci. 2008;46(9):767–71.

144. Svec F, Fréchet JMJ. Modified poly(glycidyl metharylate-co-ethylene dimethacrylate) continuous rod columns for preparative-scale ion-exchange chromatography of proteins. J Chromatogr A. 1995;702(1–2):89–95.
145. Viklund C, Svec F, Fre JMJ. Fast Ion-Exchange HPLC of Proteins Using Porous Poly (glycidyl methacrylate- co -ethylene dimethacrylate) Monoliths Grafted with Poly (2-acrylamido-2-methyl-1-propanesulfonic acid). 1997;597–600.
146. Jiao X, Shen S, Shi T. One-pot preparation of a novel monolith for high performance liquid chromatography applications. J Chromatogr B Anal Technol Biomed Life Sci [Internet]. 2015;1007:100–9. Available from: http://dx.doi.org/10.1016/j.jchromb.2015.10.028
147. Lin Z, Huang H, Sun X, Lin Y, Zhang L, Chen G. Monolithic column based on a poly(glycidyl methacrylate-co-4-vinylphenylboronic acid-co-ethylene dimethacrylate) copolymer for capillary liquid chromatography of small molecules and proteins. J Chromatogr A [Internet]. 2012;1246:90–7. Available from: http://dx.doi.org/10.1016/j.chroma.2012.02.056
148. Sabarudin A, Huang J, Shu S, Sakagawa S, Umemura T. Preparation of methacrylate-based anion-exchange monolithic microbore column for chromatographic separation of DNA fragments and oligonucleotides. Anal Chim Acta [Internet]. 2012;736:108–14. Available from: http://dx.doi.org/10.1016/j.aca.2012.05.039
149. Terborg L, Masini JC, Lin M, Lipponen K, Riekolla ML, Svec F. Porous

polymer monolithic columns with gold nanoparticles as an intermediate ligand for the separation of proteins in reverse phase-ion exchange mixed mode. J Adv Res [Internet]. 2015;6(3):441–8. Available from: http://dx.doi.org/10.1016/j.jare.2014.10.004

150. Wang M, Xu J, Zhou X, Tan T. Preparation and characterization of polyethyleneimine modified ion-exchanger based on poly(methacrylate-co-ethylene dimethacrylate) monolith. J Chromatogr A. 2007;1147(1):24–9.
151. Wei Y, Huang X, Liu R, Shen Y, Geng X. Preparation of a monolithic column for weak cation exchange chromatography and its application in the separation of biopolymers. J Sep Sci. 2006;29(1):5–13.
152. Quigley WWC, Dovichi NJ. Quigley.CEreview.101113.pdf. 2004;76(16):4645–58.
153. Peterson DS, Rohr T, Svec F, Fréchet JMJ. Enzymatic microreactor-on-a-chip: Protein mapping using trypsin immobilized on porous polymer monoliths molded in channels of microfluidic devices. Anal Chem. 2002;74(16):4081–8.
154. Ueki Y, Umemura T, Li J, Odake T, Tsunoda KI. Preparation and application of methacrylate-based cation-exchange monolithic columns for capillary ion chromatography. Anal Chem. 2005;76(23):7007–12.
155. Huo Y, Schoenmakers PJ, Kok WT. Efficiency of methacrylate monolithic columns in reversed-phase liquid chromatographic separations. J Chromatogr A. 2007;1175(1):81–8.
156. Armenta JM, Gu B, Thulin CD, Lee ML. Coupled affinity-hydrophobic

monolithic column for on-line removal of immunoglobulin G, preconcentration of low abundance proteins and separation by capillary zone electrophoresis. J Chromatogr A. 2007;1148(1):115–22.

157. Fresco-Cala B, Cárdenas S, Valcárcel M. Preparation and evaluation of micro and meso porous silica monoliths with embedded carbon nanoparticles for the extraction of non-polar compounds from waters. J Chromatogr A [Internet]. 2016;1468:55–63. Available from: http://dx.doi.org/10.1016/j.chroma.2016.09.047
158. Hebb AK, Senoo K, Bhat R, Cooper AI. Structural control in porous cross-linked poly(methacrylate) monoliths using supercritical carbon dioxide as a “pressure-adjustable” porogenic solvent. Chem Mater. 2003;15(10):2061–9.
159. Safa KD, Nasirtabrizi MH. Ring opening reactions of glycidyl methacrylate copolymers to introduce bulky organosilicon side chain substituents. Polym Bull. 2006;57(3):293–304.
160. Samanta S, Chatterjee DP, Layek RK, Nandi AK. Nano-structured poly(3-hexyl thiophene) grafted on poly(vinylidene fluoride) via poly(glycidyl methacrylate). J Mater Chem. 2012;22(21):10542–51.
161. Labbé A, Brocas AL, Ibarboure E, Ishizone T, Hirao A, Deffieux A, et al. Selective ring-opening polymerization of glycidyl methacrylate: Toward the synthesis of cross-linked (co)polyethers with thermoresponsive properties. Macromolecules. 2011;44(16):6356–64.
162. Courtois J, Szumski M, Byström E, Iwasiewicz A, Shchukarev A, Irgum K. A study of surface modification and anchoring techniques used in the

preparation of monolithic microcolumns in fused silica capillaries. J Sep Sci. 2006;29(1):14–24.

163. Alkarimi AA. terpolymers for mixed mode LC separations. 2018;(January).
164. Barner-Kowollik C, Davis TP, Stenzel MH. Probing mechanistic features of conventional, catalytic and living free radical polymerizations using soft ionization mass spectrometric techniques. Polymer (Guildf). 2004;45(23):7791–805.
165. Inkson BJ. Scanning Electron Microscopy (SEM) and Transmission Electron Microscopy (TEM) for Materials Characterization [Internet]. Materials Characterization Using Nondestructive Evaluation (NDE) Methods. Elsevier Ltd; 2016. 17–43 p. Available from: http://dx.doi.org/10.1016/B978-0-08-100040-3.00002-X
166. Assumptions THE. B.e.t. 1960;2–5.
167. Costelloe TM. Kant’s Conception of Moral Character: The "Critical" Link of Morality, Anthropology, and Reflective Judgment (review). J Hist Philos. 2001;39(3):445–6.
168. Rohr T, Hilder EF, Donovan JJ, Svec F, Fréchet JMJ. Photografting and the control of surface chemistry in three-dimensional porous polymer monoliths. Macromolecules. 2003;36(5):1677–84.

Appendix

Statistical Calculations:

Appendix (A)

Below are the special relationships for calculating the values of standard deviation, percentage standard deviation (% R.S.D), percentage error (% E_{rel}) and percentage recovery (% Rec).

1- $\bar{y} = \frac{\sum y_i}{n}$

Whereas:

$\bar{Y}$: Absorption rate

n:Number of readings

2- $\sigma = \sqrt{\frac{\sum (Y_i - \bar{Y})\text{^}2}{n-1}}$

σ = S.D : standard deviation

3- $\boldsymbol{RSD\%} = \frac{\sigma}{\bar{\boldsymbol{Y}}} \times 100$

R.S.D% : Percentage measurement deviation

4- $\%E_{rel} = \frac{d}{\mu} \times 100$

% E_{rel} = percentage error

d : The absolute error is equal to the difference between the measured analytical value and the true value (μ)of the concentrations.

5- Recovery% = E% + 100

Or

Recovery% = $\mathbf{x_i/u} \times 100$

$\mathbf{X_i}$: Analytical result measured (concentration)

u : The real result (the concentrations).

Appendix (B)

The special relationships for calculating the correlation coefficient(r), the slope(b), the point of intersection(a), the straight line equation, the different curves, the standard deviation of the slope, the point of intersection, and the special relationships for calculating the detection of limit(LOD) and the quantitative detection limit(LOQ)

1- $$r = \frac{\sum\left[(x_i - \bar{x})(y_i - \bar{y})\right]}{\sqrt{\left[\sum(x_i - \bar{x})^2\right]\left[\sum(y_i - \bar{y})^2\right]}}$$

r : The correlation coefficient

$\bar{Y}$: Absorption rate or respond

$\bar{x}$: Concentration rate

2- $$b = \frac{\sum\left[(x_i - \bar{x})(y_i - \bar{y})\right]}{\sum(x_i - \bar{x})^2}$$

b : The slope

3- $a = \bar{y} - b\bar{x}$

a : intersection

4- Y= a + bx

X: The concentration of the substance

5 - $$S_{y/x} = \sqrt{\frac{\sum(y_i - \bar{y})^2}{(n-2)}}$$

$S_{y/x}$: Standard deviation of change of (y) values of residual

$\bar{Y}$:Absorption rate or respond

X_i: The value of the response or absorption

6- $$S_b = \frac{S_{y/x}}{\sum (x_i - \bar{x})^{1/2}}$$

S_b : Standard deviation of slope (b)

7-

S_a : Standard deviation of the point of intersection(a)

Relationships for calculating the detection limit and the quantitative detection limit :

1- $$L.O.D = \frac{3 \times \sigma \times C}{\bar{y}}$$

L.O.D=L.D: The detection of limit

σ : Standard deviation

C : The lowest concentration that the device can sense, represented by the concentration of the plank used under study.

$\bar{Y}$:Absorbance or response rate for a series of (n) measurements not less than ten.

2-L.O.D= 3.3Sa/Slope

S_a : Standard deviation of the point of intersection(a)

b : Slope

3- L.O.D= a+3S**yx**

$S_{y/x}$: Standard deviation of change of (y) values

a : intersection point.

4- L.O.D= 3.3S**yx**/Slope

5- L.O.D= $X_{\mathbf{blank}}+3S_{\mathbf{blank}}$

or

L.O.D= $X_{\mathbf{blank}}+2S_{\mathbf{blank}}$

X_{blank} :The rate of response or absorbance of Planck's solution at the wavelength of the maximum fixed absorption for model estimation (substance or element).

S_{blank} : Standard deviation of the change in values (absorption or response) of Planck's solution.

6- L.O.D= Signal to noise ratio = 3/1

Or

L.O.D= Signal to noise ratio = 2/1

7- L.O.Q= 10S**a**/Slope

L.O.Q : The quantitative detection limit.

8- L.O.Q= a+10S**yx**

9- L.O.Q=10S**yx**/Slope

10- L.O.Q= Xblank+10Sblank

11- $L.O.Q = \frac{10 \times \sigma \times C}{\overline{X}}$

Appendix (C)

Spectroscopic relations :

1- $\varepsilon = A / C.L$

ε : molar absorption coefficient ($L . mol^{-1} . cm^{-1}$)

A : Absorption

C : Concentration.

L : molar absorption coefficient (1cm).

can be found(ε) from the following relationship:

$\varepsilon = M.W \times b \times 1000$

M.W : molecular weight of the substance.

b: Slope

a : specific absorbance ($ml . g^{-1} . cm^{-1}$)

3- $S = \frac{0.001}{a}$

S : Sandal sensitivity ($\mu g . cm^{-2}$)

can be found(S) from the following relationship:

$S = M.W / \varepsilon$

Appendix

Pharmaceutical compounds	Theoretical value mg	Experimental value1 mg	Experimental value2 mg	Experimental value3 mg	RSD% N =3	E rel. %	Recovery	t-test	f-test
Propanolol (accord)	10	9.62	9.67	9.73	1.39	-0.038	99.962	0.117613257	0.284284418
Triflupromazine (Hicma)	10	9.39	9.23	9.4	1.41	-0.061	99.939		

Pharmaceutical compounds	Theoretical value	Experimental value1	Experimental value2	Experimental value3	F-Test Two-Sample for Variances		
Propanolol (accord)	10	9.62	9.67	9.73			
Triflupromazine (Hicma)	10	9.39	9.23	9.4		*Propanolol (accord)*	*Triflupromazine (Hicma)*
					Mean	9.755	9.505
					Variance	0.0287	0.114966667
					Observations	4	4
					df	3	3
					F	0.249637576	
		0.284284418			P(F<=f) one-tail	0.284284418	
					F Critical one-tail	0.107797789	

Pharmaceutical compounds	Theoretical value	Experimental value1	Experimental value2	Experimental value3	t-Test: Two-Sample Assuming Equal Variances		
Propanolol (accord)	10	9.62	9.67	9.73			
Triflupromazine (Hicma)	10	9.39	9.23	9.4		*Propanolol (accord)*	*Triflupromazine (Hicma)*
					Mean	9.755	9.505
					Variance	0.0287	0.114966667
					Observations	4	4
					Pooled Variance	0.071833333	
					Hypothesized Mean Difference	0	
					df	6	
					t Stat	1.319143363	
		0.117613257			P(T<=t) one-tail	0.117613257	
					t Critical one-tail	1.943180281	
		0.235226515			P(T<=t) two-tail	0.235226515	
					t Critical two-tail	2.446911851	

v1	v2	Ave.	Stdev	RSD	Corr.	Slope	Intersection (a)	Standard deviation	Standard deviation of the slope	Standard deviation for(a)	LOD	LOQ
0.1	17	8.55	11.9501	1.40	0.997228	191.4637	165.7	1437.511	-4.04623	371906.8	0.005	0.036
0.3	161	80.65	113.6321	1.41								
0.5	303	151.75	213.8998	1.41								
1	480	240.5	338.7041	1.41								
3	700	351.5	492.8534	1.40								
5	1250	627.5	880.3479	1.40								
10	2100	1055	1477.853	1.40								
20	3954	1987	2781.758	1.40								
4.9875	1120.625	equal to av.										

v1	v2	Ave.	Stdev	RSD	Corr.	Slope	Intersection (a)	Standard deviation	Standard deviation of the slope	Standard deviation for (a)	LOD	LOQ
0.1	55	27.55	38.82016	1.41	0.996083	127.5623	120.1356	1539.342	-3.42051	1072014	0.007	0.054
0.3	100	50.15	70.49855	1.41								
0.5	200	100.25	141.0678	1.41								
1	350	175.5	246.7803	1.41								
5	620	312.5	434.8707	1.39								
10	1500	755	1053.589	1.40								
20	2870	1445	2015.254	1.39								
30	3800	1915	2665.793	1.39								
8.3625	1186.875	equal to average										

الخلاصة

يعتبر الفصل الكروموتوغرافي السائلي عالي الاداء (High-Pressure Liquid Chromatography) (HPLC) احد اكثر التقنيات شيوعا المستخدمة في الكيمياء التحليلية لفصل وتقدير المركبات الصيدلانية.

تم في هذه الدراسة تحضير عمود فصل كروماتوغرافي.مونوليثيي عمود فصل كروماتوغرافي هو (Glycidylmetharylate-Co-Ethylenedimethacrylate-Co- Acrylamide) لتقدير وفصل المركبات الصيدلانية.

تم استخدام انبوب بوروسيليكات طوله (60mm) وبقطر داخلي وخارجي (1.5mm) و (3.5mm) على التوالي للبلمرة المشتركة باستخدام مصدر ضوء الاشعة فوق البنفسجية (365nm). تم اذابة المونمرات (Glycidylmetharylate) (Acrylamide) ورابط (Ethylenedimethacrylate) وبادئ (2,2-dimethoxy-2-phenylacet phenone) في مذيبات مناسبه وهي (1-propanol) و (hexanol).

وجد ان البوليمر تكون بعد ٣ دقائق بعدها تم فتح مجموعة الايبوكسي في (glycidyle methacrylate) لتشكيل مجموعات ديول بضخ HCL (0.2M) لمدة ٣ ساعات بمعدل تدفق ($20\mu L.min^{-1}$) .

تم تشخيص واثبات تكون المونوليث باستخدام تقنيات متنوعه مثل (SEM) و(BET) و(^{1}HNMR) و (FT-IR) .وقد تمت دراسة خصائص البولمر المتكون مثل المساحة السطحية وحجم الفجوات الموجودة داخل المونوالث.بتم دراسة الظروف المثلى لتكوين البولمر مثل وقت التشعيع، نفاذية المونوليث، المسامية ،الانتفاخ والمسافه بين مصدر الاشعاع والعمود.

تم استخدام المونوليث المحضر لتقدير وفصل المركبات الصيدلانية مثل مثل (Propranolol Hydrochloride) و (TriFluoperazinedi Hydrochloride) بأستخدام تقنية (HPLC) بسبب الدور الحيوي لها في علاج العديد من الامراض التي تصيب الانسان.

اتسمت طريقة التقدير بحد كشف (LOD) ($0.005\ \mu g.mL^{-1}$) , حد كشف كمي (LOQ) ($0.036\ \mu g.mL^{-1}$) و حساسية ساندل ($0.0052\mu g/cm^2$) لمركب (Propranolol Hydrochloride) بينما لمركب(TrifluoperazinediHydro chloride) كانت ذات حد كشف (LOQ) ($0.007\ \mu g.mL^{-1}$) ,حد كشف كمي (LOQ) ($0.036\ \mu g.mL^{-1}$) وحساسية ساندل ($0.00783\ \mu g/cm^2$) .

تم استخدام عمود المونوليث المحضر في فصل المركبات الصيدلانية باستخدام تقنية (HPLC) وظهرت قمة عند زمن احتجاز قدره (1.4 min) لمركب (Propranolol Hydrochloride) , بينما لمركب (Trifluoperazine dihydorchloride) ظهرت قمة بعد زمن احتجاز قدره (2.6min) . وجد ان هذه المركبات تتأثر مع مكونات العمود وكان الفصل ناجحاً . وجد ان عدد الصفائح النظرية (N) وارتفاع الصفيحة النظرية للعمود الكروماتوغرافي المونوليثي (Propranolol Hydrochloride) و (TriFluoperazinedi Hydrochloride) (110.995plates) و (2.19mm/plates) و (111.102plates) و(2.22mm/plates) على التوالي .

وجد ان العمود المونوليث المحضر يتمتع بخصائص مهمة هي انه منخفض الكلفة وذا دقة وضبط عاليين ,وان عمر العمود المونوليث الكرموتوغرافي (45) يومياً.

وزارة التعليم العالي والبحث العلمي

جامعة بابل /كلية العلوم

قسم الكيمياء

تحضيرعمود فصل كروموتوغرافي يستخدم لفصل وتقدير المركبات الصيدلانية

رسالة ماجستير مقدمة

الى مجلس كلية العلوم – جامعة بابل

وهي جزء من متطلبات نيل درجة الماجستير في العلوم / الكيمياء

من قبل

نرجس صلاح فلاح مشعل السلطاني

بكالوريوس علوم كيمياء – جامعة بابل – ٢٠١٣

بأشراف

ا.د. احمد علي عبد الصاحب الكريمي

ا.م. ابتسام عبد الواحد رشيد

2022م ١٤٤٤ هـ